SPECTROSCOPIC STUDIES OF ELEMENTARY PROCESSES ON EXCITED ATOMS IN PLASMA

KENZO MIYAZAKI

1976

SPECTROSCOPIC STUDIES OF ELEMENTARY PROCESSES ON EXCITED ATOMS IN PLASMA

by

KENZO MIYAZAKI
Department of Engineering Science
Faculty of Engineering
Kyoto University
Kyoto

Kyoto University
1976

CONTENTS

Section			Page
		Chapter I	
		Introduction	1
		References	5
		Chapter II	
		Measurement of Population Density of Excited Helium Levels by the Hook Method	7
		Synopsis	7
1		Introduction	8
2		Principle	9
3		Experiment and Results	10
4		Calculations	11
5		Discussion	12
	5.1	Estimation of experimental errors	12
	5.2	Comparison with line absorption mesurement	13
	5.3	Comparison with calculations	14
		References	16
		Figure captions	18
		Figures	19
		Tables	25
		Chapter III	
		The Interferometric Population Measurement with Dye Lasers	26
		Synopsis	26
1		Introduction	27
2		Principle of the hook Method	28

Chapter III (continued)

Section		Page
3	Experimental Detailes	29
4	Experimental Results	32
5	Calculation	33
6	Discussion	35
	Acknowledgement	37
	Appendix	38
	References	39
	Figure captions	40
	Figures	42
	Tables	59

Chapter IV

	Excitation Mechanism of 3250 and 4416 Å Laser Lines in the Cataphoretic He-Cd Laser Discharge	62
	Synopsis	62
1	Introduction	63
2	Experimental Procedure	65
2.1	Measurement of population density by the hook method	66
2.2	Determination of population density of the 3250 Å upper level	68
3	Results and Discussion	69
3.1	Dependence of population densities on discharge current	70
3.2	Dependence of population densities on Cd atom concentration	72
3.3	Penning-excitation cross section	73
	References	77

Chapter IV (continued)

Section		Page
	Figure captions	79
	Figures	81
	Tables	92

Chapter V

	Dispersion and Absorption Studies on the Doubly-Excited $5p^2\ ^3P_{0,1,2}$ States of CdI	93
	Synopsis	93
1	Introduction	94
2	Experimental	95
2.1	Population and f-value measurements by the hook method	96
2.2	Absorption measurement for the autoionizing transitions	97
3	Experimental Results	98
4	Discussion	99
	References	103
	Figure captions	104
	Figures	105
	Tables	114
	Acknowledgement	116

Chapter I

Introduction

There has been a growing interest in excited atoms in the low-lying levels including metastable atoms with long life time in various types of plasma. In connection with the recent progress in astrophysics, plasma physics and laser physics, the requirement of detailed knowledge on the excited atoms in plasmas has appreciably increased. In fact the excited atoms play an important role in elementary atomic processes such as photoionization in steller atomospheres, excitation transfer or chemical reaction in laser media and collisional ionization or recombination in laboratory plasmas.[1-4] Furthermore, these subjects on the excited atoms include many aspects of intrinsic importance in the study of atomic structure.[5,6] However, it is only in recent years that many attempts have been made to obtain physical quantities of the excited atoms in the low-lying levels for the atomic processes.[7-12]

This thesis describes spectroscopic investigations of several elementary processes on the excited atoms in the plasmas which are produced by stationary dc discharge, pulsed discharge, cataphoretic discharge and high-frequency discharge.

In performing the experiment, the detection of the excited atoms, especially of the non-radiative metastables, seems to be a serious problem, as well as the production method of excited species. In the course of the present experiments, the classical interferometric method invented by Rozhdestvenskii[13] is applied

to the population measurement of excited atoms in the low-lying levels under plasma conditions. This technique which is called the hook method requires measurement of anomalous dispersion near spectral lines and has been used extensively for the oscillator strength measurement in atomic and molecular spectra and the concentration measurement of atoms in gas dynamic researches.[14-16] The hook method in the present studies provides us with the values of population density which are reliable enough to allow the detailed discussion of the atomic processes on the excited atoms.

Chapter II describes the population measurement of excited He atoms in the 2^1S, ^1P and 2^3S, ^3P levels in the positive-column discharge plasma by means of the hook method.[17] The results are compared with the data given by the line absorption method and also with the calculation based on the collisional-radiative model of plasma. The accuracy of population density obtained is discussed.

In the study of time-dependent phenomena, a flash lamp has been usually employed as the light source for the photographic measurement in the hook method with a Mach-Zehnder interferometer, and use of the flash lamp has given a limitation in time resolution of the hook method.

Chapter III contains an improved experimental apparatus for the sake of the time-resolved hook measurement and its application to the population measurement of excited atoms in the low-lying He and Ne levels in the pulsed discharge.[18,19] The experimental setup constructed has dye lasers pumped by

a pulsed N_2 laser as the continuum light source, and its resolution in time is about 5 nsec. The population density measured in the experiment shows a peculier change as a function of time. From the view point of atomic processes in plasma, the characteristic population change and population mechanism are examined by the calculation based on a simple model of plasma.

In chapter IV is described the excitation mechanism of Cd^+ laser lines in a cataphoretic He-Cd laser discharge.[20] Since the invention of metal vapor lasers, much attention has been paid to the $He-Cd^+$ laser owing to the relatively high output power at 4416 Å and a convenient UV laser source at 3250 Å for its simple structure. However, there have been alternative and competitive propositions on the excitation mechanism of these laser lines. In this experiment under typical discharge condition for lasing, the population densities of He and Cd levels which are important in the laser excitation processes are obtained by the hook method and by the line intensity measurement combined with the hook method. The experimental results conclusively demonstrate that the upper laser levels of Cd ions are mainly populated by Penning collisions of the ground state Cd atoms with the metastable He atoms. The cross section for the Penning excitation in the He-Cd mixtures is estimated.

Chapter V is concerned with the metastable Cd atoms in the $5s5p\ ^3P$ levels and the doubly-excited atoms in the autoionizing $5p^{2}\ ^3P_2$ level.[21-23] Stationary Cd plasma excited in a long

cylindrical vessel by a high-frequency device produces relatively high concentration of the metastable Cd atoms, which is determined by the hook method. The absorption cross section for the autoionizing transitions $5s5p\ ^3P_{1,2} - 5p^2\ ^3P_2$ represents the Lorentzian profile with the same half-width. The observed profile is in contrast to the ordinary asymmetric profile, so-called Beutler-Fano shape,[2] for an autoionization resonance, and moreover there are in itself no continuum states of even parity available for autoionization of the $p^2\ ^3P$ states in pure LS coupling. The experimental results contrary to these general principles are discussed according to the configuration-interaction theory for autoionization. The absolute values of oscillator strength for the transitions $5s5p\ ^3P_{0,1,2} - 5p^2\ ^3P_{0,1,2}$ are also presented.

References

1) G.V.Marr: Photoionization Processes in Gases (Academic Press, New York, 1967).

2) A.Temkin ed.: Autoionization, - Astrophysical, Theoretical and Laboratory Experimental Aspects - (Mono Book Corp., Baltimore, 1966).

3) C.S.Willett: Introduction to Gas Lasers - Population Inversion Mechanisms (Pergamon Press, Oxford, 1974).

4) M.Venugopalan ed.: Reactions under Plasma Conditions (Wiley-----Interscience, New York, 1971) Vol.I and II.

5) D.R.Bates ed.: Atomic and Molecular Processes (Academic Press, New York, 1962).

6) H.S.W.Massey and E.H.S.Burhop: Electronic and Ionic Impact Phenomena (Oxford University Press, London, 1969) Vol.I and II.

7) D.R.Long and R.Geballe: Phys. Rev. A 1 (1970) 260.

8) W.L.Borst: Phys. Rev. A 9 (1974) 1195.

9) L.C.Johnson and E.Hinnov: Phys. Rev. 187 (1969) 143.

10) D.J.Bradley, P.Ewart, J.V.Nicholas, J.R.D.Show and D.G. Thompson: Phys. Rev. Letters 31 (1973) 263.

11) J.L.Carlsten, T.J.McIlrath and W.H.Parkinson: J. Phys. B 8 (1975) 38.

12) R.F.Stebbings, F.B.Dunning, F.K.Tittel and R.D.Rundel: Phys. Rev. Letters 30 (1973) 815.

13) D.S.Rozhdestvenskii: Ann. Phys. 39 (1912) 307.

14) N.P.Penkin: J. quant. Spectrosc. radiative Transfer 4 (1964) 41.

15) W.C.Marlow: Appl. Optics 6 (1967) 1715.

16) M.C.E.Huber: Modern Optical Methods in Gas Dynamic Research, ed. D.S.Dosanjh (Plenum Press, New York, 1971) p.85.

17) T.Fujimoto, K.Miyazaki and K.Fukuda: J. quant. Spectrosc. radiative Transfer 14 (1974) 377.

18) K.Miyazaki, R.Nakata, Y.Tomita, M.Suemitsu, S.Watanabe and K.Fukuda: Japan J. appl. Phys. 14 (1975) 1075.

19) K.Miyazaki and K.Fukuda: To be published.

20) K.Miyazaki, Y.Ogata, T.Fujimoto and K.Fukuda: Japan. J. appl. Phys. 13 (1974) 1866.

21) K.Miyazaki and K.Fukuda: J. Phys. Soc. Japan: 38 (1975) 906.

22) K.Miyazaki, T.Watanabe and K.Fukuda: J. Phys. Soc. Japan 38 (1975) 1551.

23) K.Miyazaki, T.Watanabe and K.Fukuda: J. Phys. Soc. Japan 40 (1976) 233.

Chapter II

Measurement of Population Density of Excited Helium Levels by the Hook Method*

Synopsis

The hook method has been applied to the positive-column discharge plasma of helium and the population density of the lowest-lying excited levels, $2^{1,3}S$ and $2^{1,3}P$, was measured. The results are compared with data obtained by use of the line absorption method, and discrepancies between these data are discussed. The result is also compared with a calculation based on application of the collisional-radiative model.

---

* Published in J. quant. Spectrosc. radiative Transfer 14 (1974) 377.

§ 1. Introduction

In the spectroscopic study of plasmas, the population densities of the lowest-lying excited levels, such as metastable levels, are frequently measured by the line absorption or re-absorption method. In these cases, it is an essential requirement to know the profile of the line from the light source and that from the plasma itself near the line center. However, it is often difficult to determine the line profile accurately and, therefore, the derived population densities may be uncertain. Furthermore, the plasma must have an optical thickness of order smaller than unity at the line center to be measured by this method.

On the other hand, the hook method, which employs anomalous dispersion of refractivity outside the line core, does not require detailed knowledge of the profile near the line center, and there is no restriction on the allowable upper limit to the optical thickness. Several experiments have been made which determine population density by this method. The first of these was an experiment by Ladenburg,[1] who measured the population densities of excited neon levels in a positive-column discharge and showed the existence of negative dispersion

In what follows, we describe measurements of population density of helium $2^{1,3}S$ and $2^{1,3}P$ levels in a positive-column plasma by this method. The results are compared with data obtained by the line absorption measurement by Mewe.[2] Calculation of the population density is also presented and the result is compared with the experimental data.

§ 2. Principle

If one is interested in the spectral region outside the cores of spectral lines so that the effect of line broadening is neglected, the refractivity of plasma is given by

$$n_\lambda - 1 = \frac{r_0}{4\pi} \sum_p \sum_{q>p} \frac{f_{pq} \lambda_{pq}^3 n(p)}{\lambda - \lambda_{pq}} \left[1 - \frac{g(p) n(q)}{g(q) n(p)} \right], \qquad (2.1)$$

where r_0 is the classical electron radius, λ the wavelength considered, λ_{pq} and f_{pq} the wavelength and the absorption oscillator strength, respectively, of the spectral line combining the lower level p and the upper one q, and n(p) and g(p) are the population density and the statistical weight of the level p, respectively. The summations are taken over all the levels and q>p means that the level q lies above the level p.

In the spectrum of the interference fringe in the hook method, hooks are formed at those wavelengths which are real roots of

$$\sum_p \sum_{q>p} \frac{f_{pq} \lambda_{pq}^3 n(p)}{(\lambda - \lambda_{pq})^2} = \frac{4\pi K}{r_0 l}, \qquad (2.2)$$

where the negative dispersion term in eq.(2.1) has been neglected, K is the hook-method constant, and l is the plasma length.

For a well-separated line, all terms but one in eq.(2.2) can be dropped and the simple relation

$$n(p) f_{pq} = \frac{\pi K}{r_0 l \lambda_{pq}^3} \Delta^2 \qquad (2.3)$$

is derived, where Δ is the hook separation.

If the oscillator strengths are known, one can determine the population density, n(p), by observing the hooks and using eqs.(2.2) and (2.3).

§ 3. Experment and Results

A Mach-Zehnder interferometer and a spectrograph constituted the optical system. A short xenon arc lamp was used as the light source for the interferometer. The discharge cell was placed in the test beam section. Windows and compensation plates were made of fused quartz of 5 mm thickness. Measurements were made on the two cells. The cell A was 16 mm in inner diameter and 98 cm in active length and B was 3mm in diameter and 67 cm in length. The cell was evacuated to 2×10^{-7} Torr and the cold cathode was outgassed before filling with gas. Helium was introduced to a pressure of 0.2 - 5 Torr. The plasma was produced by a stationary dc discharge of 25 - 200 mA. The interferometer was mounted on an iron block supported by damping rubbers and sufficient stability was obtained for quantitative observations.

The spectral lines employed for the measurement are given in Table I. An Ebert-mount spectrograph, with a focal length of 170 cm (Shimadzu GE-170) and a grating of 1200 grooves/mm, was used. The order (all are negative) and reciprocal linear dispersion are also shown for each line. Lower-order spectra were eliminated by placing a glass filter before the entrance slit. The slit width was 20 - 50 μm and the exposure time

was 15 - 90 sec. The light bundle, which was 2 - 3 mm in height and about 1 mm in width, passed through the center of the cell and was focused onto the slit by a cylindrical lens. Some examples of hook spectrum are shown in Fig.1.

As is clearly seen in the 5876 Å line and less distinctly in the 3889 Å line, the triplet lines show multiple structure due to the fine structure so that eq.(2.2) must be applied. Since L-S coupling is valid for the levels involved and statistical equilibrium can be assumed among the population densities of the sublevels, the solution is straightforward. Using the known oscillator strengths[3,4] for the fine structure of the levels,[5] the population densities are obtained. On the other hand, the analysis for the singlet lines is made on the basis of eq.(2.3). Some examples of the results are shown in Figs. 2 (a) and (b) for cells A and B, respectively. Figures 3 (a) and (b) give the pressure dependences of the population densities for cell A.

§ 4. Calculations

Collisional-radiative calculations have been performed for the helium plasma.[6] The grouping of the levels is the same as in ref.7 but, in the present case, 59 groups of the levels having principal quantum numbers smaller than 20 are considered. The excitation cross-section formulas in ref.7 are adjusted to fit recent data.[8] The collisional-radiative and population coefficients are obtained over a wide range of plasma parameters.

The population densities for the positive-column plasma are also calculated in the same way as in ref.9. An ambipolar-diffusion model is assumed for the recombination of ions[10,11] and, as the destruction processes of metastable atoms, diffusion to the wall,[12] Penning ionization[13] and collisions with normal atoms[12] are considered in addition to the collisional-radiative processes. Trapping of radiation is taken into account according to the method of Holstein[14] for transitions terminating to the ground level and to the two metastable levels. Some examples of the results are shown in Figs.2 and 3, where the electron density is related to the discharge current with the aid of data from refs.2 and 15. Figure 4 shows the population density distribution among the excited levels.

§ 5. Discussion

5.1 Estimation of experimental errors

In the typical hook spectrum shown in Fig.1, the hook-method constants are 5700, 7700, 4050 and 4670 for 5016 Å, 3889 Å, 6678 Å and 5876 Å, respectively. These constants can be determined with an accuracy of one per cent.

Equation (2.1) neglects the influence of natural and Doppler broadening on the refractivity. The correction of the hook separation due to the "inner hooks" is discussed by Marlow[16] and by Huber.[17] In the present experiment, the hook separation is 0.2 - 3.2 Å, while natural and Doppler broadening are, at most, 0.01 Å and 0.02 Å, respectively. According to Huber's diagram, the correction is within 0.3 - 2.0

per cent.

It is known that, in a positive-column plasma, the population density of excited levels decreases rapidly with increasing principal quantum number.[9] The present calculation also shows this feature (Fig.4), i.e., $g(p)n(q)/g(q)n(p)$ is of the order of 10^{-3} for the present case. Therfore, the neglect of the negative dispersion term in eq.(2.1) is well justified.

The oscillator strengths for the four transitions concerned are estimated to be accurate to 1 - 3 per cent.

Accuracy of the measurement on the separation of hooks depends on the sharpness of the spectrogram, on the slope of the fringes and on the hook separation itself. The accuracy is estimated to be within 3 - 15 per cent, leading to an uncertainty of 6 - 30 per cent for the resulting population density.

The overall uncertainty of n(p) is shown in Figs.2 and 3 by error bars.

5.2 Comparison with line absorption measurement

As an example of a line absorption measurement, the data by Mewe[2] are plotted on Figs.3 (a) and (b); the tube diameter and the discharge current of Mewe were 22 mm and 400 mA, respectively. Since the experimental conditions were not exactly the same in both investigations, direct comparison between the the results is not possible. However, the figures show some striking features. Thus, the scattering of data points in the present experiment is not as large as that observed in the line-absorption experiment. Next, the hook method gives

population densities 3 - 10 times as large as those derived from line absorption.

The reasons for the discrepancies will now be considered. First, the discharge tube diameter of Mewe is 1.4 times as large as the present one. The calculations show that this difference leads to a difference in the population density of the excited levels in the opposite sense by nearly the same amount. This result is also suggested from a comparison of Figs.2 (a) and (b). The second discrepancy lies in the problem of optical thickness τ; for instance, τ for the 5876 Å line is 10 according to the present result. Such a large τ may lead to a severe error in absorption measurements. The third discrepancy is associated with moving striations, which occur for higher pressure ($\gtrsim$0.5 Torr) in Mewe's experiment. Since the absorption data are taken at right angles with respect to the tube axis, averaging over the data under striated conditions for a long period does not give the averaged population density unless $\tau \ll 1$. On the other hand, the hook method yields an averaged density along the tube axis. The discrepancy of Mewe's data from the present results is probably associated with the last two phenomena considered. Indeed, both sets of data show agreement within a factor of 2 for low-excitation and unstriated discharges (current density $\approx$ 10 mA/cm^2).

5.3 Comparison with calculations

As seen in Figs.2 and 3, the dependences of the calculated population density on the discharge current and on the pressure

explain the experimental data. The absolute value of the calculated density for the triplet levels is in good agreement with the experiment. However, for the singlet levels, the calculated values are a factor of 2 - 4 larger than the observed values.

Figure 4 shows high population densities for the lowest-lying excited levels and a rapid decrease in the density of higher-lying levels with increasing principal quantum number. This feature is observed in experiments on helium[18,19] and on argon plasmas.[20]

References

1) R.Ladenburg: Rev. mod. Phys. 5 (1933) 243.

2) R.Mewe: Physica 47 (1970) 373 and 398.

3) W.L.Wiese, M.W.Smith and B.M.Glennon: Atomic Transition Probabilities (U.S.Government Printing Office, Washington, 1966) Vol.I, p.9.

4) L.C.Green, N.C.Johnson and E.K.Kolchin: Astrophys. J. 144 (1966) 369.

5) C.E.Moore: Atomic Energy Levels (U.S.Government Printing Office, Washington, 1949) Vol.I, p.4.

6) Y.Ogata and K.Fukuda: Mem. Fac. Engng., Kyoto Univ. 35 (1973) 177.

7) L.C.Johnson and E.Hinnov: Phys. Rev. 187 (1969) 143.

8) For instance, P.G.Burke, J.W.Cooper and S.Ormonde: Phys. Rev. 183 (1969) 245.

9) T.Fujimoto, Y.Ogata, I.Sugiyama, K.Tachibana and K.Fukuda: Japan. J. appl. Phys. 11 (1972) 718.

10) W.Schottky: Phys. Zeit. 25 (1924) 635.

11) A.Dalgarno: Phil. Trans. 250 (1958) 426.

12) H.S.W.Massey, E.H.S.Burhop and H.B.Gilbody: Electronic and Ionic Impact Phenomena, 2nd ed. (Oxford Univ. Press, London, 1971) Vol.III, p.1780.

13) A.W.Johnson and J.B.Gerardo: Phys. Rev. A 7 (1973) 925.

14) T.Holstein: Phys. Rev. 83 (1951) 1159.

15) S.C.Brown: Basic Data of Plasma Physics, 2nd. ed. (MIT Press, Cambridge, 1966) p.80.

16) W.C.Marlow: Appl. Optics 6 (1967) 1715.

17) M.C.E.Huber: Modern Optical Methods in Gas Dynamic Research, ed. D.S.Dosanjh (Plenum Press, New York, 1971) p.85.

18) O.P.Bochkova and L.P.Razumovskaya: Optics and Spectrosc. 18 (1965) 438.

19) D.W.Swallom and P.D.Scholz: J. quant. Spectrosc. radiative Transfer 12 (1972) 107.

20) K.Tachibana and K.Fukuda: Japan. J. appl. Phys. 12 (1973) 895.

Figure captions

Fig.1. Examples of hook spectrum.

Fig.2. Population density as a function of discharge current. ——: present calculation. (a): The cell A. Filling pressure is 0.4 Torr. (b): The cell B. Pressure is 1.8 Torr.

Fig.3. Population density as a function of filling pressure for the cell A. Discharge current is 200 mA.
(a) ●, ○, ——: 2^1S and ■, □, ---: 2^1P. ●, ■: present experiment and ——, ---: present calculation.
○, □: Mewe's experiment (ref.2)
(b) The notations are the same as in (a) except that "2^1S" and "2^1P" are replaced by "2^3S" and "2^3P", respectively.

Fig.4. Calculated population-density distribution among the excited levels for the cell A. Filling pressure and discharge current are 0.4 Torr and 200 mA, respectively. Electron density and temperature are 5.3×10^{10} cm^{-3} and 6.4×10^4 K, respectively.

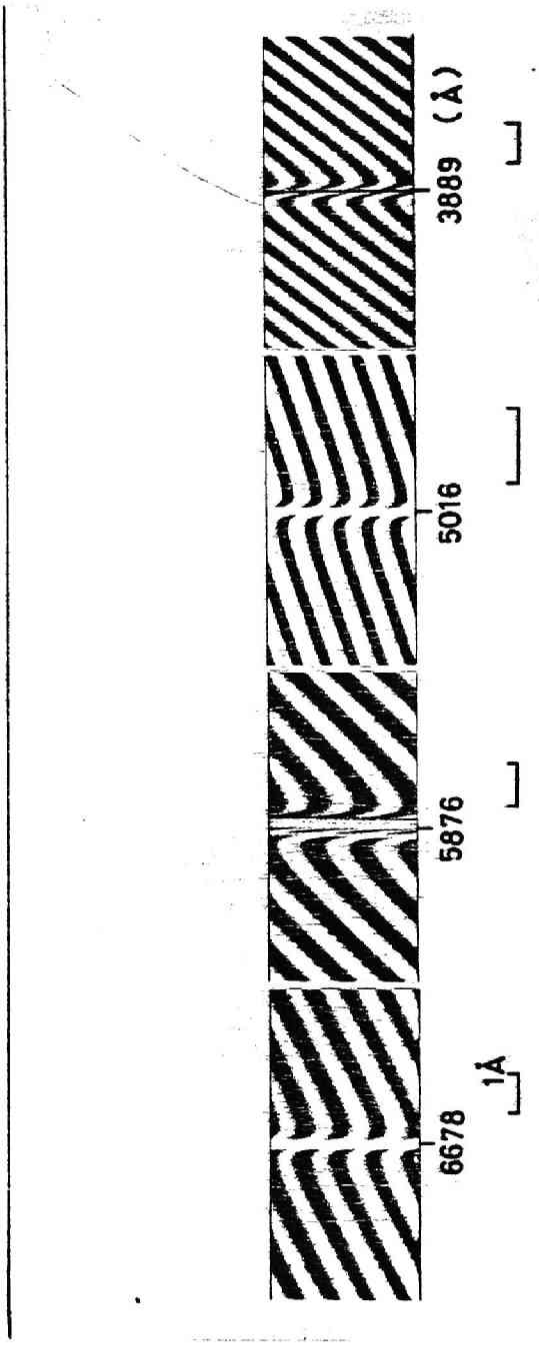

Fig.1

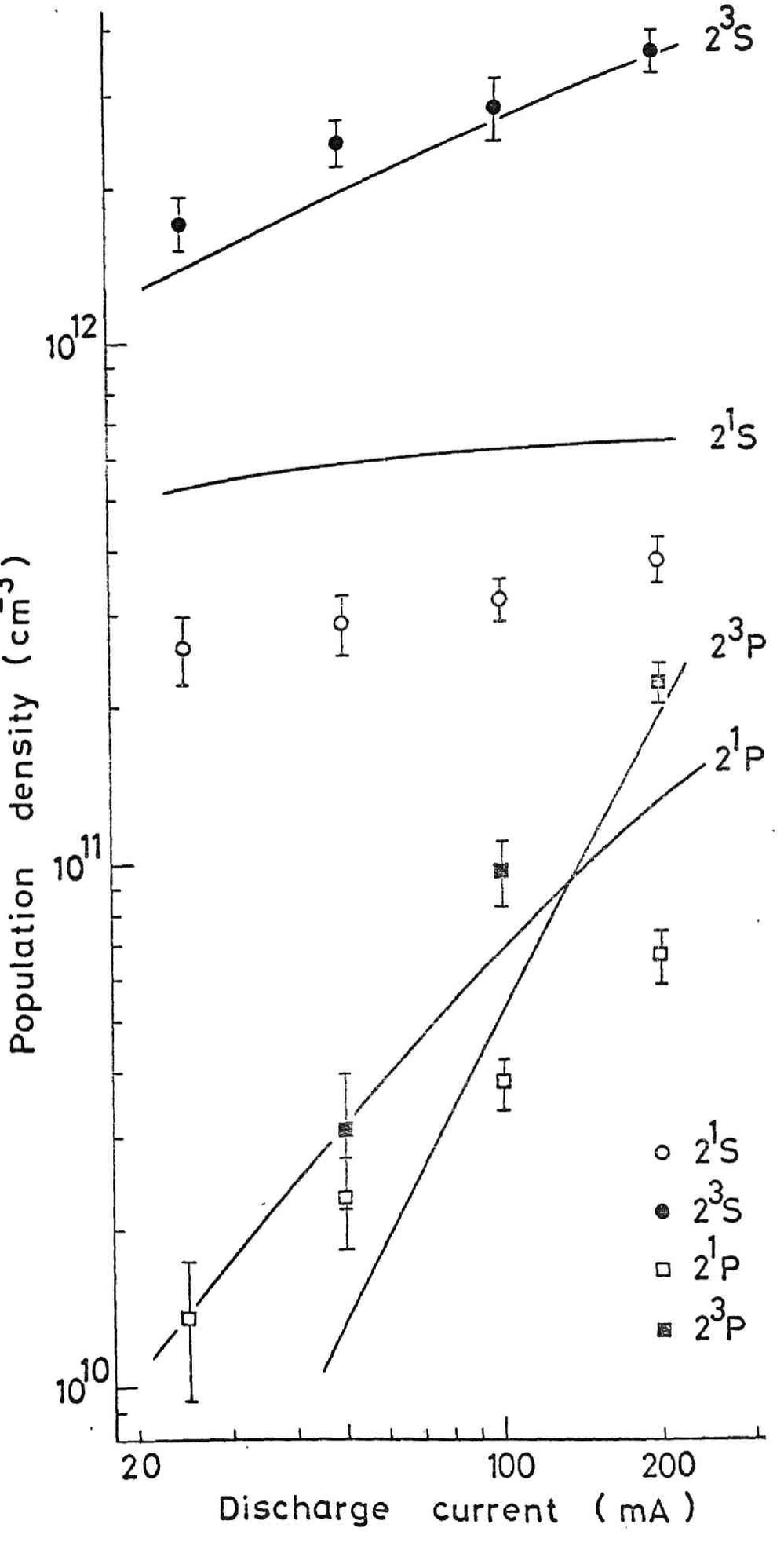
2^3S
10^{12}
2^1S
2^3P
2^1P
10^{11}
Population density (cm^{-3})
10^{10}
2^1S
2^3S
2^1P
2^3P
20
100
200
Discharge current (mA)

Fig.2(a)

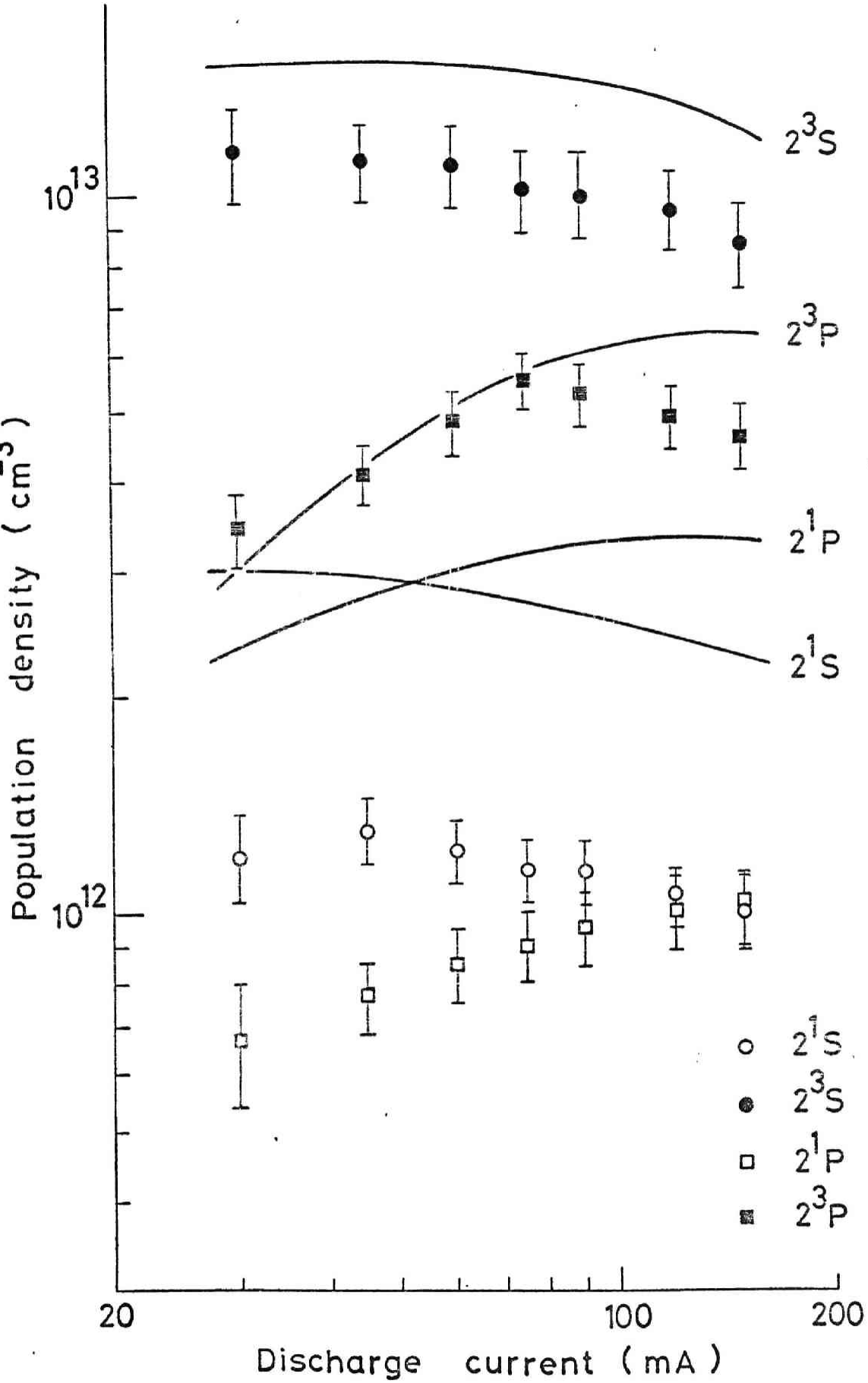
Population density (cm^{-3})
10^{13}
10^{12}
2^3S
2^3P
2^1P
2^1S
20
100
200
Discharge current (mA)

Fig.2(b)

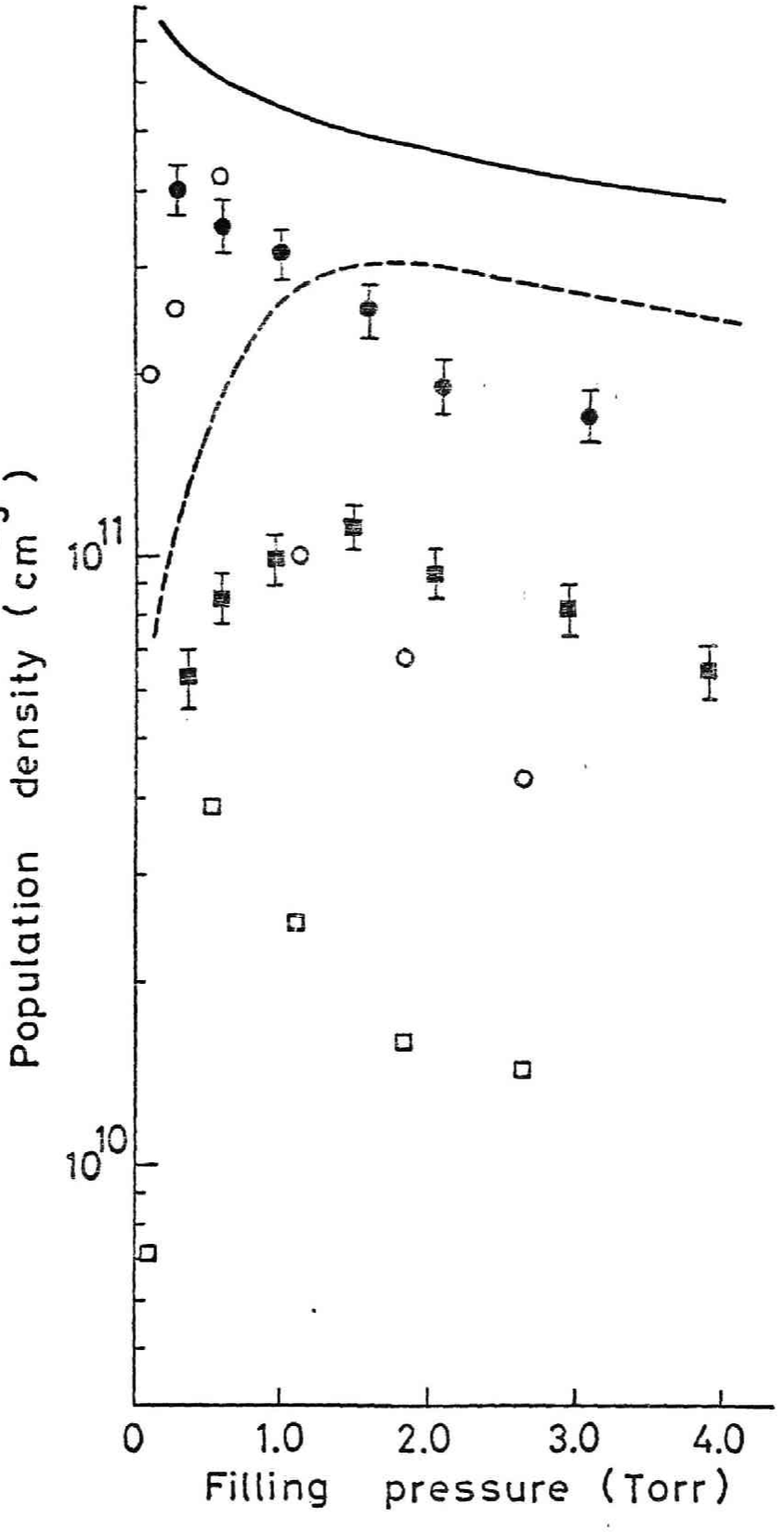
Population density (cm^{-3})
10^{11}
10^{10}
0
1.0
2.0
3.0
4.0
Filling pressure (Torr)

Fig.3(a)

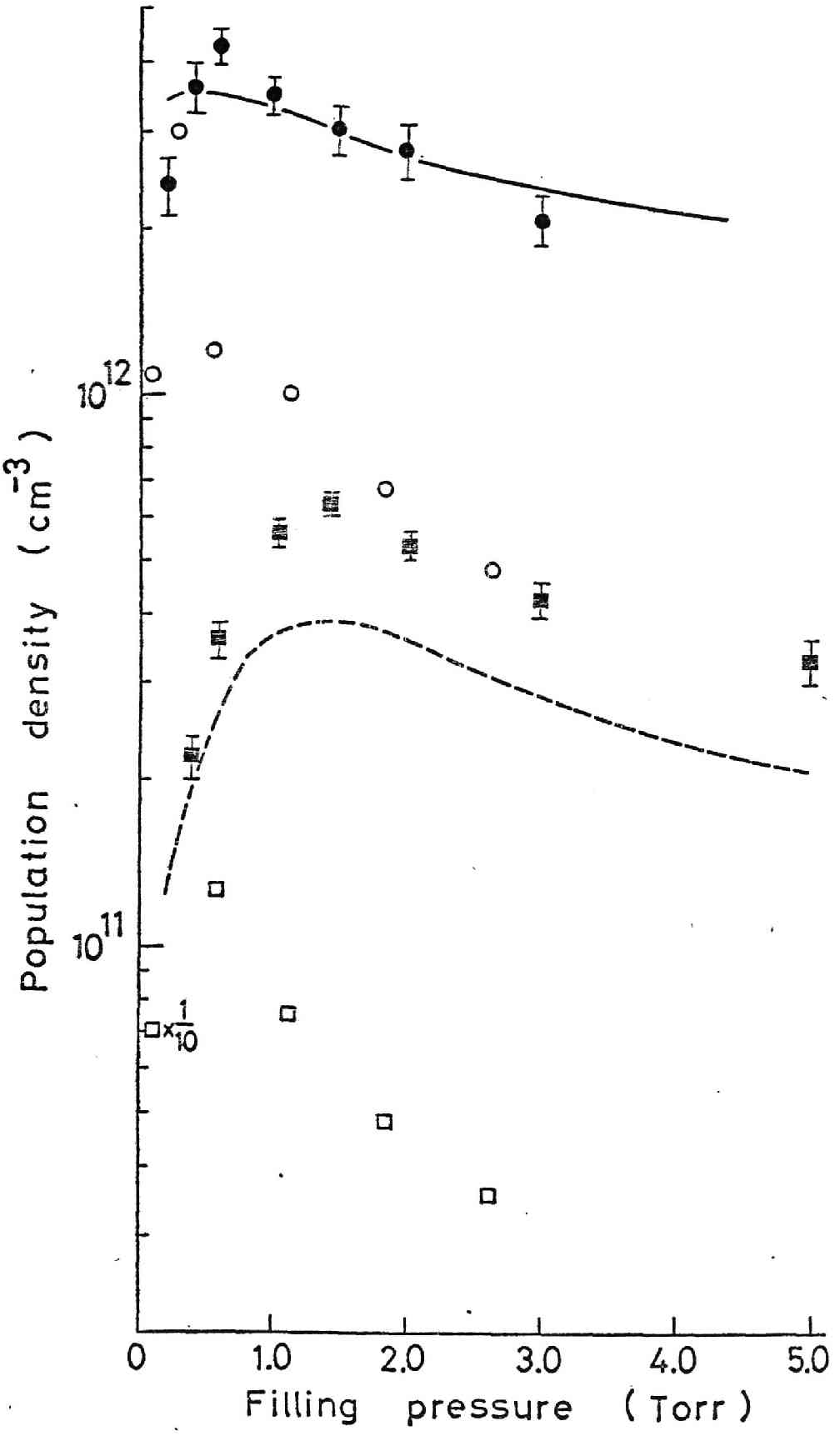
Population density (cm^{-3})
10^{12}
10^{11}
$\times\frac{1}{10}$
0
1.0
2.0
3.0
4.0
5.0
Filling pressure (Torr)

Fig.3(b)

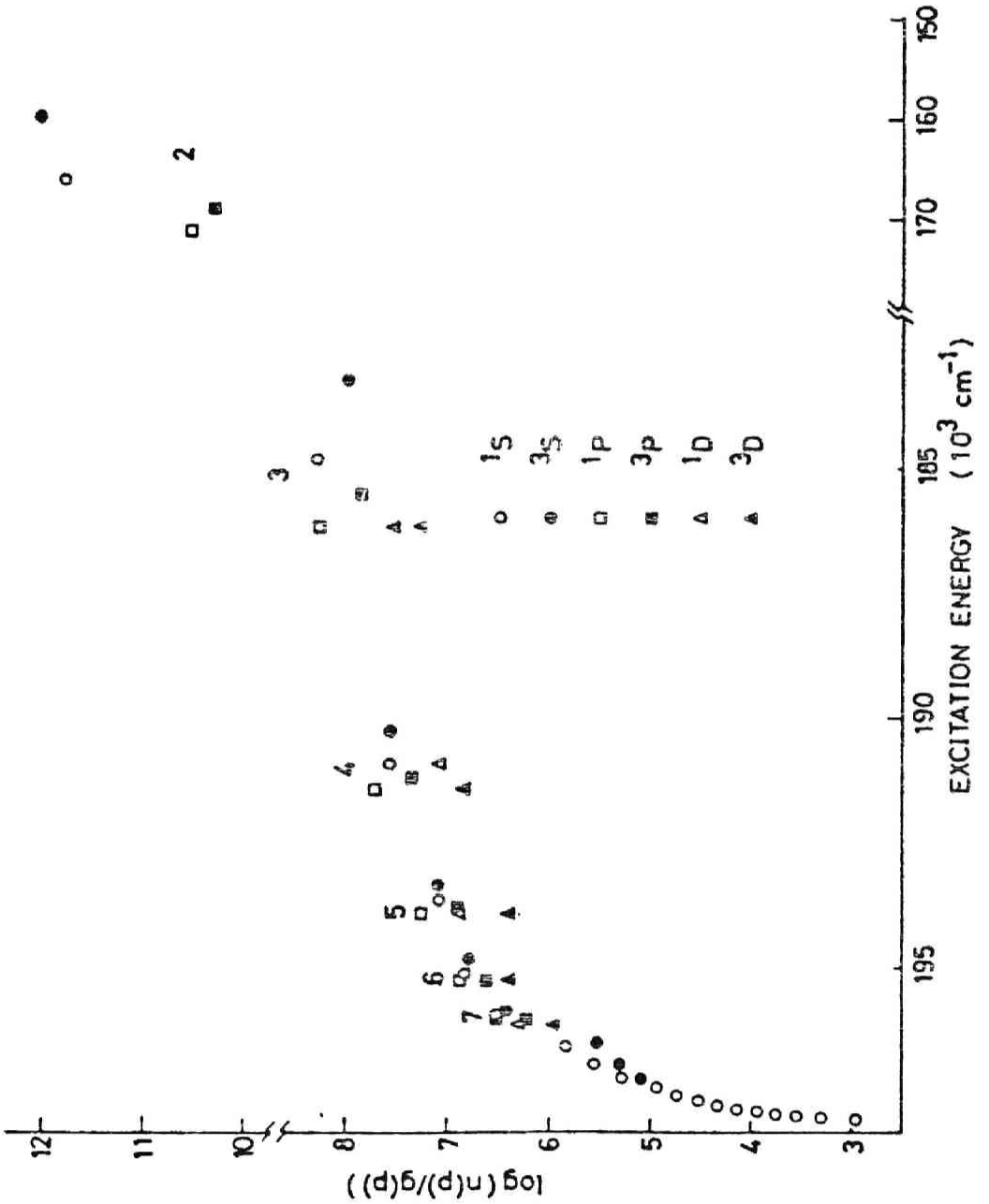

Fig.4

Table I. Data on the hook spectra shown in Fig.1.

Level	Spectral line (Transition)	Order	Reciprocal dispersion (Å/mm)	Film
2^1S	5016 Å ($2^1S - 3^1P$)	3rd	0.704	Fuji Neopan F
2^3S	3889 Å ($2^3S - 3^3P$)	3rd	1.17	Fuji Neopan F
2^1P	6678 Å ($2^1P - 3^1D$)	2nd	1.47	Kodak 103F
2^3P	5876 Å ($2^3P - 3^3D$)	2nd	1.74	Fuji Neopan F

Chapter III

The Interferometric Population Measurement with Dye Lasers*

Synopsis

Dye lasers pumped by a pulsed N_2 laser have been applied to the hook method as the continuum light source for an interferometer. The apparatus, which has a time resolution of about 5 nsec, has been employed for the population measurement of He and Ne atoms in the low-lying excited levels in the pulsed discharge with current duration of about 3 μsec. Two maxima of the population density peculier to the discharge have been found, one of which is during the current pulse of discharge and the other is in the early stage of afterglow. Calculation of electron temperature T_e and population density is made on the basis of a simple model of plasma, and the result shows that the characteristic population change is owing to the rapid decrease of T_e in the transient plasma. The population mechanisms dominant in the discharge and afterglow plasma are also demonstrated.

---

* Partly published in Japan. J. appl. Phys. 14 (1975) 1075.

§ 1. Introduction

An extensive use has been made of the hook method for population measurement in gas dynamic researches.[1-5] The hook method requires a continuum light source for the interferometric and photographic measurement of anomalous dispersion near spectral lines of a test medium. A flash lamp has been usually employed as the light source to investigate time-dependent phenomena by making use of the method.[1] It has been crucial and fairly difficult to construct the flash lamp with short-pulsed emission of continuum intense enough to photograph the hook spectrum, and then the time resolution is of the order of 1 μsec at most. Accordingly, there has been a limitation in the application of the hook method to the transient phenomena with faster change, so far as the flash lamp is used.

Recently, the authors have applied dye lasers pumped by a pulsed N_2 laser to the hook method as the continuum light source, and the time resolution of the method has been improved considerably.[6] In this paper we describe in detail the experimental setup and its application to the population measurement of low-lying excited levels in the pulsed He and Ne discharges with the current duration of about 3 μsec. The next section contains a short description of principle of the hook method. The experimental apparatus and procedure for the measurement are described in §3 and the results are presented in §4. In §5 we calculate the electron temperature and population density in the pulsed He discharge on the basis

of a simple model of He plasma, so as to explain the characteristic population change found in the measurement. The last section examines the atomic processes dominant for populating the excited He levels in the pulsed discharge.

§ 2. Principle of the Hook Method

Near an isolated transition at the wavelength λ_{ij} but outside the core of the spectral line, refractive index n of plasma is expressed as[7)]

$$n - 1 = \frac{r_0}{4\pi} \frac{f_{ij}\lambda_{ij}^3 N_i}{\lambda - \lambda_{ij}} \left(1 - \frac{g_i N_j}{g_j N_i}\right), \tag{2.1}$$

where N_i and N_j are the population density of the lower level i and the upper level j of the transition, respectively, g_i is the statistical weight of level i, r_0 is the classical electron radius and f_{ij} is the absorption oscillator strength of the transition.

In the hook method, one observes spectrum of the refractive index as the interference fringe pattern. The high-order fringes form maxima and minima or hooks of the intensity profile about the transition at λ_{ij}. When the negative dispersion term is neglected in eq.(2.1), i.e., $g_i N_j / g_j N_i \ll 1$, the wavelength separation Δ between the maxima and minima gives the population density N_i in terms of the relation 1,2,8)

$$N_i f_{ij} = \frac{\pi K}{r_0 \lambda_{ij}^3 l} \Delta^2, \tag{2.2}$$

where l is the length of absorption medium and K is a constant which can be easily and accurately determined.

§ 3. Experimental Details

The Pyrex discharge tube used in the experiment was 17 mm in inner diameter and 101 cm in length and had a cold cathode in the side arm. The ends of the tube were closed by quartz flat windows at a right angle to the tube axis for the interferometric measurement. The initial filling gas pressure p of He and Ne was 10 and 15 Torr. The repetitive pulsed-discharge at 10 Hz was made with 0.05 μF capacitor charged to the voltage V of 12 or 15 kV and a thyratron was employed as a switch of the discharge circuit. The duration of current pulse was about 3 μsec, and the peak current was about 800 A at p = 10 Torr and V = 12 kV in He. An example of the current wave form is shown in Fig.1.

The experimental arrangement for the population measurement is illustrated in Fig.2. The optical setup for the hook method consisted of a Mach-Zehnder interferometer, an Ebert-mount spectrograph of 170 cm focal length (Shimadzu GE-170) with a grating of 1200 grooves/mm blazed at 3000 Å and a dye laser pumped by the pulsed N_2 laser (AVCO C950A) as the light source. The interferometer was mounted on an iron block supported by damping rubbers to prevent mechanical vibration. The discharge tube and another tube with compensation quartz-windows were placed in the test and reference beam sections of the interferometer, respectively. The dye cell was 6 cm

in length and the dye-laser cavity was formed by a 100 % plane mirror and a glass wall of the cell.

The rectangular shape of the N_2 laser output at 3371 A, which was triggered by delayed pulses, was focused with a cylindrical lens to a line in the dye cell. The dye-laser beam passed through the centers of both tubes at the time t delayed from the initiation of the pulsed discharge, and was focused onto the slit of the spectrograph. The dye-laser signal out of the interferometer was always monitored on an oscilloscope (Tektronix 485) together with the discharge current to know the time t.

Near the wavelength of the transitions to be measured, single-mode operation of the dye laser was essential to the requirement of continuum for the hook method. The dye-laser emission spectrum in multi-mode operation displayed strong channeling, probably due to beating between oscillations in longitudinal modes of the optical cavity or between the resonances of parallel surfaces in the optical system. The channeling often obscured the maximum and minimum positions of hooks. Examples of the hook spectrogram taken in the single- and multi-mode operations are shown in Fig.3.

The present apparatus allowed the population measurement with the time resolution of about 5 nsec, the pulse length of the dye laser oscillation, and without being worried by electric noise of the discharge at all.

The population measurements were carried out in the range of t from 0.4 to 20 μsec in the pulsed He discharge

and from 0.5 to 50 μsec in Ne. Table I shows the excited He and Ne levels, whose population density N was measured, the spectral lines λ for the hook measurement, the lasing compounds employed for dye lasers,[9,10] the concentration of the compounds and the observed maximum separation Δ_m of hooks for the each transition. The tabulated values of oscillator strength[11] for the transitions were used to determine N.

To obtain high order fringes of reasonable slopes appropriate to the hook measurement, the optical path difference of 1, 5 and 7 mm was produced between two arms of the interferometer, using quartz plates of 4, 5 and 7 mm in thickness. The hook spectra were photographed with the slit width of 50 μm on Kodak 103a-F plates and Fuji neopan-F films in the first order spectrum for the transition at 3889 Å and in the second order for the other transitions. The exposure time was 5 - 20 sec. The reciprocal linear dispersion was 4.77 Å/mm at 3889 Å in the first order and 1.56 Å/mm at 6402 Å in the second order. Figures 4 (a) and (b) show the temporal variations of the hook spectrum at 3889 Å in He and of the spectra at 6383 and 6402 Å in Ne, respectively.

We observed small hooks near the transitions $2p_5 - 4s_1$" at 5872 Å and $2p_8 - 4d_4$ at 5820 Å only in the range of t from 1.0 to 2.5 μsec in the Ne discharge, but these hooks were too small to be measured. Therefore, the negative-dispersion effect was not taken into account for the transitions in Table I over the whole range of t.

Time-dependent behaviour of the emission lines from the

discharge plasma was also observed to compare with the temporal change in N of the low-lying excited levels measured by the hook method. The emission lines observed are those of the transitions $n^3P - 2^3S$, $n^3D - 2^3P$, $n^1P - 2^1S$ and $n^1D - 2^1P$ in He and np - 1s in Ne. The output signal of a photomultiplier (HTV 1P28) on a 25 cm monochromator (Nikon G-250) was introduced to a boxcar integrator (Princeton Applied Research Model 164 and 162) synchronized with the trigger pulse of discharge and was displayed on a X-Y recorder. The gate width of the integrator was 0.5 μsec.

The electron density n_e at the time t in the He discharge, which would be used in the calculation later on, was estimated from the last discernible line for the transitions $n^3P - 2^3S$, i.e., from the Inglis-Teller relationship.[12] The boxcar-gate was fixed at t and then the higher-member spectrum of the series was observed through the end window of the discharge tube using the 170 cm spectrograph equipped with a photomultiplier (EMI 6256B). An example of the spectrum is shown in Fig.5.

§ 4. Experimental Results

Figure 6 shows the temporal variations of N of the 2^3S and 2^3P levels in the He discharge. It is found that the short-pulsed discharge brings about a characteristic change in N of the excited levels: The concentration N has a sharp peak during the current pulse of discharge and then reaches a high maximum value again in the early stage of afterglow.

The characteristic behaviour of N in He is clearly seen in the variation of hook spectrogram in Fig.4(a).

Figure 7 represents the time-dependent changes in N in the Ne discharge.

Figure 8 shows examples of the temporal change in emission lines from the discharge plasmas. The emission intensities I have also two maxima during the time range concerned.

Figure 9 shows the measured electron density n_e.

§ 5. Calculation

In order to examine the population mechanism governing the characteristic change in N, the electron temperature T_e and N are calculated in the time range from 1.5 to 7.0 μsec for the He discharge at p = 10 Torr. A simple model of the He plasma is employed for the calculation. The rate equations for N in the plasma are described on the only four excited $2^3S,P$ and $3^3P,D$ levels of HeI, where the atomic processes illustrated in Fig.10 are incorporated. The other excited levels and atomic processes are not considered. On the assumption that the relaxation time is very short for the excited levels considered and the plasma is optically thin, we obtain a steady-state solution of the rate equations at t.

In general, the magnitude of Te is of the order of 10^4 K in the positive-column plasma and of 10^3 K or lower in the afterglow plasma. Therefore, the rate coefficients of the atomic processes concerned are first calculated for the range of T_e from 1×10^3 to 6×10^4 K. Here we employ Drawin's

semiempirical formula[13] of the rate coefficients for the electronic collision processes by adjusting cross sections to the published data, the rate coefficient given by Johnson and Geraldo[14] for Penning ionization and those by Phelps[15] for diffusion and molecular formation processes. The rate equations with n_e given in Fig.9 are solved for several values of T_e, and then we decide such a value of T_e at t as the calculated population density N of the 2^3S level coincides with the experimental one.

Figure 11 shows the temporal variation of the calculated electron temperature T_e for the pulsed He discharge at p = 10 Torr. In spite of the simple model of He plasma, T_e shows the plausible value and change as a function of t: The high electron temperature T_e of about 3.3×10^4 K decreases with the fast decrease of discharge current, changes slowly in the time range from 3 to 4 μsec where the damping current exists (see Fig.1) and then falls rapidly to the order of 10^3 K in the afterglow region.

The calculated population density N in the same discharge is shown in Fig.12. The calculated and experimental values of N of the 2^3P level are in fairly good agreement in temporal change as well as in absolute value. The higher excited 3^3P and ^3D levels have also two maxima of N in the time range of interest, but the time-dependent behaviours do not always reappear the experimental changes in the emission intensities at 3889 Å ($3^3P - 2^3S$) and at 5876 Å ($3^3D - 2^3P$) shown in Fig.8. The disagreement between the temporal changes in N and these

emissions is mainly owing to the large imprisonment effect of radiation on the line intensity measurements, rather than owing to the uncertainty in the calculation based on the simple model of He plasma. According to Holstein's theory on the imprisonment effect,[16] for example, N of 3×10^{13} cm^{-3} of the 2^3S level and N of 7×10^{12} cm^{-3} of the 2^3P level reduce the line intensities at 3889 and 5876 Å from the He plasma by about an order of magnitude and by about two order, respectively, in comparison with the intensities expected in the optically thin case. Therefore, the maxima of the emission intensity observed are displaced from the actual population maxima of upper levels of emission lines.

§ 6. Discussion

To investigate the dominant atomic processes in the time range of interest, the temporal changes in the ratio of population and depopulation rates for the $2^3S,P$ and 3^3D levels are shown in Figs.13(a) and (b), respectively.

In the range of t from 1.5 to 3 μsec where n_e ranges from 1.3×10^{16} to 2.8×10^{15} cm^{-3}, the following balance nearly holds for the 2^3S and 2^3P levels, respectively,

$$C_{01}n_eN_0 + F_{21}n_eN_2 = C_{12}n_eN_1, \tag{6.1}$$

$$C_{12}n_eN_1 = F_{21}n_eN_2 + C_{23}n_eN_2, \tag{6.2}$$

where the numerals 0,1,2 and 3 indicate the 1^1S, 2^3S, 2^3P and 3^3D levels, respectively, N_i is the population density of level i, C_{ij} is the rate coefficient for electonic exci-

tation from level i to level j, and F_{ji} is the rate coefficient for electronic deexcitation from level j to level i. The eqs.(6.1) and (6.2) lead to

$$N_1 = \frac{C_{01}}{C_{12}}(1 + \frac{F_{21}}{C_{23}})N_0 \approx \frac{C_{01}}{C_{23}} \frac{F_{21}}{C_{12}} N_0$$

$$= \frac{C_{01}}{C_{23}} N_0 \frac{g_1}{g_2} \exp(\frac{E_{12}}{kT_e}), \qquad (6.3)$$

$$N_2 = \frac{C_{01}}{C_{23}} N_0, \qquad (6.4)$$

respectively, where E_{12} is the excitation energy of about 20 eV from the level 1 to the level 2, and g_i is the statistical weight of level i. As T_e decreases from 3.3 to 1.1 x 10^4 K in the time range of interest, C_{01}/C_{23} decreases rapidly (see Table II in Appendix) in contrast to the slow increasing function of $\exp(E_{12}/kT_e)$. Therefore, it is explained that the first decrease of N_1 in this time range is due to the decrease of T_e accompanied with the rapid decrease of electronic excitation rate from the ground state.

In the afterglow region of t from 3 to 7 μsec where T_e ranges from 1.1 to 0.27 x 10^4 K, the similar consideration shows the population mechanisms of the excited He levels as follows. As is seen in Fig.13, the dominant processes to populate and depopulate the metastable 2^3S level are the electronic excitation and deexcitation from and to the 2^3P level, respectively, but the rates of these opposite processes nearly balance. Therefore, the 2^3S level is mainly populated

and increased by the radiative cascade from higher excited levels. As is also seen in the figure, the higher excited levels such as 3^3P and ^3D are populated by the recombination processes of ions and electrons in this time range.

Figures 7(a) and 8 represent the similar temporal changes in N and emission in Ne to those in He, respectively. The same mechanisms as in the He plasma may be dominant to populate the excited Ne levels during the current pulse and in the afterglow region of interest in the Ne discharge.

The metastable He atoms or other metastable rare-gas atoms are often produced by a pulsed discharge in the afterglow experiment, atomic-beam experiment and so on. The present experiment and analysis suggest the method for effective production of large number density of the metastables by means of the pulsed discharge. A transient discharge plasma with high electron density n_e and subsequent rapid decrease of T_e produces high density of the metastables, as is discussed above, by the radiative cascade process of higher-excited atoms resulting from the recombination of ions and electrons.

Acknowledgement

The authors wish to express their thanks to Dr. T.Fujimoto for his help in construction of the experimental apparatus and to Mr. Y.Tomita and Mr. S.Watanabe for their assistance in performing the experiment.

Appendix

In Table II are presented the rate coefficients calculated for the electronic collision processes in the range of T_e from 1×10^3 to 6×10^4 K. Here the numerals 0, 1, 2, 3 and 4 indicate the 1^1S, 2^3S, 2^3P 3^3D and 3^3P levels of HeI, respectively, and

C_{ij}: the rate coefficient for the electronic excitation from level i to level j in the unit of cm^3sec^{-1},

S_i: the rate coefficient for the ionization from level i by the electron collisions in cm^3sec^{-1},

α_i: the rate coefficient for the radiative recombination of electron and He ion to level i in cm^3sec^{-1},

β_i: the rate coefficient for the three body recombination of electrons and He ion to level i in cm^6sec^{-1}.

The rate coefficient β_4 which is not included in the table is given by $\beta_4 = (3/5)\beta_3$.

The rate coefficient F_{ji} for the inverse process of C_{ij}, i.e., the electronic deexcitation, may be derived from the principle of detailed balance:

$$F_{ji} = C_{ij} \frac{g_i}{g_j} \exp(E_{ij}/kT_e),$$

where E_{ij} is the excitation energy from level i to level j.

References

1) M.C.E.Huber: Modern Optical Methods in Gas Dynamic Research, ed. D.S.Dosanjh (Plenum Press, New York, 1971) p.85.

2) N.P.Penkin: J. quant. Spectrosc. radiative Transfer 4 (1964) 41.

3) T.Fujimoto, K.Miyazaki and K.Fukuda: J. quant. Spectrosc. radiative Transfer 14 (1974) 377.

4) K.Miyazaki, Y.Ogata, T.Fujimoto and K.Fukuda: Japan. J. appl. Phys. 13 (1974) 1866.

5) K.Miyazaki, T.Watanabe and K.Fukuda: J. Phys. Soc. Japan 40 (1976) 233.

6) K.Miyazaki, R.Nakata, Y.Tomita, M.Suemitsu, S.Watanabe and K.Fukuda: Japan. J. appl. Phys. 14 (1975) 1075.

7) S.A.Kopff and G.Breit: Rev. mod. Phys. 4 (1932) 471.

8) W.C.Marlow: Appl. Optics 6 (1967) 1715.

9) K.H.Drexhage: Dye Lasers, ed. F.P.Schäfer (Springer-Verlag, New York, 1973) p.144.

10) C.E.Moeller, C.M.Verber and A.H.Adelman: Appl. Phys. Letters 18 (1971) 278.

11) W.L.Wiese, M.W.Smith and B.M.Glennon: Atomic Transition Probabilities (U.S.Government Printing Office, Washington, 1966) Vol.I.

12) D.R.Inglis and E.Teller: Astrophys. J. 90 (1939) 439.

13) H.W.Drawin: EUR-CEA-FC 383 (revised) Report (1967).

14) A.W.Johnson and J.B.Gerardo: Phys. Rev. A 7 (1973) 925.

15) A.V.Phelps: Phys. Rev. 99 (1955) 1307.

16) T.Holstein: Phys. Rev. 83 (1951) 1159.

Figure captions

Fig.1. Current wave form of the He discharge at p = 10 Torr and V = 12 kV.

Fig.2. Schematic diagram of the experimental arrangement.

Fig.3. Examples of the hook spectrogram taken in (a) single mode and (b) multi-mode operations of the dye laser. (a): the second order spectrum. (b): the first order spectrum.

Fig.4. Temporal variations of the hook spectrogram. (a): photographs in He at p = 10 Torr and V = 12 kV. (b): photographs in Ne at p = 15 Torr and V = 12 kV.

Fig.5. Emission spectrum of higher members for the transitions $n^3P - 2^3S$ in He.

Fig.6. Temporal variations of population density of the 2^3S and 2^3P levels in He. (a): p = 10 Torr and V = 12 kV. (b): p = 15 Torr and V = 15 kV.

Fig.7. Temporal variations of population density of the low-lying excited levels in Ne. (a): p = 10 Torr and V = 12 kV. (b): p = 15 Torr and V = 12 kV.

Fig.8. Temporal changes in the intensity of emissions from the pulsed discharges.

Fig.9. Temporal variation of the measured electron density in the pulsed He discharge at p = 10 Torr and V = 12 kV.

Fig.10. The He levels and atomic processes considered in the calculation. The solid lines indicate electronic collision processes: excitation, deexcitation,

ionization and three-body recombination. The dashed lines are the radiative processes: radiative cascade and recombination. p, d and m are Penning ionization, diffusion and molecular formation processes, respectively.

Fig.11. Temporal variation of the calculated electron temperature in the pulsed He discharge at p = 10 Torr and V = 12 kV.

Fig.12. Temporal variations of the calculated population density of the excited He levels. The measured population density is plotted for comparison. The discharge condition is the same as in Fig.11.

Fig.13. Temporal changes in the ratio of the calculated rates for (a) the population to and (b) the depopulation from the indicated levels. A: radiative transition. p: Penning ionization. He^+: ionization in (a) and recombination in (b). Otherwise: transitions by electron collisions. The discharge condition is the same as in Fig.11.

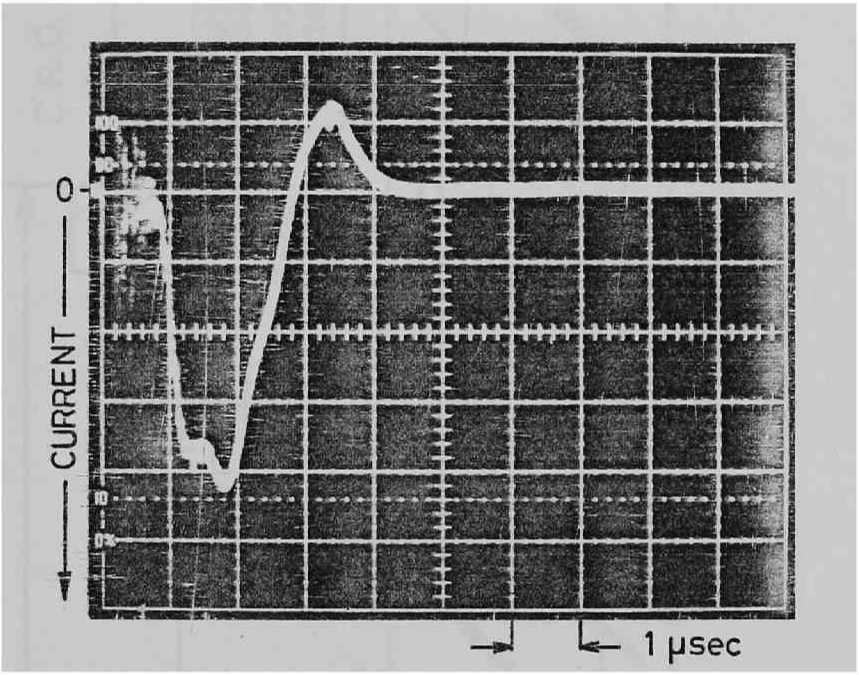

Fig.1

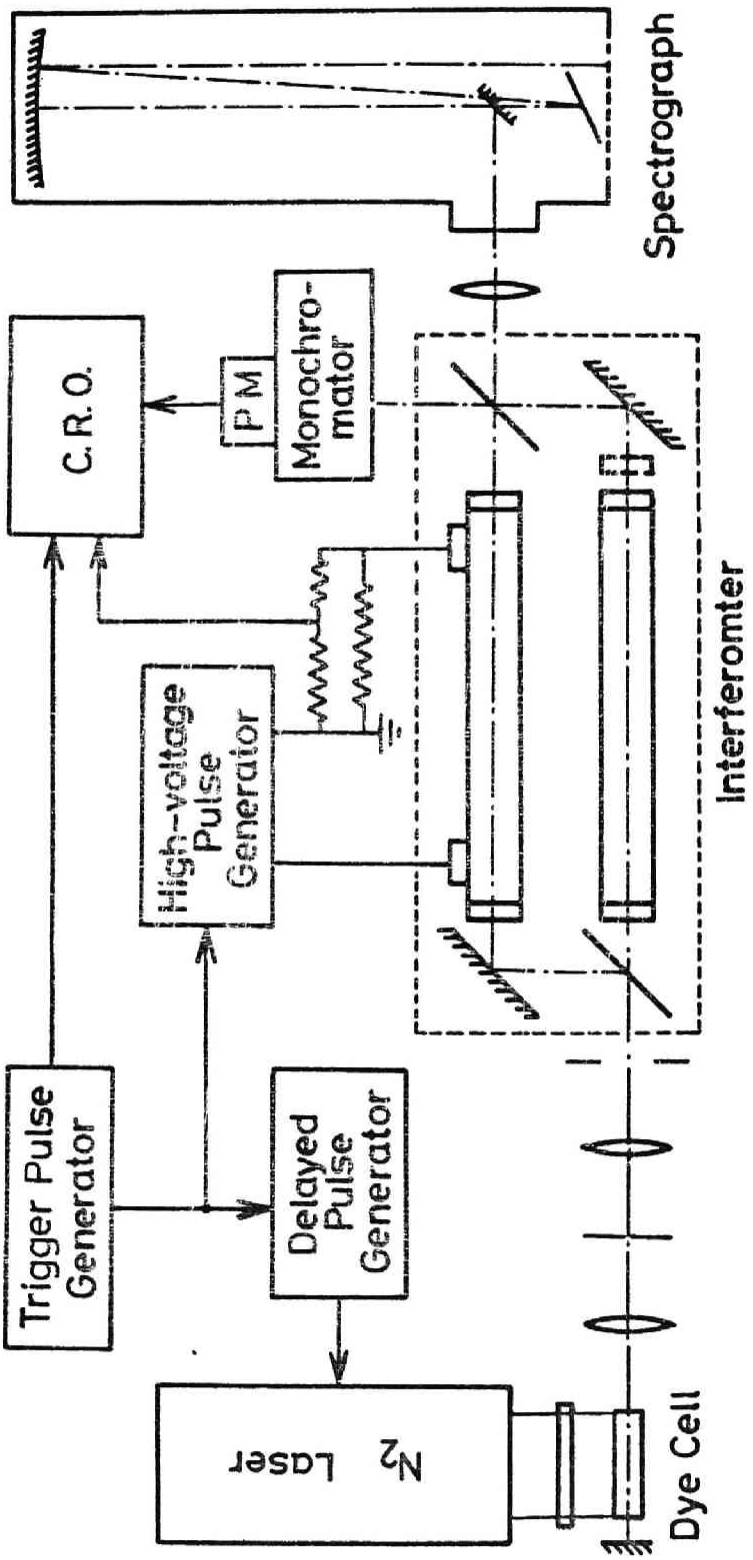
Spectrograph
C.R.O.
PM
Monochro-
mator
High-voltage
Pulse
Generator
Interferomter
Trigger Pulse
Generator
Delayed
Pulse
Generator
N2 Laser
Dye Cell

Fig.2

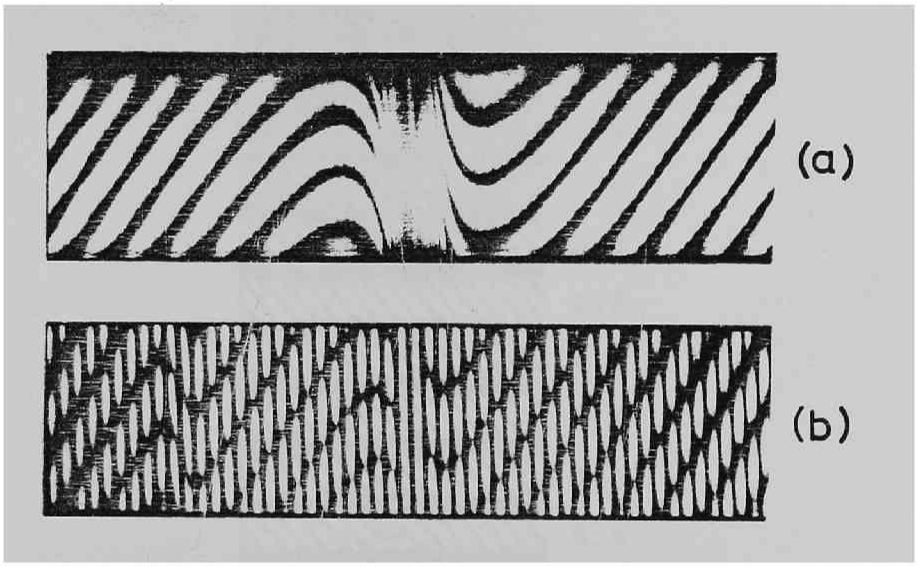

Fig.3

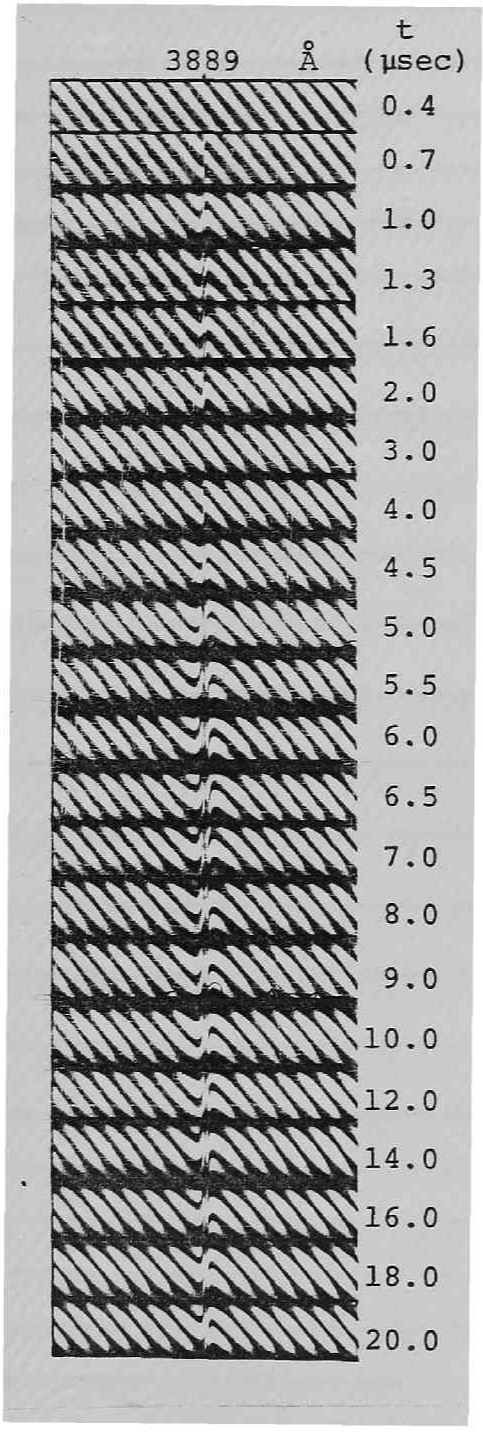
3889 Å
t
(μsec)
0.4
0.7
1.0
1.3
1.6
2.0
3.0
4.0
4.5
5.0
5.5
6.0
6.5
7.0
8.0
9.0
10.0
12.0
14.0
16.0
18.0
20.0

Fig.4(a)

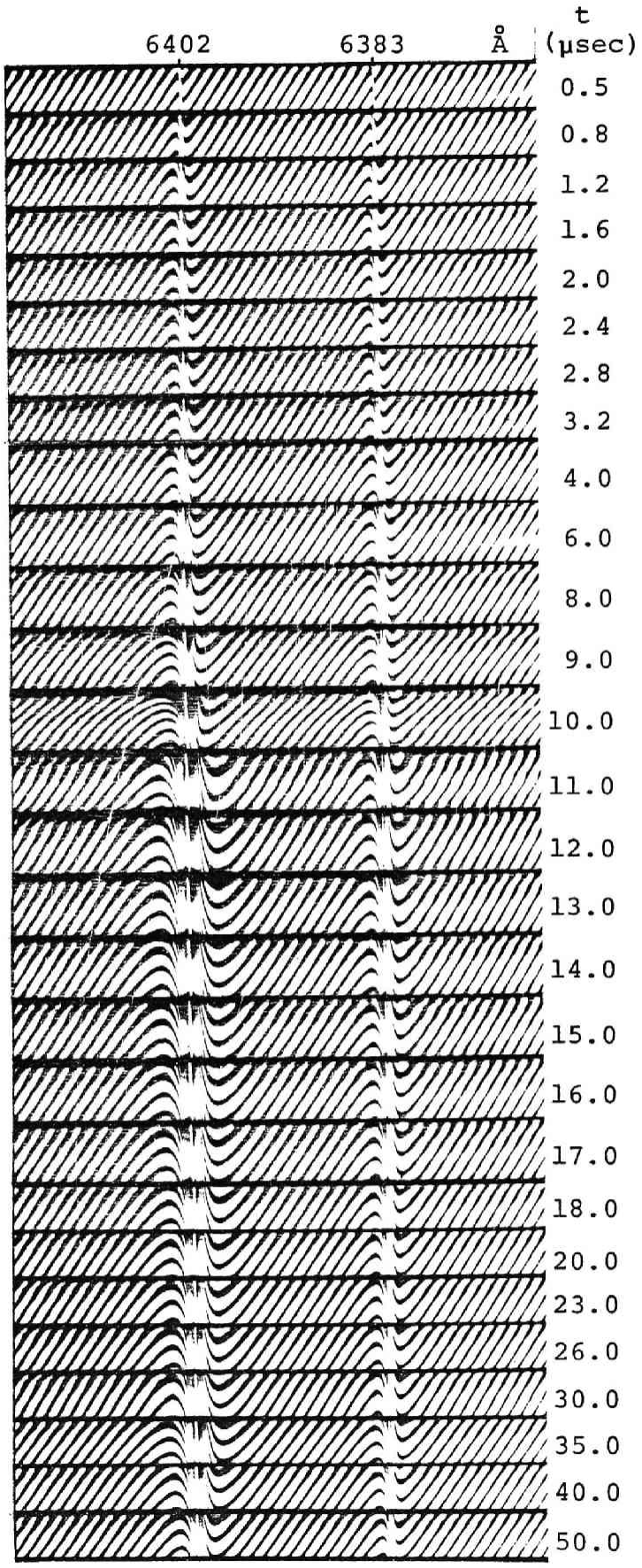
6402
6383
Å
t
(μsec)
0.5
0.8
1.2
1.6
2.0
2.4
2.8
3.2
4.0
6.0
8.0
9.0
10.0
11.0
12.0
13.0
14.0
15.0
16.0
17.0
18.0
20.0
23.0
26.0
30.0
35.0
40.0
50.0

Fig.4(b)

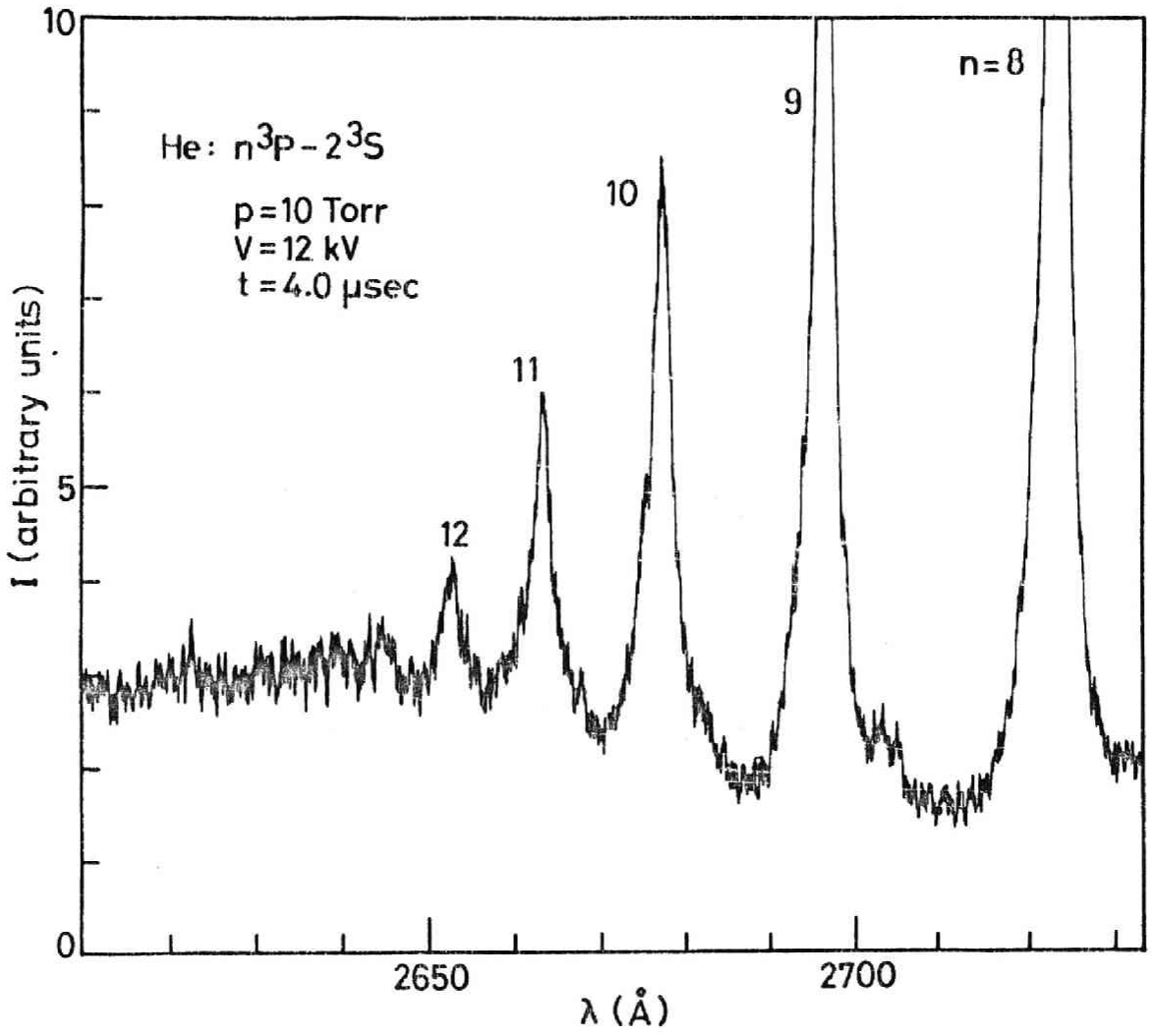
10
5
0
I (arbitrary units)
He: n³P - 2³S
p = 10 Torr
V = 12 kV
t = 4.0 μsec
12
11
10
9
n = 8
2650
2700
λ (Å)

Fig.5

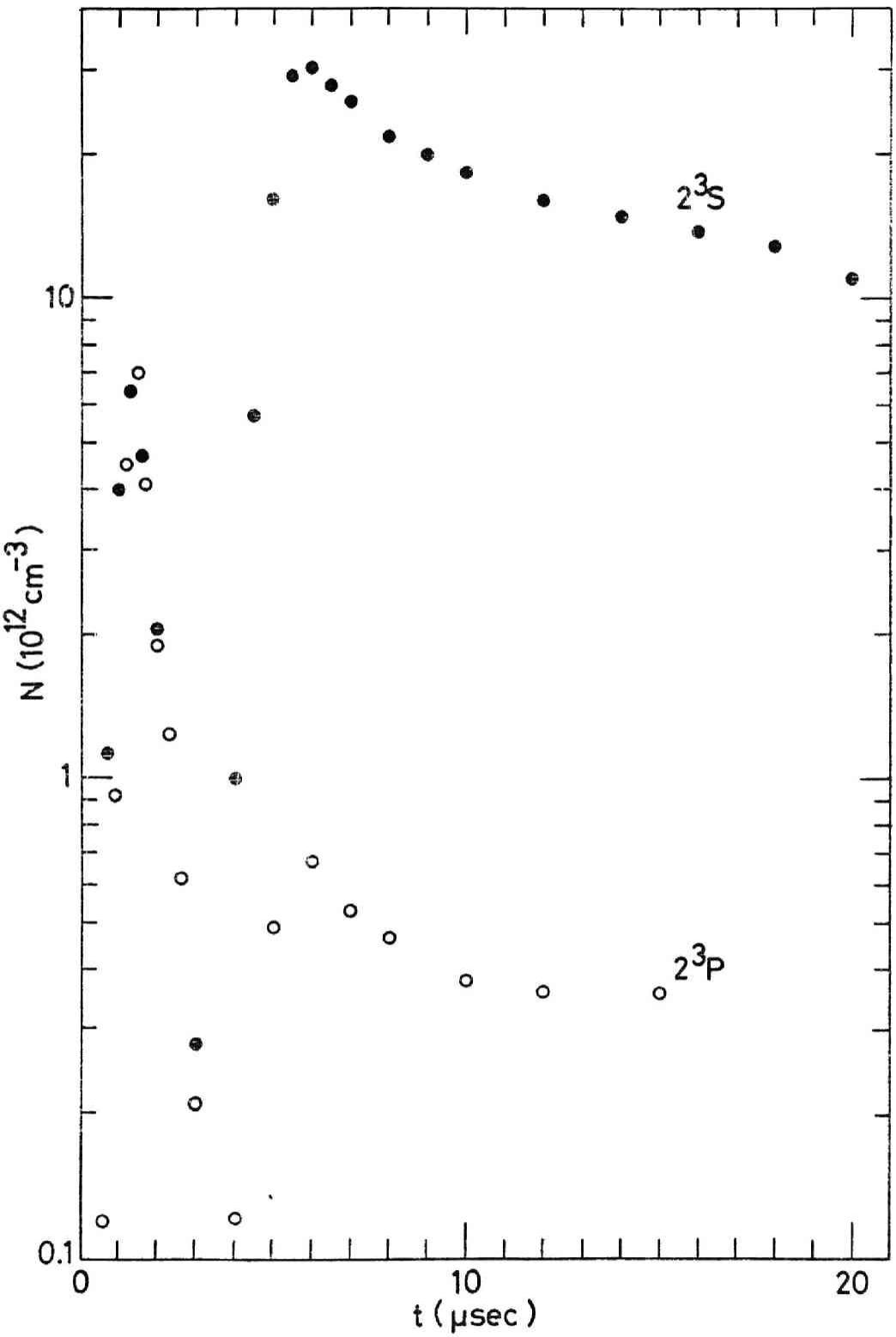

Fig.6(a)

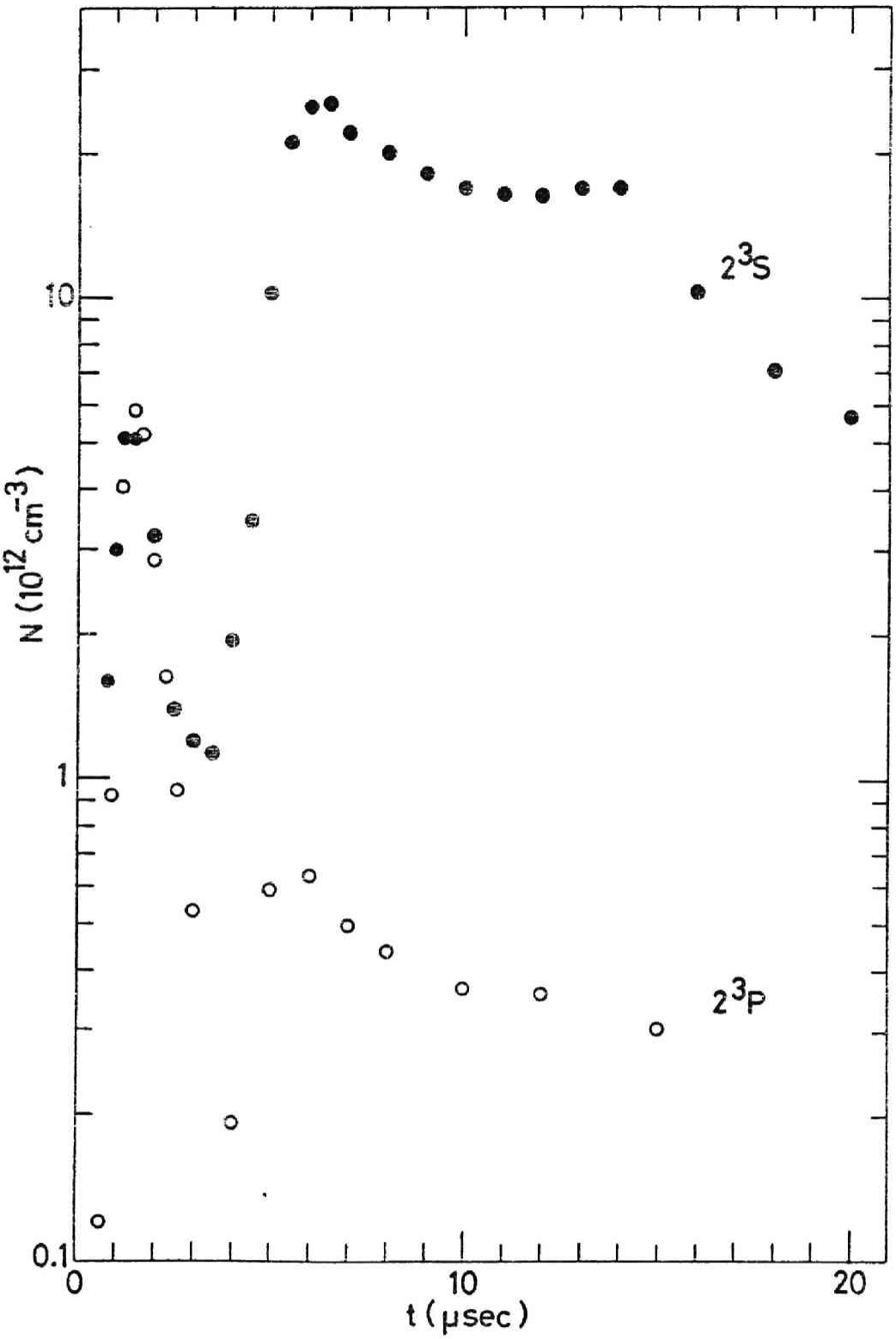

Fig.6(b)

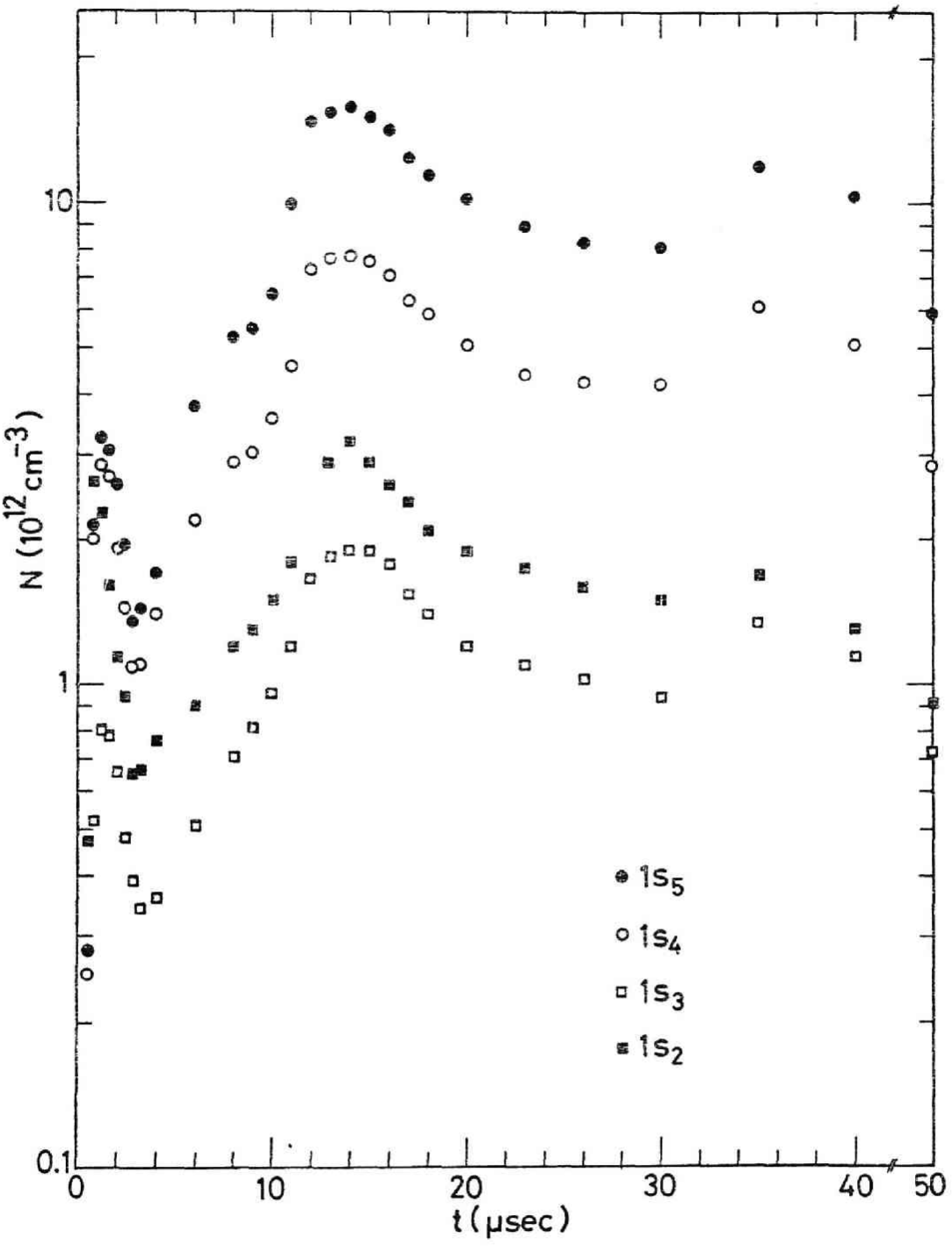

Fig.7(a)

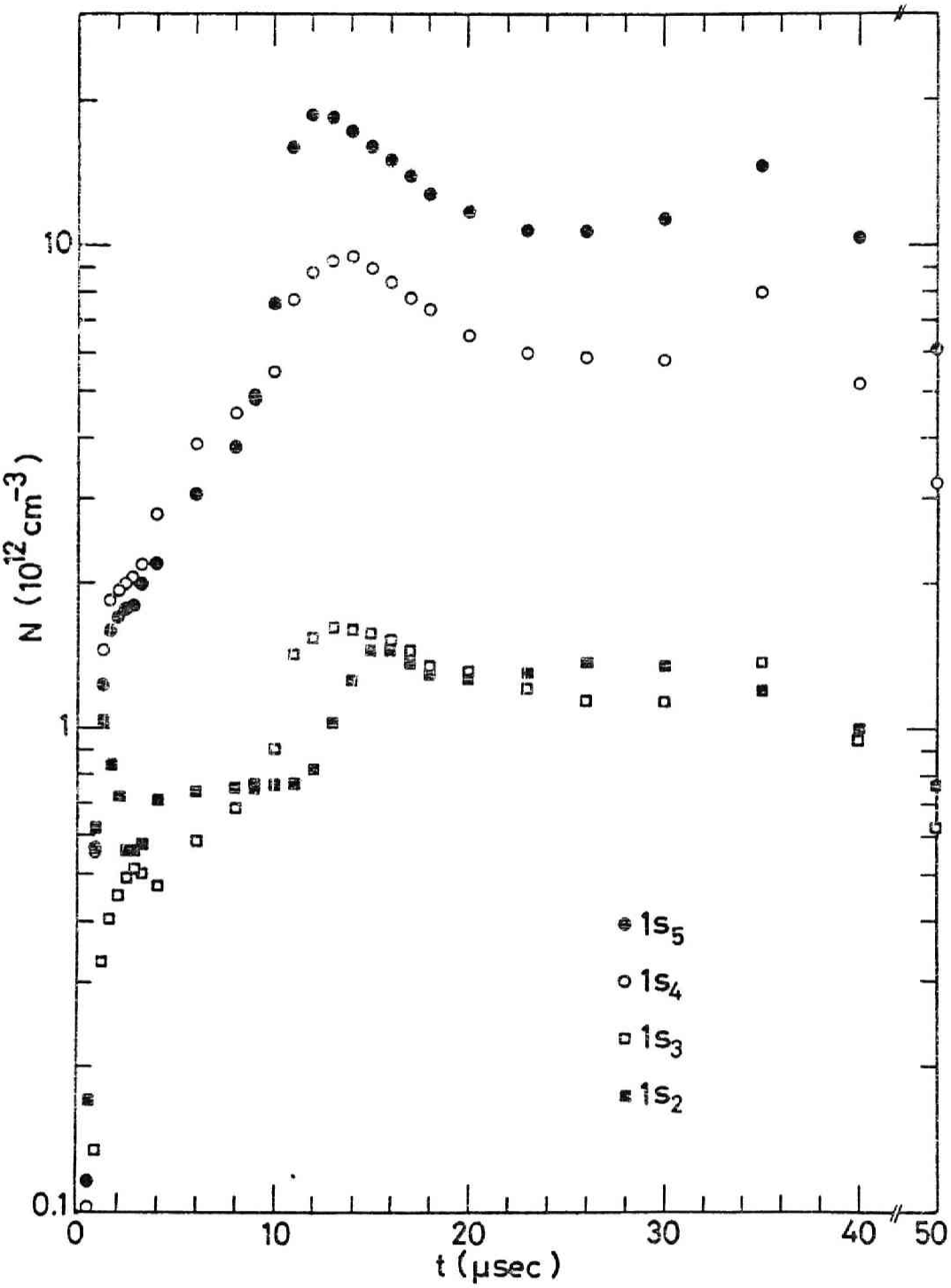

Fig.7(b)

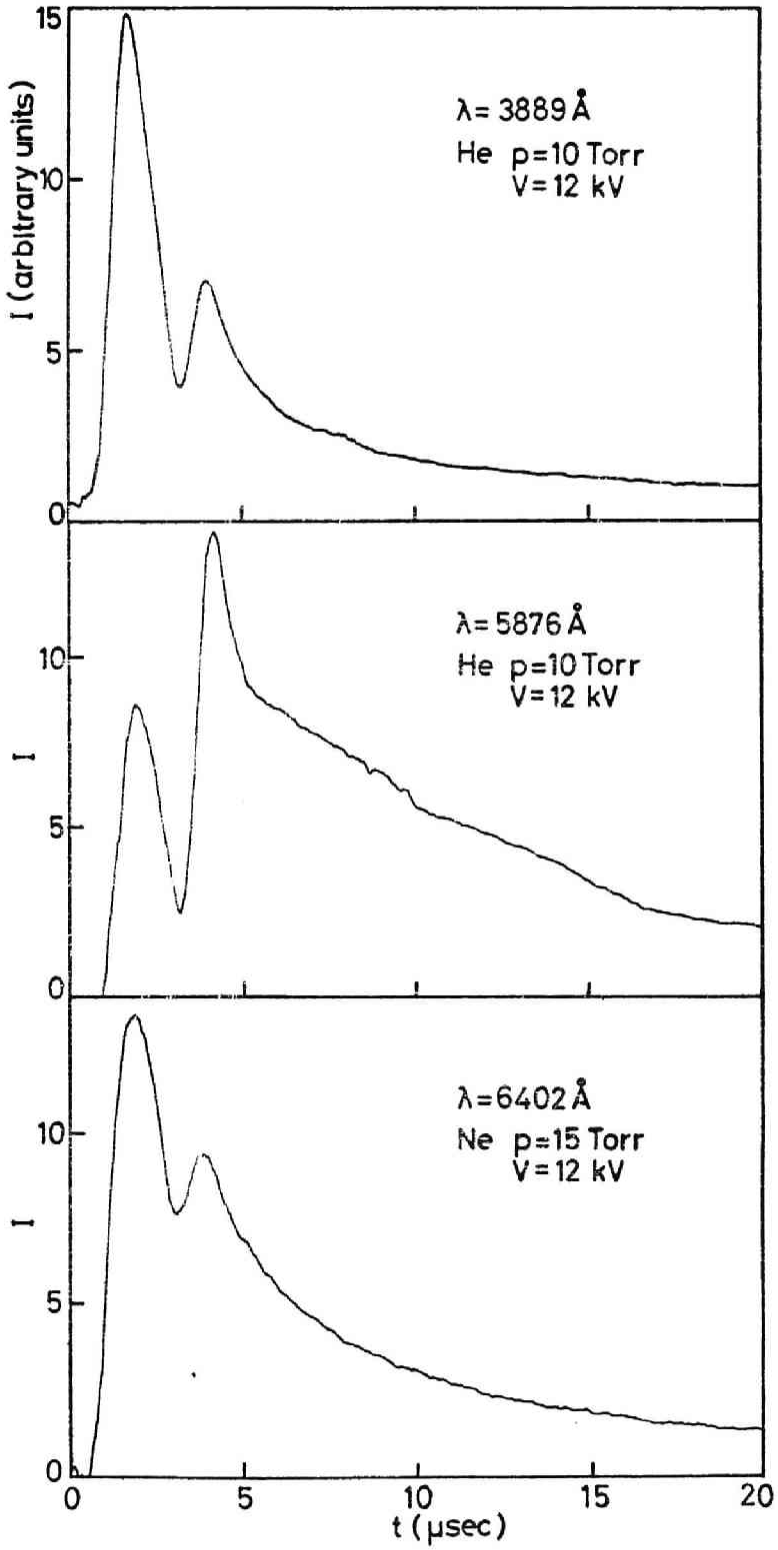
I (arbitrary units)
λ= 3889 Å
He p=10 Torr
V=12 kV
λ= 5876 Å
He p=10 Torr
V=12 kV
λ=6402 Å
Ne p=15 Torr
V=12 kV
I
t (μsec)
0
5
10
15
20

Fig.8

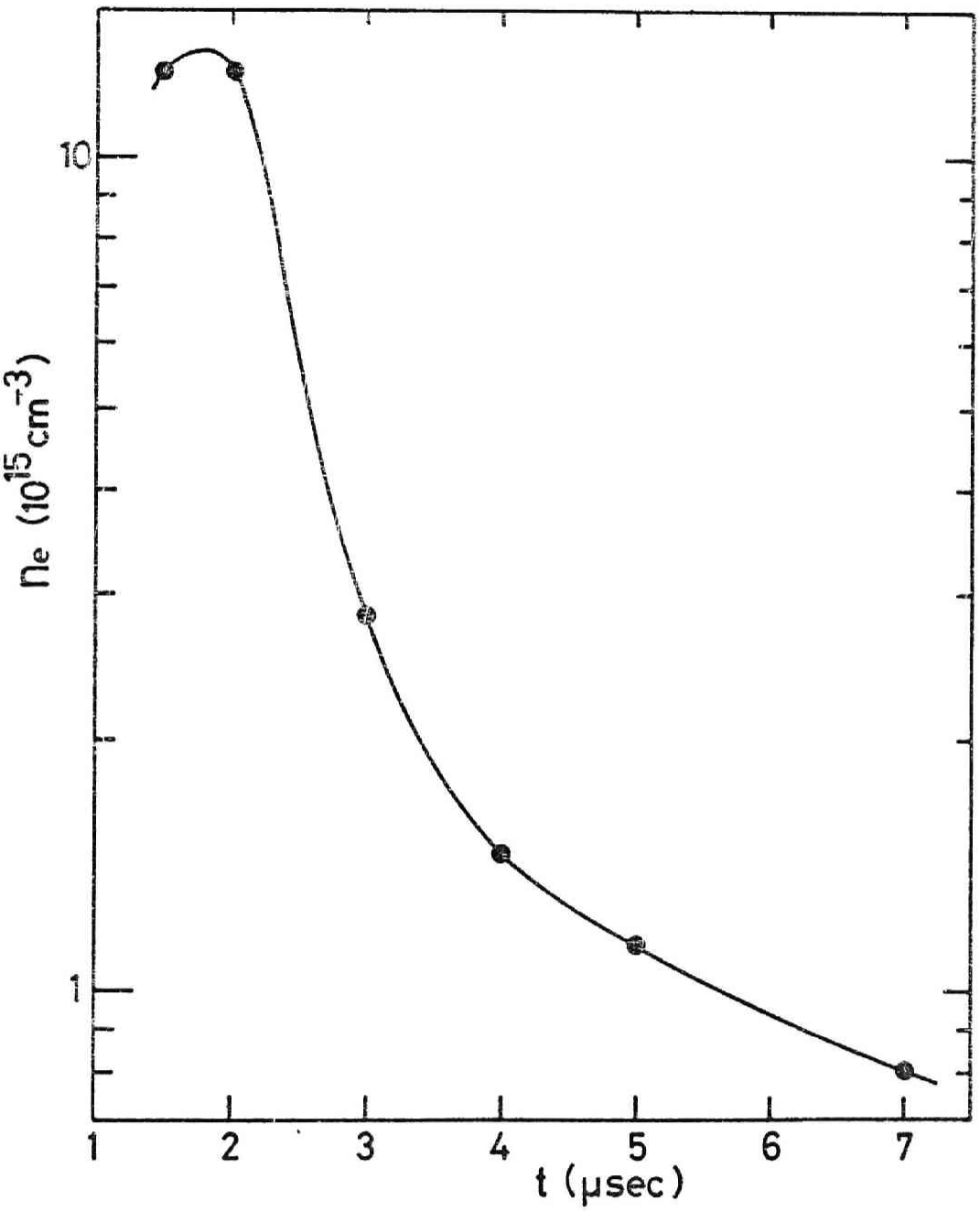

Fig.9

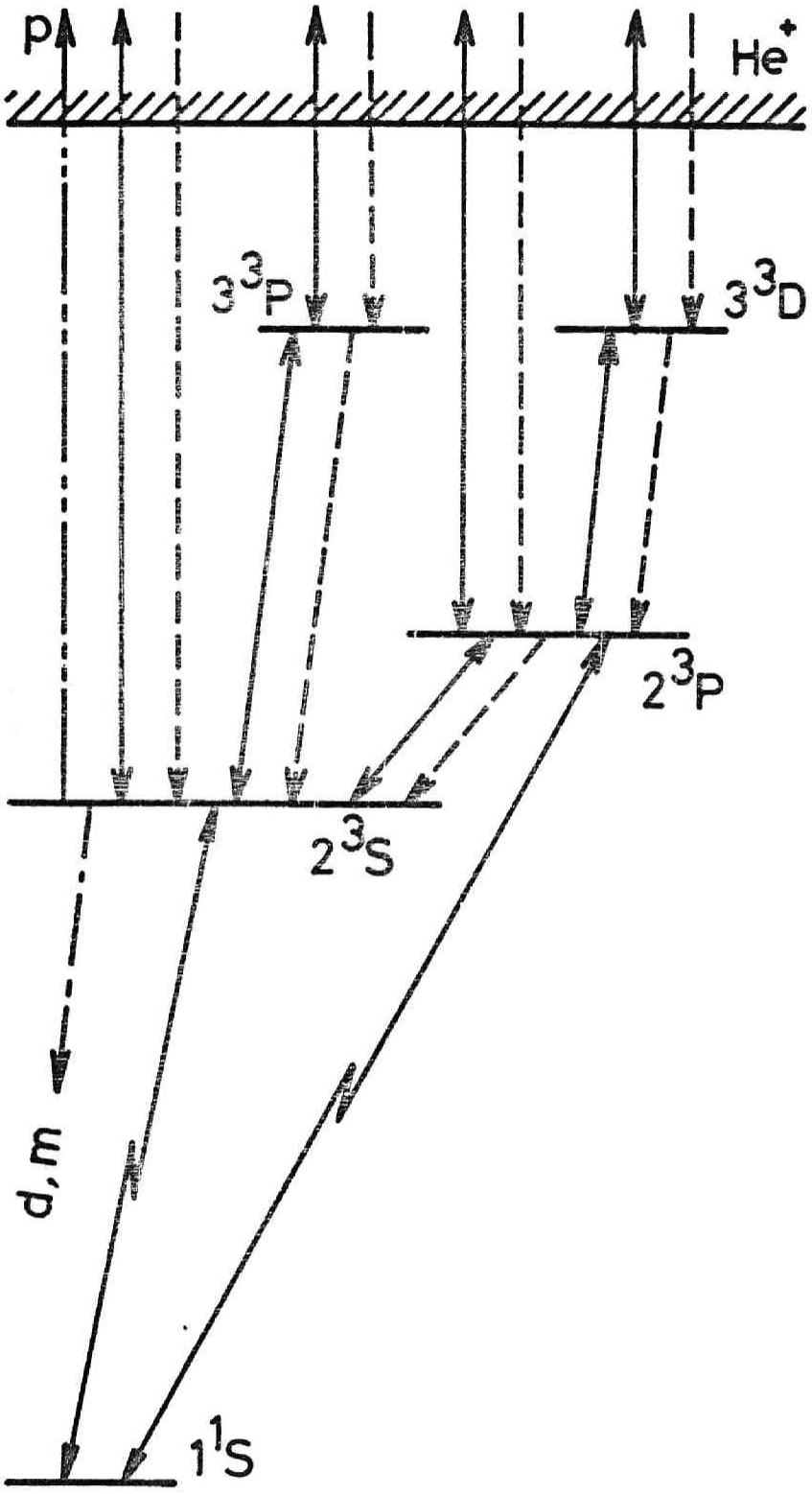

Fig.10

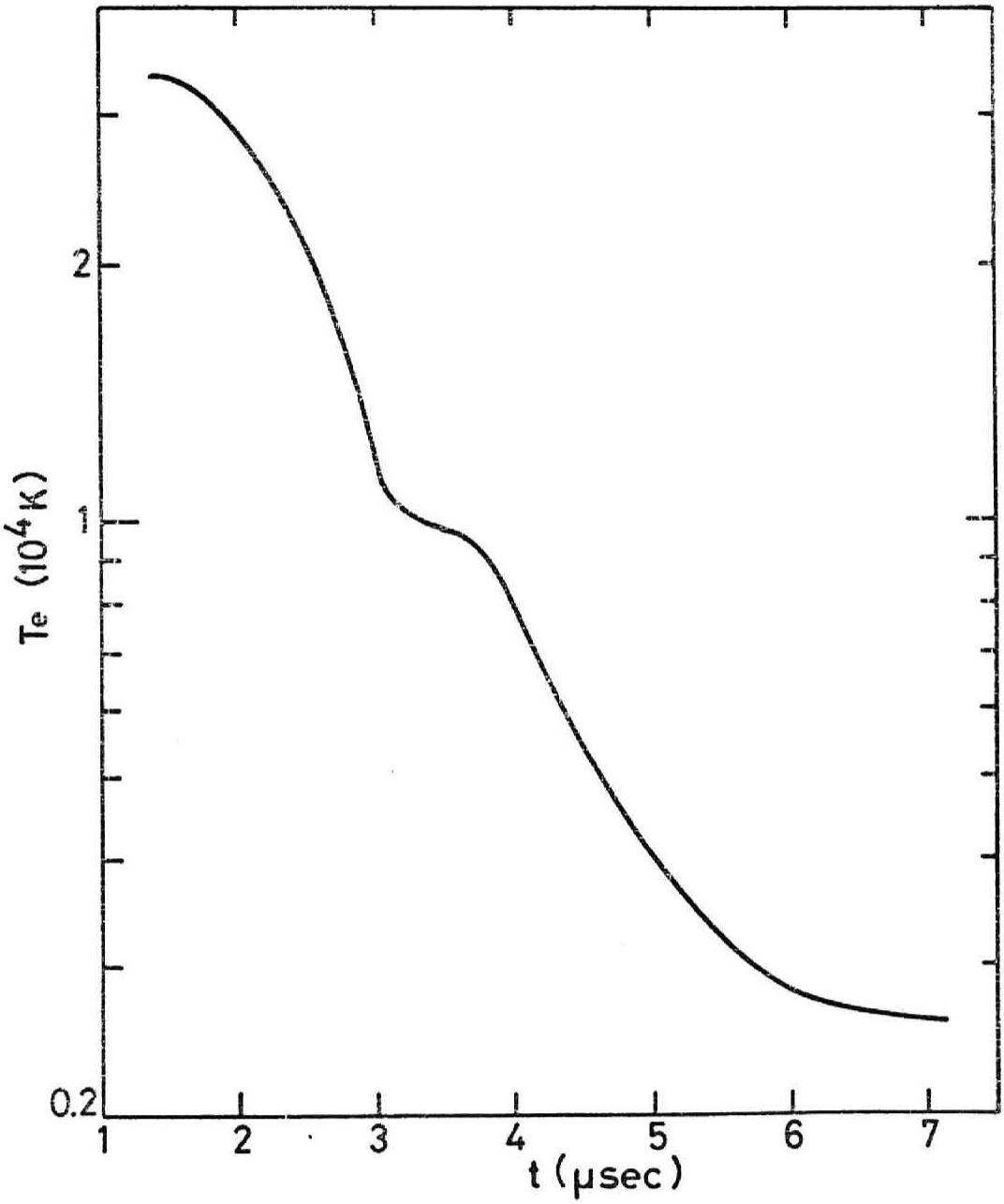

Fig.11

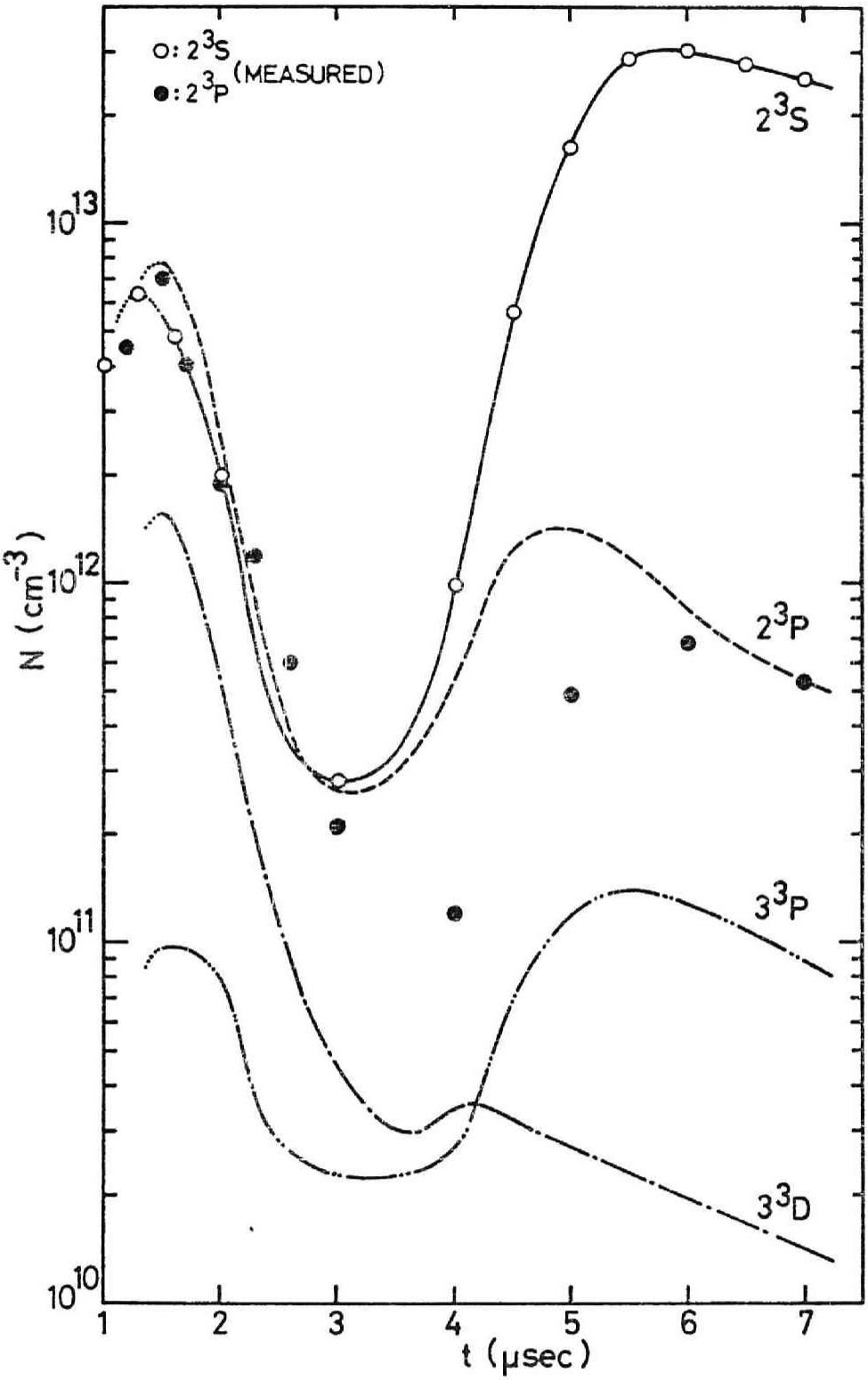
o: 2³S
●: 2³P (MEASURED)
2³S
2³P
3³P
3³D
N (cm⁻³)
10¹³
10¹²
10¹¹
10¹⁰
1
2
3
4
5
6
7
t (μsec)

Fig.12

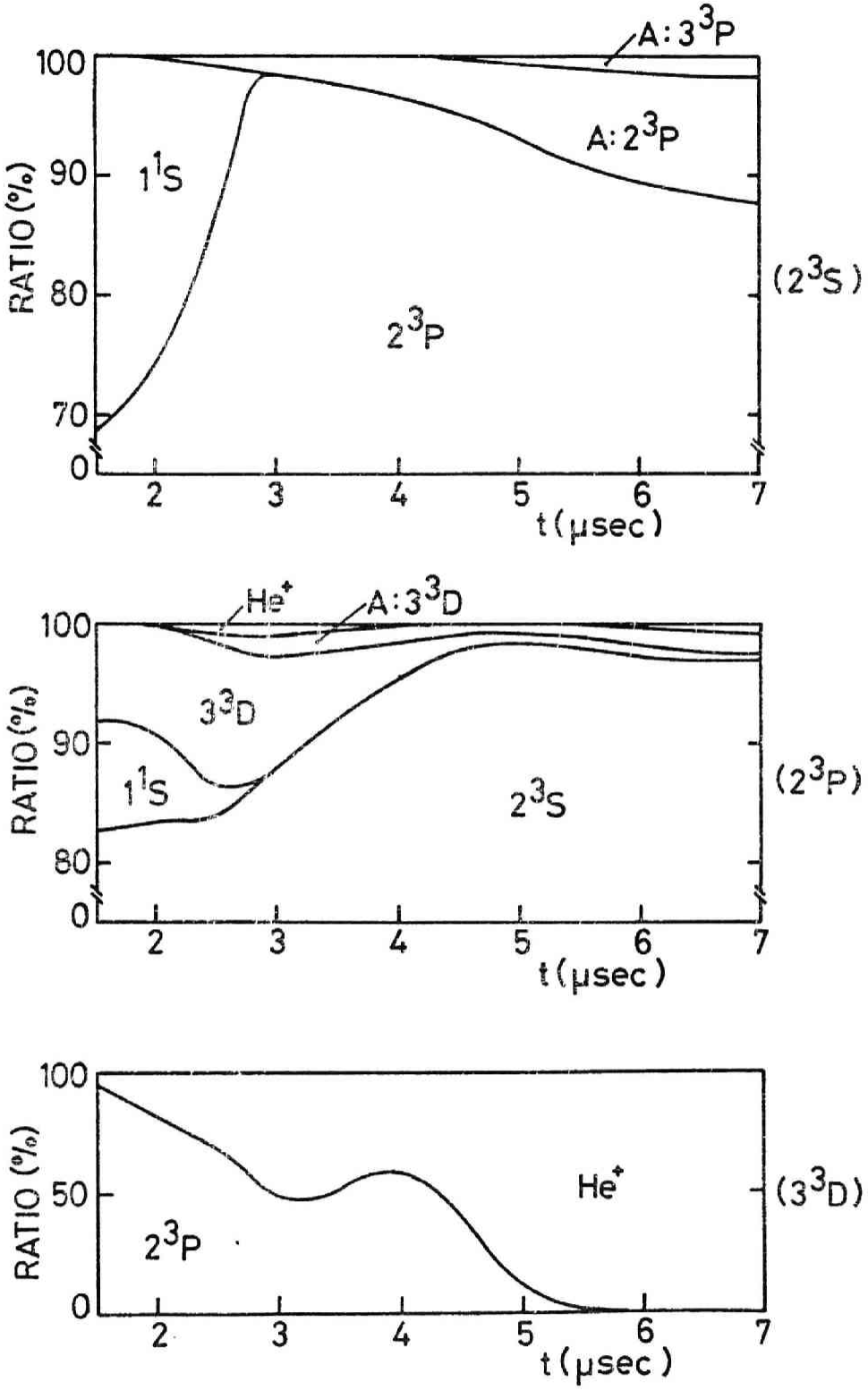
A:3³P
100
A:2³P
1¹S
90
RATIO(%)
80
(2³S)
2³P
70
0
2
3
4
5
6
7
t(μsec)
He⁺
A:3³D
100
3³D
90
1¹S
2³S
(2³P)
RATIO(%)
80
0
2
3
4
5
6
7
t(μsec)
100
He⁺
(3³D)
50
2³P
RATIO (%)
0
2
3
4
5
6
7
t(μsec)

Fig.13(a)

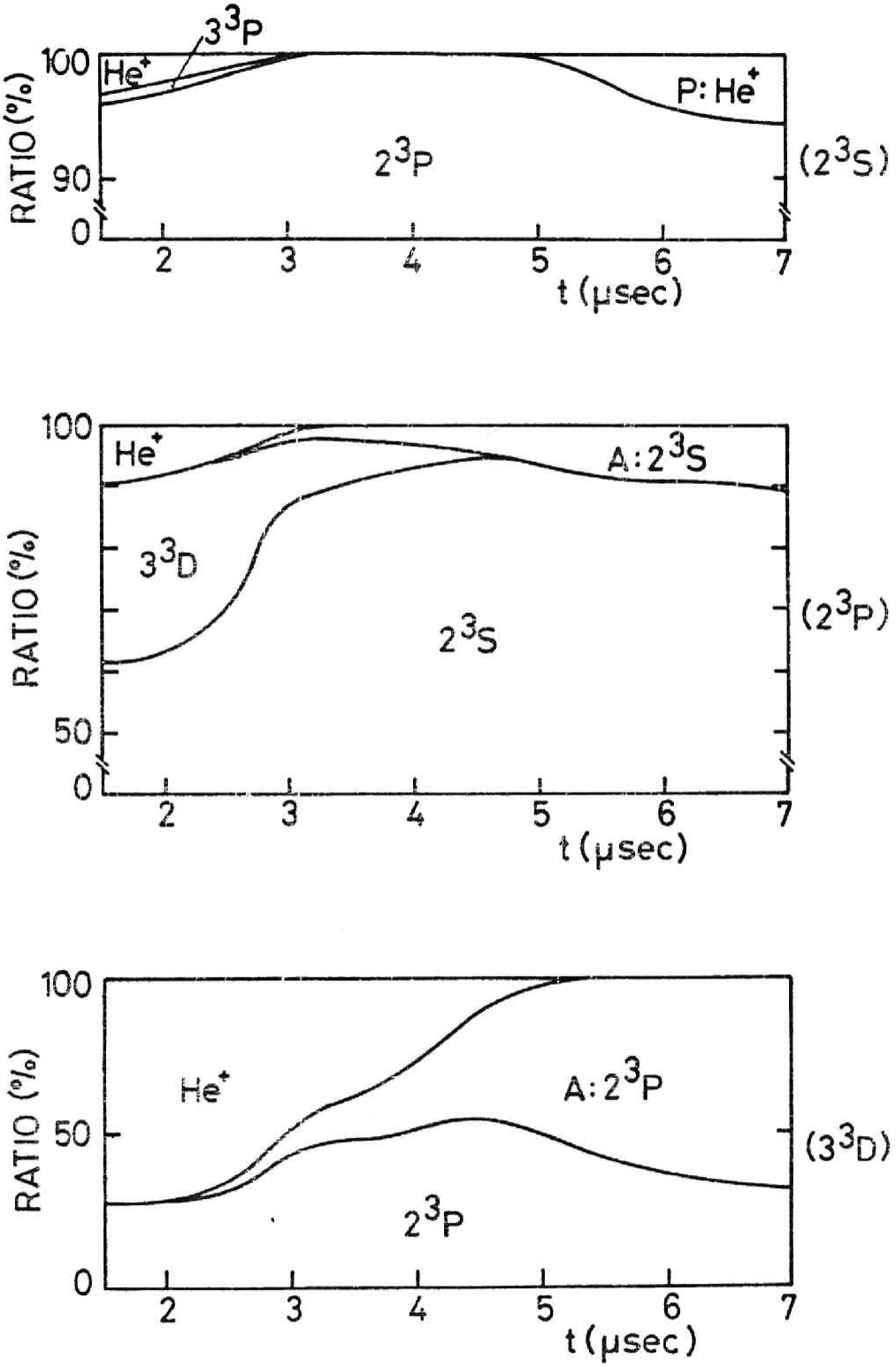
3³P
100
He⁺
P: He⁺
RATIO (%)
90
2³P
(2³S)
0
2
3
4
5
6
7
t (μsec)
100
He⁺
A: 2³S
3³D
RATIO (%)
2³S
(2³P)
50
0
2
3
4
5
6
7
t (μsec)
100
He⁺
A: 2³P
RATIO (%)
50
(3³D)
2³P
0
2
3
4
5
6
7
t (μsec)

Fig.13(b)

Table I. Data on the hook measurement. Solvent (a): dioxane and (b): ethanol. Δ_m: observed maximam hook separation.

	Level	λ(Å)	Transition	Compound(solvent)	Concentration (mol/l)	Δ_m(Å)
He	2^3S	3889	$2^3S - 3^3P$	BBD (a)	2×10^{-3}	2.8
	2^3P	5876	$2^3P - 3^3D$	Rhodamine 6G (b)	5×10^{-3}	4.3
Ne	(Paschen) $1s_2$	5852	$1s_2 - 2p_1$	Rhodamine 6G (b)	3×10^{-3}	1.3
	$1s_3$	6266	$1s_3 - 2p_5$	Cresyl violet (b)	1×10^{-4}	1.7
				(Rhodamine 6G*)	(5×10^{-3})	
	$1s_4$	6383	$1s_4 - 2p_7$	Cresyl violet (b)	1×10^{-4}	2.7
				(Rhodamine 6G*)	(5×10^{-3})	
	$1s_5$	6402	$1s_5 - 2p_9$	Cresyl violet (b)	1×10^{-4}	5.5
				(Rhodamine 6G*)	(5×10^{-3})	

* Rhodamine 6G is mixed in the solution as the intermediary dye for the cresyl-violet dye laser.[10)]

Table II. The rate coefficients for electronic collision processes.

T_e(K)	1000	3000	5000	6000	8000	10000	11000	13000	16000
C_{01}	——	——	1.5(29)	4.90(26)	1.19(21)	3.48(19)	3.10(18)	7.73(17)	2.05(15)
C_{02}	——	——	2.5(31)	3.4(27)	9.89(23)	5.56(20)	1.21(18)	1.33(17)	4.58(16)
C_{12}	2.6(13)	4.16(9)	3.22(8)	5.75(8)	1.20(7)	1.82(7)	2.09(7)	2.69(7)	3.44(7)
C_{14}	1.7(25)	1.95(14)	3.65(12)	1.37(11)	8.56(11)	2.31(10)	3.57(10)	6.88(10)	1.27(9)
C_{23}	1.0(18)	3.01(11)	1.04(9)	2.62(9)	9.09(9)	1.90(8)	2.53(8)	4.13(8)	6.32(8)
S_1	2.0(32)	2.31(16)	5.63(13)	4.12(12)	4.63(11)	2.07(10)	3.53(10)	1.12(9)	2.32(9)
S_2	9.9(27)	3.44(14)	1.36(11)	6.22(11)	4.53(10)	1.47(9)	2.30(9)	5.50(9)	9.89(9)
S_3, S_4	2.2(15)	7.66(10)	1.19(8)	2.46(8)	6.26(8)	1.15(7)	1.39(7)	2.02(7)	2.77(7)
α_1	4.3(14)	2.46(14)	1.91(14)	1.74(14)	1.51(14)	1.35(14)	1.29(14)	1.18(14)	1.07(14)
α_2	1.7(13)	1.25(13)	9.11(14)	8.00(14)	7.13(14)	5.92(14)	5.61(14)	5.00(14)	4.26(14)
α_3, α_4	1.2(13)	7.90(14)	5.60(14)	5.05(14)	4.18(14)	3.44(14)	3.23(14)	2.94(14)	2.48(14)
β_1	2.2(28)	6.60(29)	3.86(29)	3.29(29)	2.30(29)	1.80(29)	1.65(29)	1.40(29)	1.13(29)
β_2	5.6(28)	2.90(28)	1.99(28)	1.65(28)	1.30(28)	1.02(28)	9.39(29)	7.80(29)	6.33(29)
β_3	4.6(27)	2.87(27)	1.90(27)	1.63(27)	1.28(27)	1.07(27)	9.57(28)	8.42(28)	6.49(28)

R_1 1.2.10(18) = 3.10 x 10^{-18}

Table II. (continued)

T_e(K)	19000	24000	30000	33000	40000	50000	60000
C_{01}	2.02(14)	2.46(13)	1.66(12)	3.58(12)	1.16(11)	3.53(11)	7.01(11)
C_{02}	5.13(15)	7.51(14)	5.83(13)	1.23(12)	4.29(12)	1.46(11)	2.99(11)
C_{12}	4.06(7)	5.22(7)	6.22(7)	6.73(7)	7.35(7)	8.33(7)	8.63(7)
C_{14}	2.14(9)	3.56(9)	5.41(9)	6.12(9)	7.78(9)	9.95(9)	1.20(8)
C_{23}	8.83(8)	1.20(7)	1.57(7)	1.74(7)	2.15(7)	2.61(7)	3.00(7)
S_1	4.51(9)	9.77(9)	1.74(8)	2.19(8)	3.26(8)	4.47(8)	5.72(8)
S_2	1.67(8)	2.97(8)	4.71(8)	5.51(8)	7.32(8)	9.35(8)	1.15(7)
S_3, S_4	3.45(7)	4.42(7)	5.65(7)	6.16(7)	7.13(7)	8.26(7)	9.02(7)
α_1	9.79(15)	8.71(15)	7.79(15)	7.43(15)	6.75(15)	6.04(15)	5.51(15)
α_2	3.94(14)	3.22(14)	2.80(14)	2.61(14)	2.19(14)	1.78(14)	1.51(14)
α_3, α_4	2.13(14)	1.70(14)	1.39(14)	1.30(14)	1.10(14)	8.82(15)	7.39(15)
β_1	9.84(30)	8.18(30)	6.58(30)	6.09(30)	5.05(30)	3.79(30)	3.05(30)
β_2	5.44(29)	4.30(29)	3.44(29)	3.07(29)	2.45(29)	1.81(29)	1.47(29)
β_3	5.42(28)	3.87(28)	3.04(28)	2.73(28)	2.16(28)	1.63(28)	1.27(28)

Read 3.10(18) = 3.10×10^{-18}.

Chapter IV

Excitation Mechanism of 3250 and 4416 Å Laser Lines in the Cataphoretic He-Cd Laser Discharge*

Synopsis

The hook method has been applied to the population measurement for low-lying excited levels of He and Cd including metastable levels as well as for the ground state of Cd in the cataphoretic He-Cd laser discharge (3 mm bore and 685 mm long) under the typical condition for lasing (He pressure of 4.0 Torr, evaporator temperature of 170 to 270 °C and dc current of 30 to 160 mA). The population density of Cd ions in the 3250 Å upper level was also obtained by the line intensity measurement combined with the hook method. The results have shown that Penning collisions of ground state Cd atoms with 2^3S metastable He atoms are dominant for the excitation of 4416 and 3250 Å laser lines. The Penning-excitation cross section of 1.7×10^{-15} cm^2 and the population density of the 4416 Å upper level have been determined, which are consistent with the result so far obtained.

---

* Published in Japan. J. appl. Phys. 13 (1974) 1866.

§ 1. Introduction

There has been much interest in the CW He-Cd^+ laser because its simple construction provides a relatively high output power at 4416 Å and a convenient UV laser source at 3250 Å, and the following two processes have been proposed for the excitation mechanism of these two laser lines. Silfvast[1,2] has suggested that Penning collisions of ground state Cd atoms with metastable He atoms are the dominant process. On the contrary, Csillag et al.[3] and Jánossy et al.[4] have proposed that the upper laser level is excited by the two-step collision processes which consist of Penning ionization of neutral Cd atoms by collisions with metastable He atoms and excitation of the resulting Cd ions by electron-ion collisions.

The dominance of Penning reaction has been proved by the population measurement of the metastable atoms in low current discharge or afterglow,[5-8] but the experimental conditions were far from those for laser oscillation. On the other hand, the two-step excitation[3,4] has been proposed by the observation of the dependence of laser output power or sidelight intensity on the discharge current in a 50 Hz ac laser discharge.

In order to demonstrate the excitation mechanism in He-Cd discharge, it is crucial to know the accurate population densities of various atomic and ionic levels which play an important role in the excitation processes. In the previous studies,[5-9] the line absorption or reabsorption method has

been utilized for the population measurement. However, the population density obtained by these methods is often accompanied with considerable uncertainty because the methods require knowledge of accurate profile near the center of a spectral line of interest. Moreover, use of the methods is restricted by the optical thickness of discharge plasma near the line center.

The aim of the present work is to make clear the excitation mechanism of the laser lines at 3250 and 4416 Å in the He-Cd discharge under the typical condition for laser oscillation. The experiment was carried out on the cataphoretic laser discharge produced in a long capillary. The hook method, which requires the measurement of anomalous dispersion outside a spectral line core, was employed to obtain population density for the four lowest excited levels of He, $2^{1,3}S$ and $2^{1,3}P$, and those of Cd, 5^1P_1 and $5^3P_{0,1,2}$, as well as for the ground state 5^1S_0 of Cd. Furthermore, the population density of the 3250 Å laser upper level was also obtained by the sidelight intensity measurement combined with the hook method.

The hook method is almost insensitive to the profile of a spectral line and never affected by the optical thickness of discharge plasma near the line center, so that it gives much more accurate value of population density than the absorption method. The experimental procedure is described in the next section and in §3 the results are presented and discussed in relation to the excitation process of the Cd laser lines.

§ 2. Experimental Procedure

A Pyrex discharge tube used in the present experiment is illustrated in Fig.1, which is of the same design as the conventional dc cataphoretic He-Cd laser tube.[10,11] However, the quartz windows were sticked on both ends perpendicularly to the tube axis for the purpose of interferometric measurement. Main bore with thick wall was 685 mm in length and 3 mm in inner diameter. Pure He and He-Cd dc discharges were produced in the bore. In the latter case, Cd metal of natural isotopic abundance was heated in the evaporator by an electric wire furnace, whose temperature was controlled within the accuracy of one percent. The tube was sufficiently outgassed and evacuated by a diffusion pump to below 5×10^{-7} Torr before introduction of pure (99.999 %) He gas.

In the cource of the experiment, filling pressure P_{He} of He was 4.0 Torr and wall temperature of the main bore was kept constant at 358 °C ± 2 % by another wire furnace. Temperature T_{ev} of the evaporator was varied in the range of 170 to 270 °C, and dc discharge current j in the range from 30 to 160 mA. These conditions are appropriate for the laser oscillations at 3250 and 4416 Å.[1,2,11,12] It took, at least, about half an hour before the cataphoretic discharge settled down in a steady state. Fluctuation of the discharge was monitored by observing spontaneous emission from Cd, and a spatially uniform and stable discharge was maintained over a time period required for measurement.

2.1 Measurement of population density by the hook method

An experimental setup consists of a Mach-Zehnder interferometer and a spectrograph of large dispersion. A xenon short arc lamp was used as a continuum light source for the interferometer. The He-Cd discharge tube was placed in the test beam section.

As is stated in detail in ref.13 or 14, the hook method leads to the following expression for the population density N_p of the level p to be measured:

$$N_p f_{pq} = \frac{\pi K}{r_0 l \lambda_{pq}^3} \Delta^2, \qquad (2.1)$$

where Δ is the wavelength separation of hooks formed outside the core of an absorption line at the wavelength λ_{pq}, f_{pq} is the absorption oscillator strength for the transition from the lower level p to the upper level q, r_0 and l are the classical electron radius and the discharge length, respectively, and K is a constant of the hook method which can be easily and accurately determined. When the oscillator strength is known, the population density N_p can be obtained from the measurement of Δ.

The energy level diagrams of CdI, II and HeI are shown in Fig.2 together with the transitions of interest. Population densities of neutral He and Cd in the following levels were measured by the hook method:

He: $2^1S(5016)$, $2^1P(4922)$, $2^3S(3889)$, $2^3P(5876)$,

Cd: $5^1S_0(2288)$, $5^1P_1(6438)$, $5^3P_0(4678)$, $5^3P_1(4800)$, $5^3P_2(5086)$,

where the transitions adopted for the hook measurement are indicated in Å in the parenthesiss. The oscillator strengths of the transitions for CdI are listed in Table I together with the transition probabilities of some CdI and II lines necessary to the present experiment. Those of the He lines are not included in the table because they are accurately known.[19]

For the transitions with multiplet structure, eq.(2.1) is not available if the separation between the multiplet components is fairly great in comparison with the separation of hooks. In the present case, the fine structure in the transitions at 3889 and 5876 Å of He was taken into account according to the treatment in ref.20.

The left side of eq.(2.1) is often modified to $N_p f_{pq}(1 - g_p N_q / g_q N_p)$ owing to upper-level effect or negative dispersion, where N_q is the population density of the upper level q, and g_p and g_q are the statistical weights of the lower and upper levels, respectively. In the experiments on both He and Cd discharges,[21,22] it has been observed that the upper-level effect is small enough to be neglected, i.e., $g_p N_q / g_q N_p \ll 1$, for the transitions listed above. This situation is also supported for the present experimental condition of He discharge by the calculations by Ogata and Fukuda,[23] and by Fujimoto et al.[20] based on the collisional-radiative model of plasma.[24]

An Ebert-mount spectrograph of 170 cm focal length, Shimadzu GE-170, with a grating of 1200 grooves/mm and 3000 Å blaze was used to record hook spectra on a photographic film.

For example, the reciprocal linear dispersion was 1.74 Å/mm at 5876 Å in the second order and the hook separation about this line was in the range from 1.5 to 3.2 Å depending on the discharge conditions. Hooks about the line 2288 Å were photographed in the first order spectrum with exposure time of 5 to 10 sec, and those about the other lines in the second or third order with exposure time of 30 to 90 sec. Some examples of the hook spectra are shown in Fig.3. Small distortion of hooks was observed near the tube wall due to the gradient of particle density along radial direction. So the population density was determined from the separation of the hooks formed near the tube axis.

2.2 Determination of population density of the 3250 Å upper level

Population density of the 3250 Å laser upper level was derived from the relative intensity between the sidelight emissions at 3250 Å (CdII, $5s^2\ ^2D_{3/2} - 5p\ ^2P_{1/2}$) and 3261 Å (CdI, $5^3P_1 - 5^1S_0$) by making use of the population density of the level 5^3P_1 determined by the hook method. In the line intensity measurement, these two lines are so close in wavelength to each other that no calibration was necessary for the detecting system and the transmission of the tube wall.

The population density N_1 of the 3250 Å upper level is given as

$$N_1 = \frac{I_1}{I_2} \frac{gA_2\nu_2}{A_1\nu_1} N_2 \qquad (2.2)$$

$$(I_1 = A_1N_1h\nu_1,\ I_2 = gA_2N_2h\nu_2),$$

where N_2 is the population density of the 3261 Å upper level 5^3P_1, which is known by the hook method, I_1 and I_2 are the spontaneous intensities, ν_1 and ν_2 are the frequencies, A_1 and A_2 are the transition probabilities for the 3250 and 3261 Å lines, respectively, and the "escape factor" g is a dimensionless quantity characteristic to the imprisonment of the 3261 Å line. When the concentration of Cd atoms in the ground state 5^1S_0 is determined by the hook method, the value of g can be estimated according to Phelps.[25)]

As is seen in the next section, the population density N_1 was determined by the above procedure under only one condition of He-Cd discharge, i.e., P_{He} = 4 Torr, T_{ev} = 258 °C and j = 120 mA, because the measurement of relative intensity of the 3250 Å line provides the values of N_1 at different discharge conditions.

§ 3. Results and Discussion

If Penning collisions of ground state Cd atoms with metastable, especially 2^3S, He atoms excite the laser lines at 3250 and 4416 Å, the population density N_i of an upper laser level is given to the first approximation by the following rate equation describing a steady state:

$$\frac{dN_i}{dt} = \langle\sigma_p v\rangle N_{Cd} N_m - \sum_j A_{ij} N_i = 0, \qquad (3.1)$$

where N_{Cd} and N_m are the number densities of the ground state Cd atoms and the 2^3S metastable He atoms, respectively, $\langle\sigma_p v\rangle$ is the velocity-averaged Penning-excitation cross section or

the Penning-excitation rate coefficient, and A_{ij} is the radiative transition probability from the upper laser level i to the lower level j.* Assuming that $\langle \sigma_p v \rangle$ is constant under the present experimental condition, eq.(3.1) becomes

$$N_i \propto N_{Cd} N_m. \tag{3.2}$$

3.1 Dependence of population densities on discharge current

The population and spontaneous emission measurements were made as a function of discharge current. Figure 4 gives the population densities of the four lowest excited He levels, $2^{1,3}S$ and $2^{1,3}P$, in the pure He discharge at P_{He} = 4 Torr. Figure 5 represents the population densities of the He levels and the concentration of the ground state Cd atoms in the He-Cd discharge at a fixed evaporator temperature T_{ev} = 258 °C, where P_{He} is also 4 Torr. Figure 6 shows the spontaneous emissions of the 4416 and 3250 Å laser lines under the same discharge condition as in Fig.5. The absolute scale of the population density of the 3250 Å upper level was determined at j = 120 mA by the method described in §2.2, where the concentration of the ground state Cd atoms is given in Fig.5 and the value of g is estimated to be 0.85 for the 3261 Å line. In order to examine the relation of eq.(3.2), the products, $N_{Cd}N_m$ and $N_{Cd}N(He^*)$, are plotted in Fig.6 by making use of the data in Fig.5, where N(He*) means the sum of the population densities

* The destruction process of the laser level is confirmed experimentally to be $\sum_j A_{ij} \sim 10$ x (radiationless decay probability), (private communication from T.Sakurai).

of the four lowest excited He levels.

In Fig.6 the spontaneous emissions from the two upper laser levels show quite the same dependence on discharge current and this dependence is also nearly the same as that of $N_{Cd}N_m$: the emission intensities increase more rapidly than $N_{Cd}N_m$ as the current increases in the low current region, but the decrease in the emission intensities occurs at high current in accordance with that of $N_{Cd}N_m$. The former fact is attributed to the rise of gas temperature on the axis of discharge[26,27] accompanied by the increase of the current, because the temperature rise makes the coefficient $\langle\sigma_p v\rangle$ of eq.(3.1) larger.

The three excited He levels, 2^1S and $2^{1,3}P$, do not contribute so much to the excitation for the upper laser levels as the 2^3S level since the population densities of the former are much lower than that of the latter as shown in Fig.5. Moreover, the decrease in the population density of the 2^3S level at high current in Fig.5 is in good accord with that in the spontaneous emissions in Fig.6. The above pronounced behavior of the 2^3S metastable level suggests that this level takes a dominant role in the Penning excitation of the ground state Cd atoms.

Figure 7 shows the spontaneous emissions of CdII 5378 and 5337 Å lines as a function of discharge current under the same condition as in Figs.5 and 6. The variation of the emissions, i.e., the monotonous increase with increasing discharge current, is clearly different from those of the emissions at 3250 and 4416 Å in Fig.6. This implies that the

upper levels of the 5378 and 5337 Å lines are too high in energy (see Fig.2) to be populated by the collisions of the ground state Cd atoms with He atoms in the four lowest excited levels, and that the other kinds of excitation processes must be introduced to explain the laser oscillation of these lines.[7,8,28)]

3.2 Dependence of population densities on Cd atom concentration

The measurements of population density and line intensity were carried out by changing the evaporator temperature, i.e., Cd atom concentration, at a constant discharge current j = 120 mA, where P_{He} was 4 Torr. The concentration of the ground state Cd atoms in the main bore was determined from the hooks about the 2288 Å resonance line and is shown in Fig.8 as a function of the evaporator temperature. Here are also shown the Cd atom concentration in the evaporator calculated from Cd vapor pressure at the temperature T_{ev} as well as the mean value of Cd concentration in the discharge measured by Browne et al.[9)]

In Fig.9 the population densities of the four excited He levels are shown as a function of Cd atom concentration. All the densities fall off remarkably when the Cd concentration exceeds 2.0×10^{13} cm^{-3}. Figure 10 gives the spontaneous emissions of the laser lines at 3250 and 4416 Å under the same condition as in Fig.9, where the product $N_{Cd}N_m$ is indicated for comparison. The variations of these emissions are in excellent agreement with that of $N_{Cd}N_m$ and the relation

of eq.(3.2) precisely holds. It is now concluded that the Penning collisions of the ground state Cd atoms with 2^3S metastable He atoms are the dominant process to populate the 3250 and 4416 Å laser upper levels over the whole range of the present experimental conditions.

It was possible for us to measure the population densities of the four lowest excited levels of Cd, 5^1P_1 and $5^3P_{0,1,2}$, by the hook method under the same discharge condition as in Fig.9. The result is shown in Fig.11 as a function of Cd concentration. The high values of these densities are noticeable and it will be interesting to examine the possibility that Cd atoms in these four levels populate some high-lying levels of Cd ions to oscillate laser lines by the collisions with He or Ne atoms in low-lying excited levels in the discharge of He-Cd or Ne-Cd, respectively.

Through the course of the present experiment, the discharge current and the evaporator temperature were very carefully controlled, and the so-called "break" observed by Jánossy et al.[4] never appeared in the measurement of the variation of spontaneous emission as a function of discharge current (Figs.6 and 7).

3.3 Penning-excitation cross section

From the above result it is easily seen that the rate coefficient of the Penning excitation for the 3250 Å laser upper level is determined from eq.(3.1) with the observed population densities, N_i, N_m and N_{Cd}, of this level, the He 2^3S metastable level and the Cd ground state, respectively.

In Figs.9 and 10, for example, $N_m = 6.4 \times 10^{12}$ cm^{-3} and $N_i = 1.7 \times 10^{10}$ cm^{-3} at $N_{Cd} = 3.0 \times 10^{13}$ cm^{-3}, at which the peak appears in the sidelight emissions at 3250 and 4416 Å, and these values lead to

$$\langle \sigma_p v \rangle = 3.4 \times 10^{-10} \text{ cm}^3\text{sec}^{-1},* \qquad (3.3)$$

where the values of A_{ij} in Table I are used for the transitions at 3250 and 3536 Å (see Fig.2). The coefficient $\langle \sigma_p v \rangle$ is reduced to $\bar{\sigma}_p \bar{v}$, where $\bar{\sigma}_p$ is the effective Penning-excitation cross section and $\bar{v}$ is the mean thermal velocity for He-Cd encounters. When gas temperature is assumed to be 460 °C, $\bar{v}$ is 2.0×10^5 cmsec^{-1} and then $\bar{\sigma}_p$ is calculated to be

$$\bar{\sigma}_p = 1.7 \times 10^{-15} \text{ cm}^2 \text{ at } P_{He} = 4 \text{ Torr and } j = 120 \text{ mA} \qquad (3.4)$$

from the relation (3.3).

Schearer and Padovani[6] and Collins[8] have obtained the total cross section of 4.5 and 6.5×10^{-15} cm^2, respectively, by the pulsed-afterglow method for the Penning ionization of Cd atoms by the collision with He atoms in the 2^3S level. From the former value, Silfvast[5] has derived the cross section of about 1×10^{-15} cm^2 for the Penning excitation from

---

* This value is, of course, valid over the whole range of Cd concentration in Fig.9, but it decreases to 1.7×10^{-10} cm^{3}sec^{-1} when the current j is reduced from 120 mA to 30 mA, as seen from Figs.5 and 6.

the He metastable to the 4416 Å upper level in the low current discharge. However, no data have been obtained under the discharge condition appropriate for the laser oscillation. The above value (3.4) is considered to be a reliable value of the cross section under this condition because it has been determined directly from the observed population densities involved.

When the Penning-excitation rate coefficient for the 4416 Å upper level is assumed to be equal to that for the 3250 Å upper level, the population density of the former level is estimated to be 5.1×10^{10} cm^{-3} at $N_{Cd} = 3.0 \times 10^{13}$ cm^{-3} in Fig.9. This value and the corresponding observed value of 1.7×10^{10} cm^{-3} for the 3250 Å upper level are in good agreement with the values obtained by the absolute line-intensity measurement,[18] 6.7 and 2.3×10^{10} cm^{-3}, respectively.* The penning excitation rate and population density of the 4416 Å upper level are easily estimated at different discharge conditions by the same way as described above.

In Fig.9 the population densities of the four lowest excited levels of He are nearly constant in the range of $N_{Cd} = 0$ to 1×10^{13} cm^{-3} but they decrease for $N_{Cd} \gtrsim 1 \times 10^{13}$ cm^{-3}. Their decreases from $N_{Cd} = 0$ to 3×10^{13} cm^{-3} in Fig.9 correspond to those from Fig.4 to 5 at j = 120 mA and the population density of the 2^3S metastable level reduces to

---

* In this experiment the dc cataphoretic discharge was produced in the tube of 3 mm bore and 70 cm length at P_{He} = 4.0 Torr and j = 140 mA.

about 70 % of its initial value. The depopulation rate from this level by Penning collisions with Cd atoms is estimated to be 2.6 x 10^{17} $cm^{-3}sec^{-1}$ at the present discharge condition, when the total cross section is assumed to be four times as larege as the value (3.4) according to Silfvast.[5] On the other hand, the collisional-radiative calculation on pure He plasma in positive column[20] gives the effective depopulation rate of 1.2 x 10^{18} $cm^{-3}sec^{-1}$ from the 2^3S level at the electron temperature of 4.2 x 10^4 K and density of 1.5 x 10^{12} cm^{-3}, which were determined by the double-probe method on the present discharge tube at P_{He} = 4.0 Torr, j = 120 mA and T_{ev} = 258 °C. The depopulation rate in the latter case is about five times as large as that in the former case, and this fact suggests that the decrease in the population density of the He 2^3S level caused by the mixing of Cd atoms is partly due to the increase in the depleting rate from the level by the Penning collisions[5] and partly to the decrease in the electron temperature of the discharge plasma or E/P value.[9]

References

1) W.T.Silfvast: Appl. Phys. Letters 13 (1968) 169.

2) W.T.Silfvast: Appl. Phys. Letters 15 (1969) 23.

3) L.Csillag, M.Jánossy, K.Kántor, K.Rózsa and T.Salamon: J. Phys. D 3 (1970) 64.

4) M.Jánossy, V.V.Itagi and L.Csillag: Acta Phys. Hungar. 32 (1972) 149.

5) W.T.Silvfast: Phys. Rev. Letters 27 (1971) 1489.

6) L.D.Schearer and F.A.Padovani: J. chem. Phys. 52 (1970) 1618.

7) G.J.Collins, R.C.Jensen and W.R.Bennet: Appl. Phys. Letters 19 (1971) 125.

8) G.J.Collins: J. appl. Phys. 44 (1973) 4633.

9) P.G.Browne and M.H.Dunn: J. Phys. B 6 (1973) 1103.

10) J.P.Goldsborough: Appl. Phys. Letters 15 (1969) 159.

11) J.R.Fendley, I.Gorog, K.G.Hernqvist and C.Sun: RCA Rev. 30 (1969) 422.

12) J.P.Goldsborough: IEEE J. Quantum Electronics QE-5 (1969) 133.

13) W.C.Marlow: Appl. Optics 6 (1967) 1715.

14) M.C.E.Huber: Modern Optical Methods in Gas Dynamic Research, ed. D.S.Dosanjh (Plenum Press, New York, 1971) p.85.

15) T.Andersen and G.Sørensen: J. quant. Spectrosc. radiative Transfer 13 (1973) 369.

16) A.R.Schaefer: J. quant. Spectrosc. radiative Transfer 11 (1971) 197.

17) M.Barrat and J.P.Barrat: Compt. Rend. 257 (1963) 1463.

18) D.T.Hodges: Appl. Phys. Letters 17 (1970) 11.

19) W.L.Wiese, M.W.Smith and B.M.Glennon: Atomic Transition Probabilities (U.S.Government Printing Office, Washington, 1966) Vol.1, p.9.

20) T.Fujimoto, K.Miyazaki and K.Fukuda: J. quant. Spectrosc. radiative Transfer 14 (1974) 377.

21) O.P.Vochkova and L.P.Razumovskaya: Optics and Spectrosc. 18 (1965) 438.

22) N.P.Penkin and T.P.Redko: Optics and Spectrosc. 20 (1966) 106.

23) Y.Ogata and K.Fukuda: Mem. Fac. Engng. Kyoto Univ. XXXV (1973) 177.

24) D.R.Bates, A.E.Kingston and R.W.P.McWhirter: Proc. Roy. Soc. A 267 (1962) 297.

25) A.V.Phelps: Phy. Rev. 110 (1958) 1362.

26) Yu.M.Kagan and N.N.Khristov: Optics and Spectrosc. 28 (1970) 311.

27) S.I.Krylova, L.A.Luizova and A.D.Khakhaev: Optics and Spectrosc. 25 (1968) 87.

28) W.K.Schuebel: Appl. Phys. Letters 16 (1970) 470.

Figure captions

Fig.1. Schematic diagram of the cataphoretic He-Cd discharge tube.

Fig.2. Energy level diagrams of CdI, II and HeI.

Fig.3. Examples of hook spectrograms. The hooks about the lines 3889 and 5086 Å are photographed in the third order, and the hooks about the line 5876 Å in the second order. The tube diameter is 3 mm as indicated.

Fig.4. Population density in the pure He discharge as a function of current. P_{He} = 4.0 Torr.

Fig.5. Population density in the He-Cd discharge as a function of current. P_{He} = 4.0 Torr and T_{ev} = 258 °C.

Fig.6. Variation of spontaneous emission under the same discharge condition as in Fig.5. N_{Cd}: the concentration of ground state Cd atoms. N_m: the population density of the He(2^3S) level. N(He*): sum of the population densities of the excited He($2^{1,3}S$, $2^{1,3}P$) levels.

Fig.7. Variation of spontaneous emission under the same discharge condition as in Fig.5.

Fig.8. The concentration of ground state Cd atoms as a function of evaporator temperature at P_{He} = 4.0 Torr and j = 120 mA. —— - ——: the mean value of the concentration obtained by Browne and Dunn (ref.9) on the discharge (3 mm bore and 3 cm long) at several He pressures for j = 100 mA. ---: the number density of Cd atoms in the evaporator calculated from vapor pressure data at T_{ev}.

Fig.9. Population density of excited He levels as a function of Cd normal-atom density under the same discharge condition as in Fig.8.

Fig.10. Variation of spontaneous emission under the same discharge condition as in Fig.8. N_{Cd}: the concentration of ground state Cd atoms. N_m: the population density of the He(2^3S) level.

Fig.11. Population density of excited Cd levels as a function of Cd normal-atom density. The discharge condition is the same as in Fig.8.

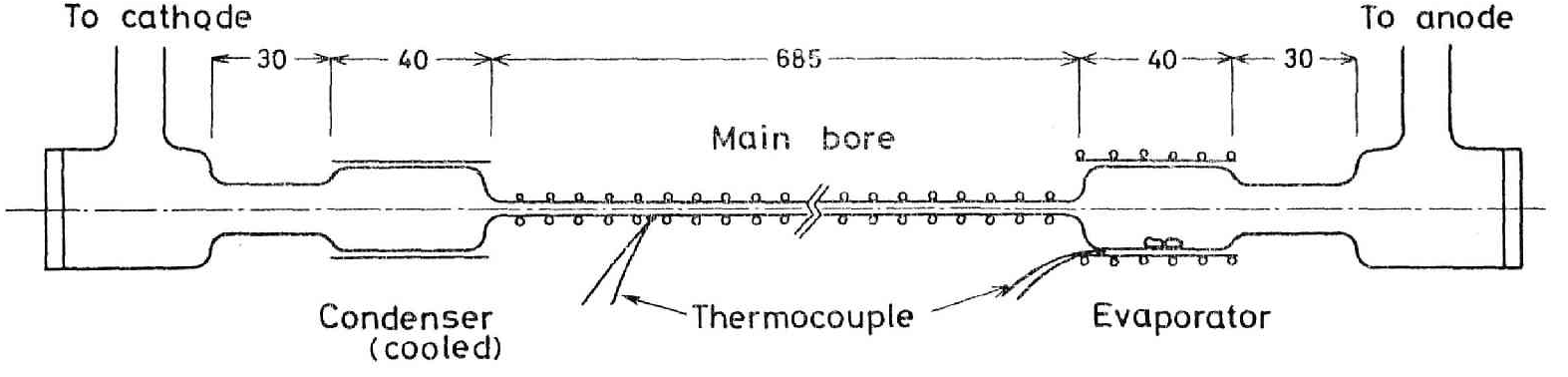
To cathode
To anode
30
40
685
40
30
Main bore
Condenser
(cooled)
Thermocouple
Evaporator

Fig.1

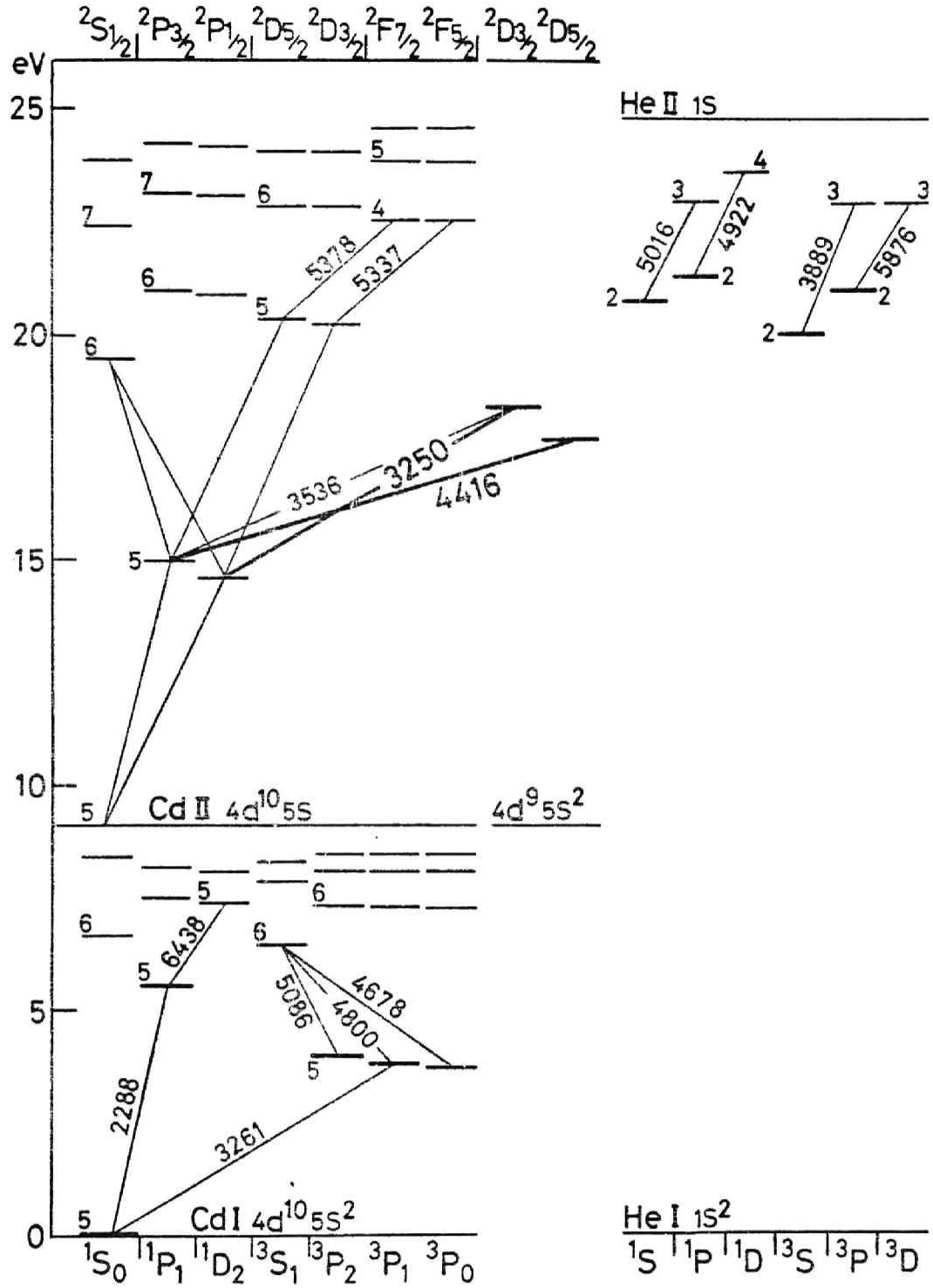
2S1/2 2P3/2 2P1/2 2D5/2 2D3/2 2F7/2 2F5/2 2D3/2 2D5/2
eV
25
20
15
10
5
0
He II 1S
5016
4922
3889
5876
5378
5337
3536
3250
4416
Cd II 4d10 5S
4d9 5S2
6438
5086
4678
4800
2288
3261
Cd I 4d10 5S2
1S0 1P1 1D2 3S1 3P2 3P1 3P0
He I 1S2
1S 1P 1D 3S 3P 3D

Fig.2

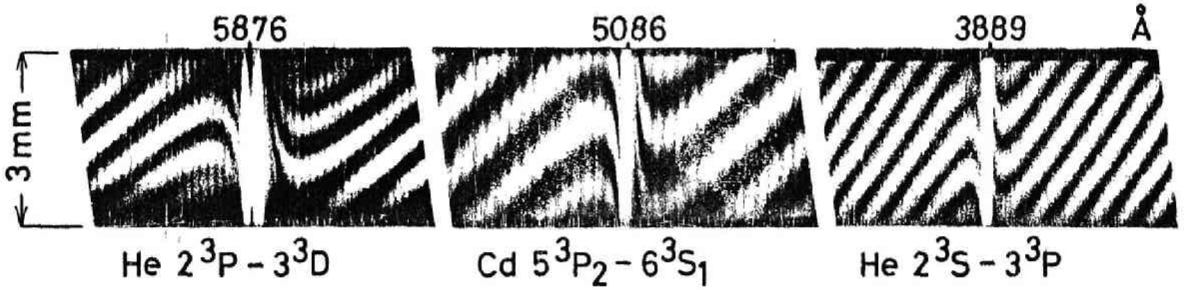

Fig.3

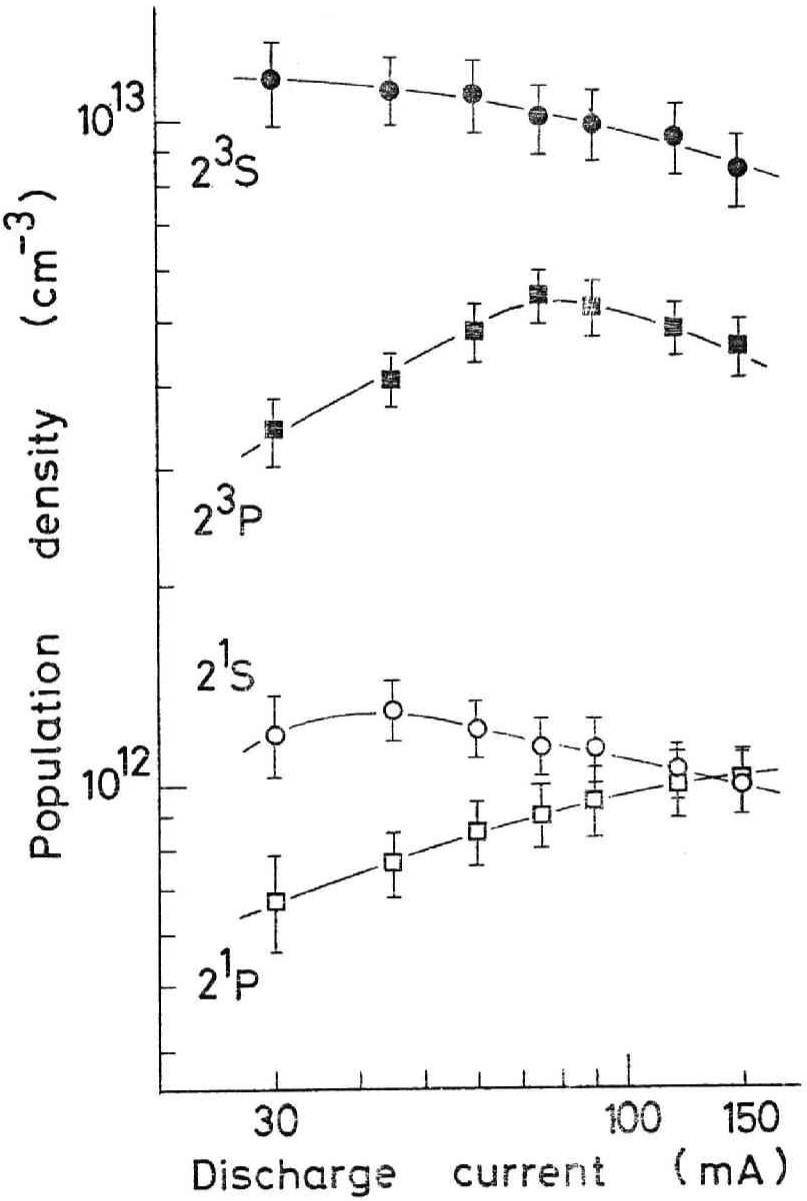
Population density (cm^{-3})
10^{13}
10^{12}
2^3S
2^3P
2^1S
2^1P
30
100
150
Discharge current (mA)

Fig.4

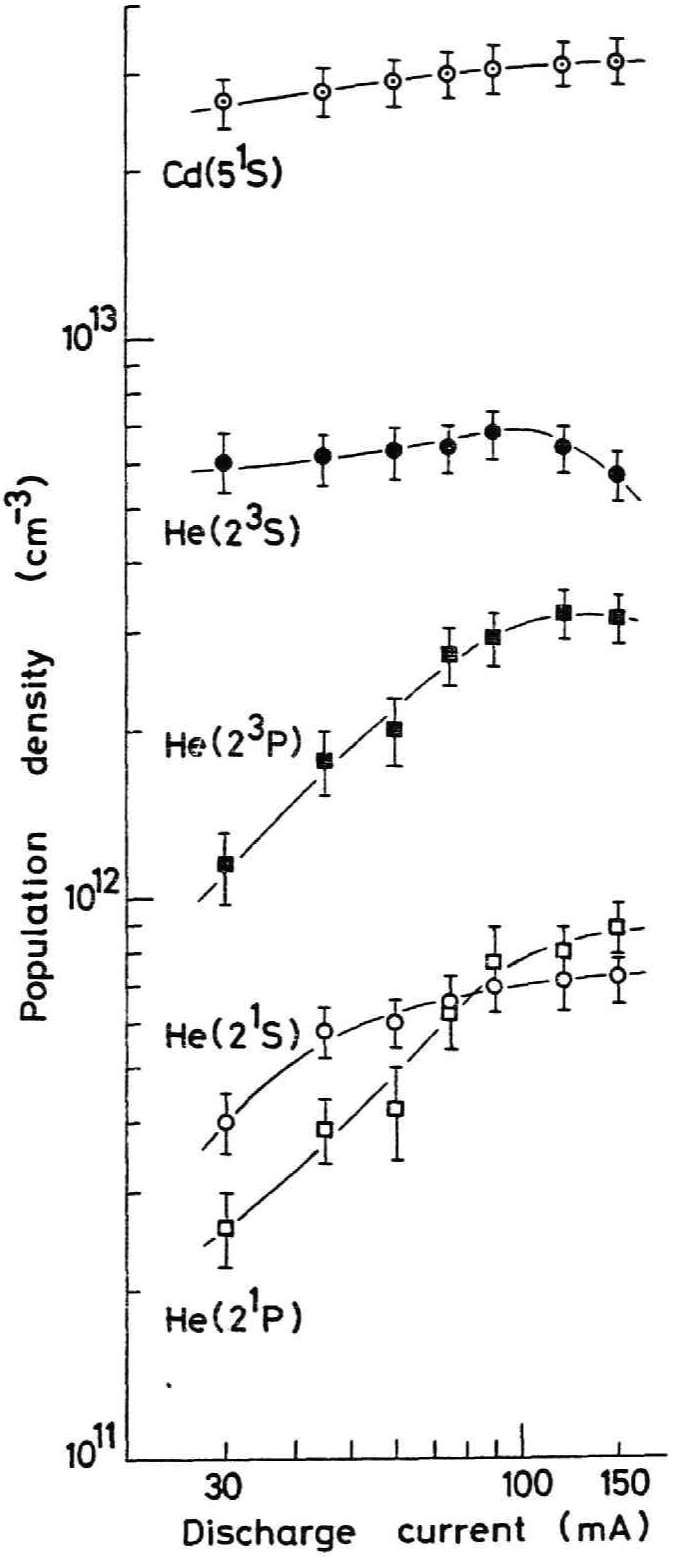
Cd(5¹S)
10¹³
He(2³S)
He(2³P)
10¹²
He(2¹S)
He(2¹P)
10¹¹
Population density (cm⁻³)
30
100
150
Discharge current (mA)

Fig.5

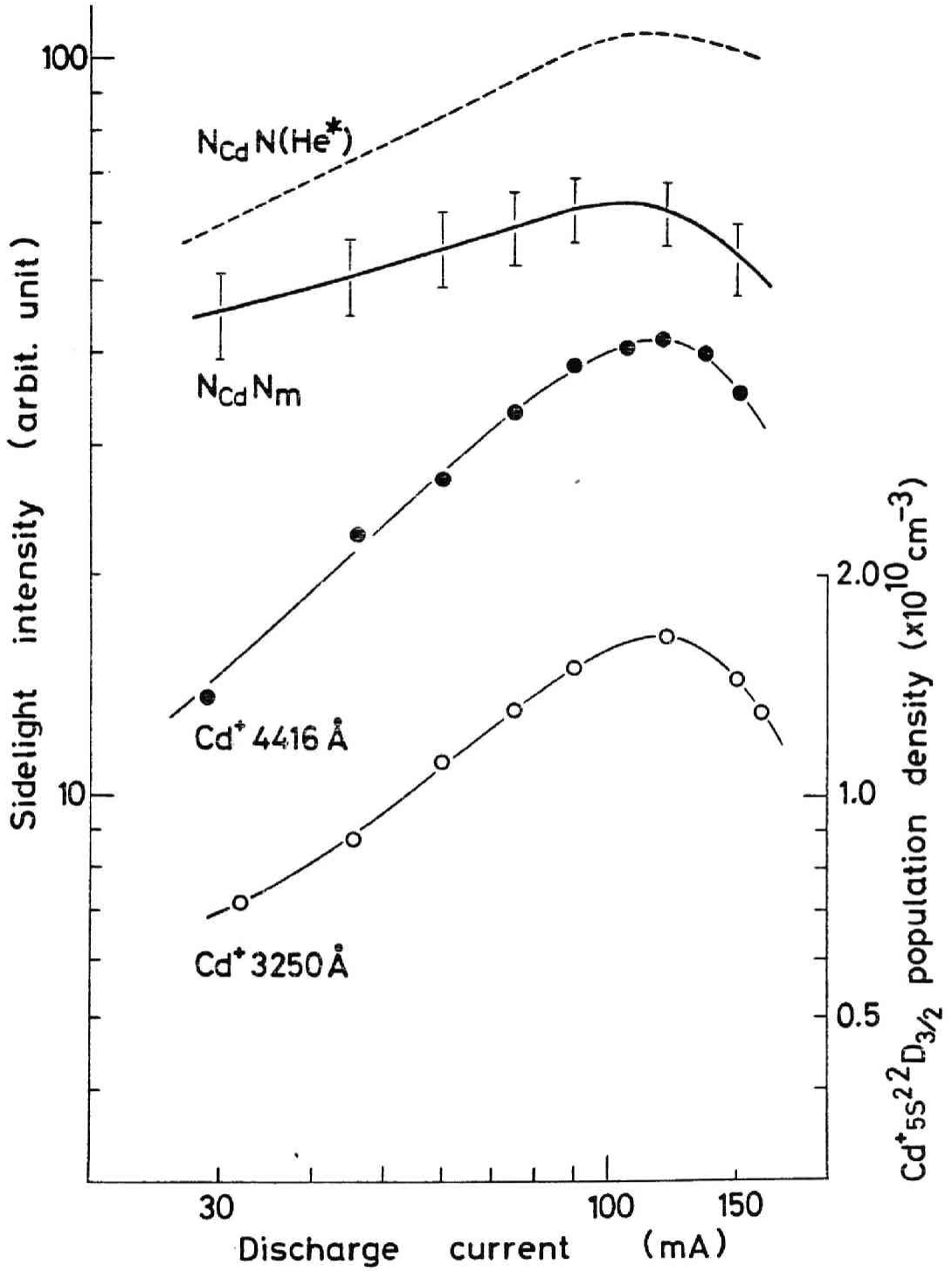
100
10
Sidelight intensity (arbit. unit)
$N_{Cd}N(He^*)$
$N_{Cd}N_m$
Cd^+ 4416 Å
Cd^+ 3250 Å
2.0
1.0
0.5
$Cd^+5S^2\,^2D_{3/2}$ population density ($x10^{10}cm^{-3}$)
30
100
150
Discharge current (mA)

Fig.6

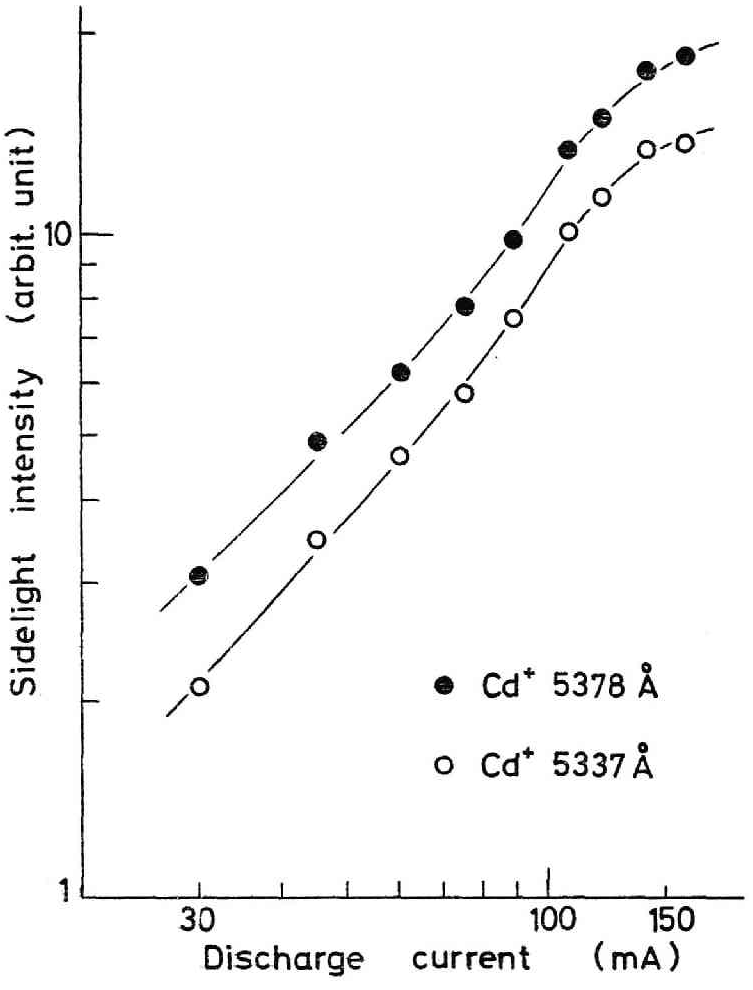
Sidelight intensity (arbit. unit)
10
1
30
100
150
Discharge current (mA)
Cd+ 5378 Å
Cd+ 5337 Å

Fig.7

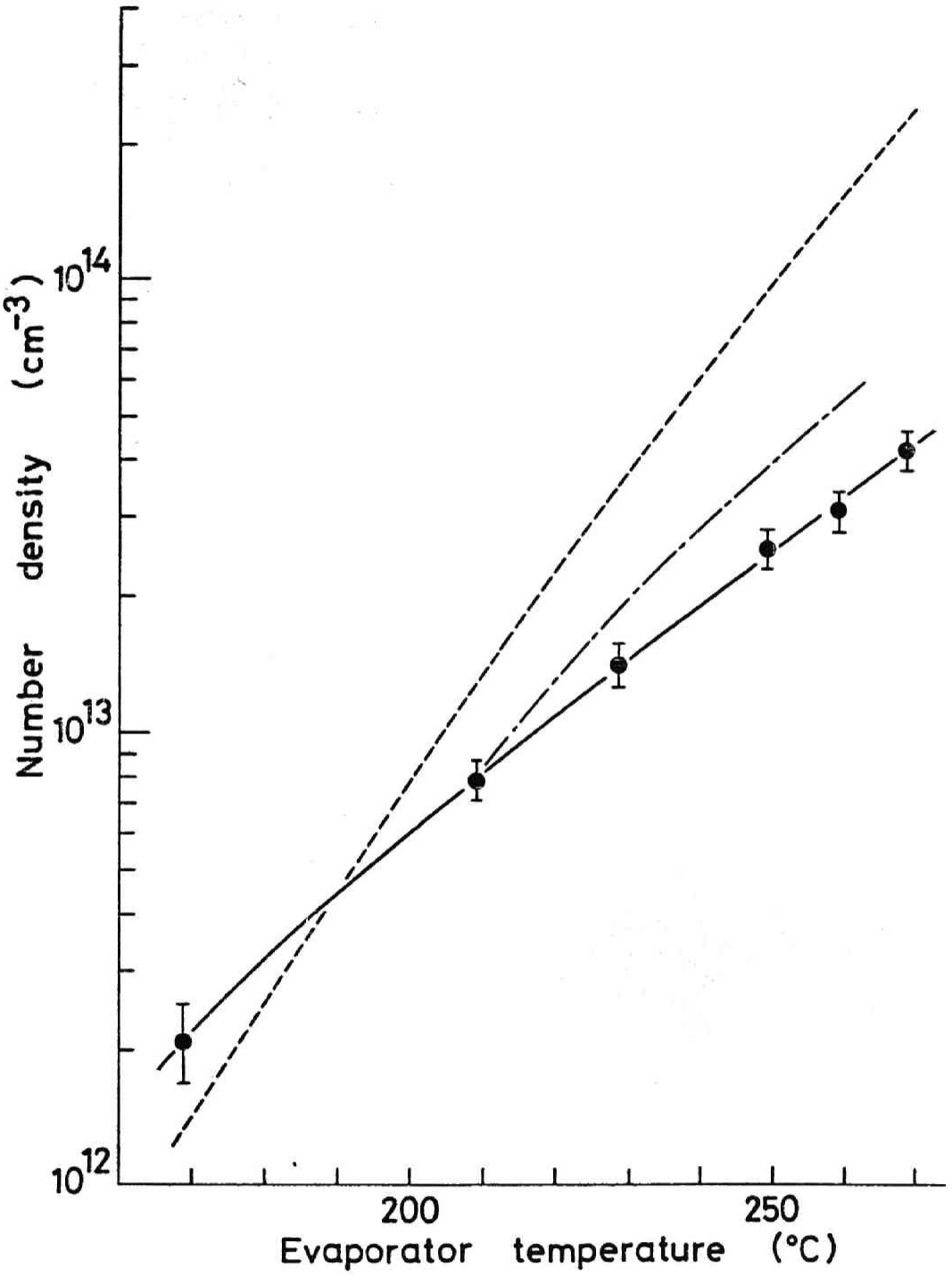
Number density (cm^{-3})
10^{14}
10^{13}
10^{12}
200
250
Evaporator temperature (°C)

Fig.8

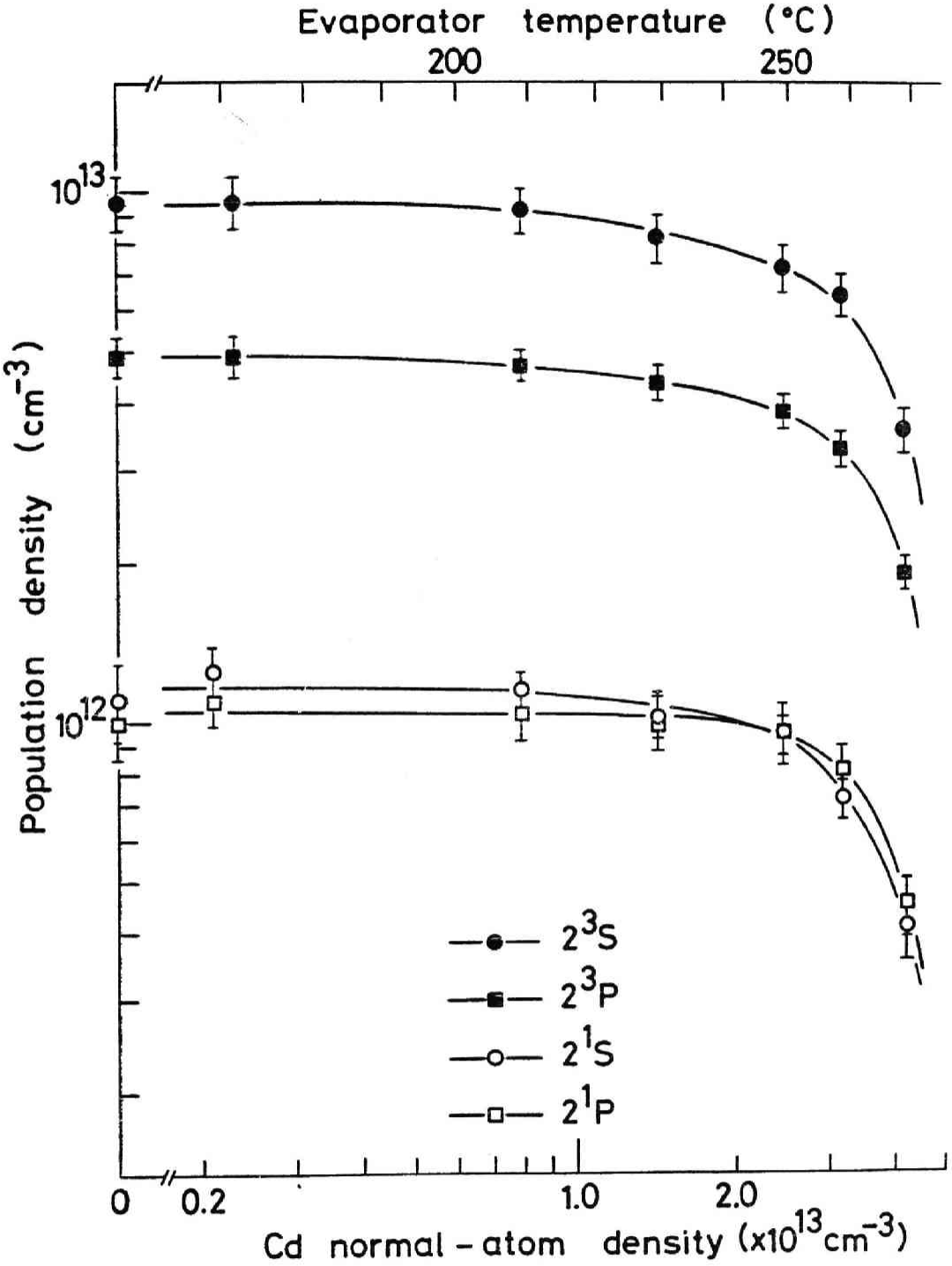
Evaporator temperature (°C)
200
250
10^{13}
10^{12}
Population density (cm^{-3})
2^3S
2^3P
2^1S
2^1P
0
0.2
1.0
2.0
Cd normal - atom density ($x10^{13} cm^{-3}$)

Fig.9

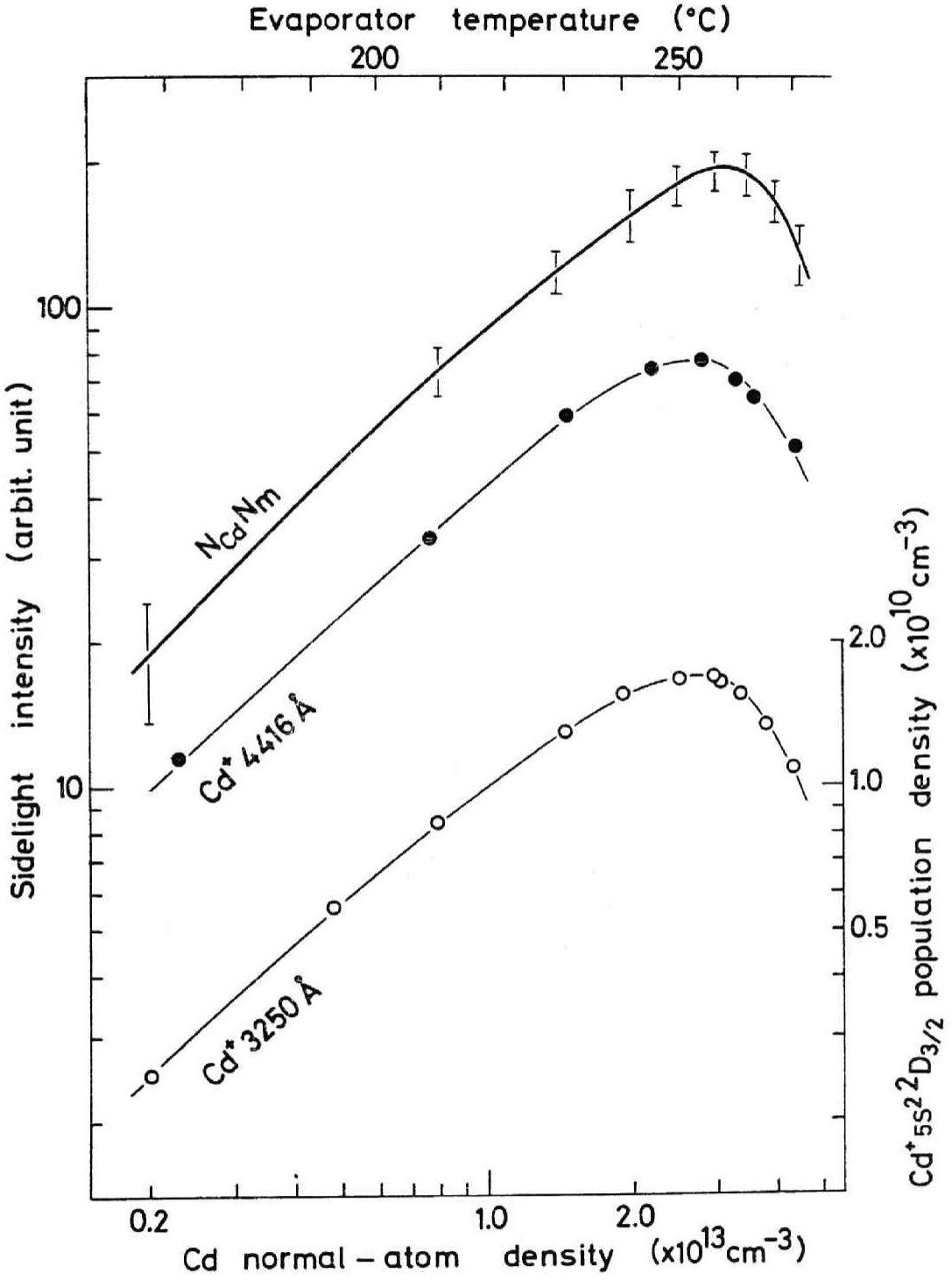
Evaporator temperature (°C)
200
250
100
10
Sidelight intensity (arbit. unit)
N_{Cd}/Nm
Cd* 4416 Å
Cd* 3250 Å
2.0
1.0
0.5
$Cd^*5s^2\,^2D_{3/2}$ population density ($x10^{10}cm^{-3}$)
0.2
1.0
2.0
Cd normal – atom density ($x10^{13}cm^{-3}$)

Fig.10

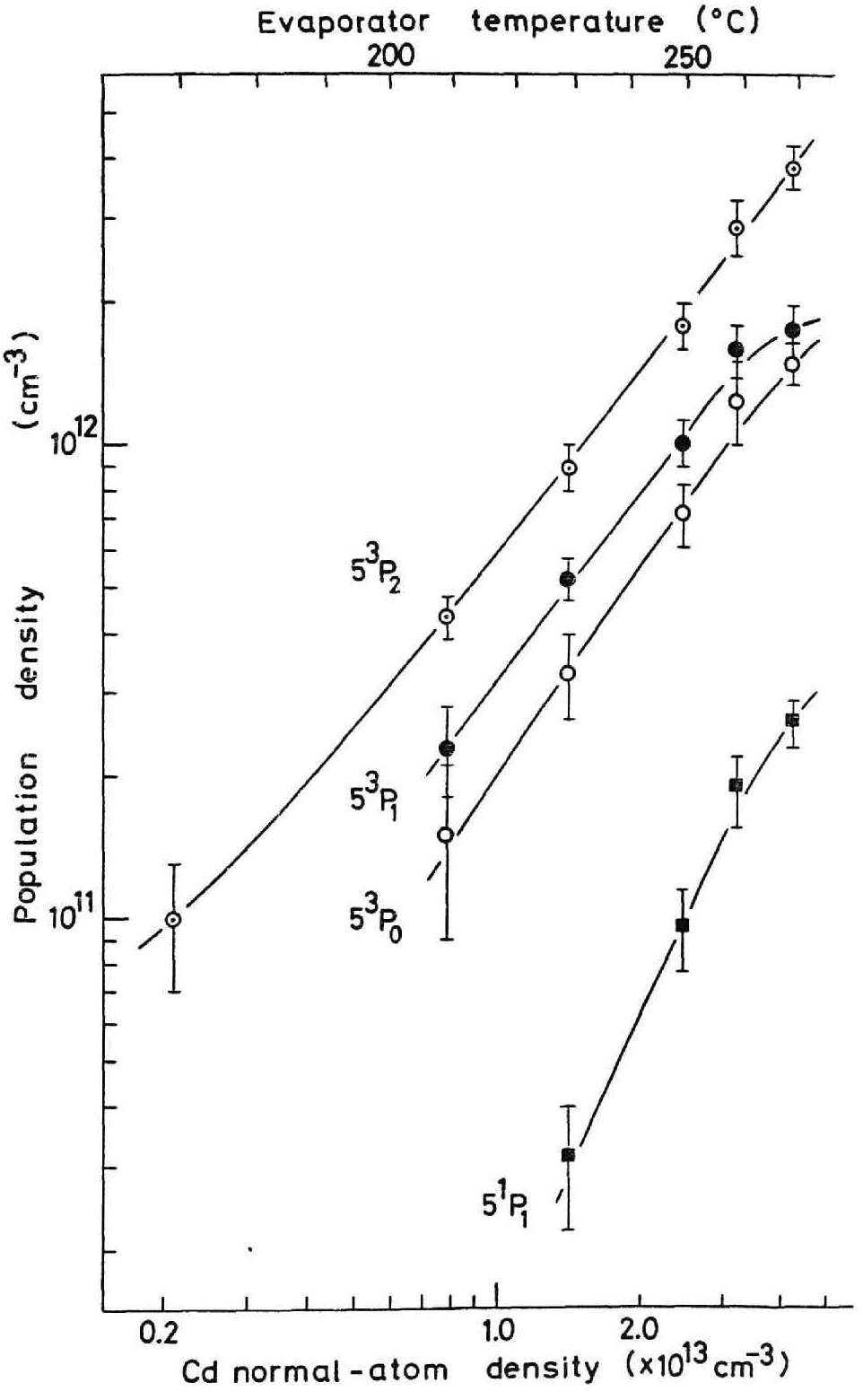
Evaporator temperature (°C)
200
250
Population density (cm⁻³)
10¹²
10¹¹
5³P₂
5³P₁
5³P₀
5¹P₁
0.2
1.0
2.0
Cd normal-atom density (x10¹³ cm⁻³)

Fig.11

Table I. Oscillator strengths and transition probabilities of CdI and II.

	Wavelength (Å)	Transition	Oscillator strength	Transition probability (10^6 sec^{-1})	Ref.
CdI	2288	$5^1S_0 - 5^1P_1$	1.24		15)
	6438	$5^1P_1 - 5^1D_2$	0.375		16)
	4678	$5^3P_0 - 6^3S_1$	0.105		15)
	4800	$5^3P_1 - 6^3S_1$	0.132		15)
	5086	$5^3P_2 - 6^3S_1$	0.117		15)
	3261	$5^3P_1 - 5^1S_0$		0.402	16)
CdII	3250	$5s^2\ ^2D_{3/2} - 5p\ ^2P_{1/2}$		3.33	17,18)
	3536	$5s^2\ ^2D_{3/2} - 5p\ ^2P_{3/2}$		0.52	17,18)
	4416	$5s^2\ ^2D_{5/2} - 5p\ ^2P_{3/2}$		1.28	17,18)

Chapter V

Dispersion and Absorption Studies on the Doubly-Excited $5p^2\ ^3P_{0,1,2}$ States of CdI*

Synopsis

Stationary Cd plasma has been produced by a high-frequency excitation device of 27.1 MHz in a discharge tube of 10 mm inner diameter and 57 cm length, and the concentration of excited Cd atoms in the $5s5p\ ^3P_{0,1,2}$ levels has been estimated by the hook method.

The absorption cross section has been measured for the autoionizing transitions $5s5p\ ^3P_{1,2} - 5p^2\ ^3P_2$ at 2212 and 2270 Å, which represent the Lorentzian profile with the same half-width of 232 cm^{-1}. The half width gives the autoionization probability 4.37×10^{13} sec^{-1} of the $5p^2\ ^3P_2$ state, and the integration of the profiles gives the oscillator strengths of the transitions. Furthermore, the oscillator strengths of the transitions $5s5p\ ^3P_{0,1,2} - 5p^2\ ^3P_{0,1}$ have been determined by the hook method.

---

* Published in J. Phys. Soc. Japan 40 (1976) 233 and partly in J. Phys. Soc. Japan 38 (1975) 906 and 1551.

§ 1. Introduction

It has long been known that the emission lines from the doubly-excited $5p^2\ ^3P_2$ level of CdI have broad width in contrast to the four sharp lines from the $5p^2\ ^3P_{0,1}$.[1] There are no ^3P-continuum states of even parity available for autoionization of the $p^2\ ^3P$ states in pure LS coupling. The observation of emission for the transition $5s5p\ ^1P_1 - 5p^2\ ^3P_2$ has shown that the $p^2\ ^3P_2$ state autoionizes to the sE(d) $^1D_2$-continuum due to the mixing of the $p^2\ ^1D_2$ component in the $p^2\ ^3P_2$ state,[2] as suggested by Majorana.[3]

The autoionization probability of the $p^2\ ^3P_2$ state has been estimated from the observed line width,[1,2] but no quantitative studies such as absorption measurement have been made on the doubly-excited levels of interest. Recently the present authors reported briefly the first observation of absorption spectrum of the autoionizing transitions $5s5p\ ^3P_{1,2} - 5p^2\ ^3P_2$ and the absolute values of absorption cross section of the transitions as well as the oscillator strength of the transitions $5s5p\ ^3P_{0,1,2} - 5p^2\ ^3P_{0,1,2}$.[4,5]

This paper gives the detailed description of the cross section and oscillator strength measurements. The next section describes the high-frequency (HF) excitation device employed to produce Cd plasma and the procedure of the dispersion and absorption measurements. The experimental results are presented in §3, and discussion in §4 deals with the observed symmetric line shape for the autoionizing transitions according to Fano.[6]

§ 2. Experimental

The Pyrex discharge tube used in the experiment is illustrated in Fig.1. The main tube, in which Cd metal was put, was 10 mm in bore diameter and 87 cm in length. The end tubes with quartz windows perpendicular to the tube axis were connected to the main tube by the brass junctions so that the main tube could be easily replaced by another one without any other changes of the experimental arrangement.

After Ar was introduced at 1.0 Torr as a buffer gas for the HF discharge, the Cd metal was vaporized by a simple electric furnace of 57 cm in length. Temperature of the furnace was monitored by a thermocouple sticked on the tube wall. The outer electrodes of thin Al plates for the HF discharge were mounted on the discharge tube at the distance of about 65 cm.

Corresponding to the furnace temperature of 267 - 366 °C, the partial pressure of Cd in the discharge ranged from 0.006 to 0.2 Torr, which was estimated by the hook method described below. The frequency and output power of the HF device were 27.1 MHz and 475 W, respectively. The discharge in Cd was very stable and uniform along the tube axis. The Cd plasma was confined in the furnace region and clearly separated from the outer region where only Ar discharge was observed. Furthermore, the Ar discharge was perfectly terminated at the brass junctions due to large loss of the HF power. Therefore, contamination of the windows, which is a serious problem in metal discharge, was never recognized in the course of the

experiment. The fairly accurate boundary of the Cd plasma was also convenient to the definition of absorption length.

2.1 Population and f-value measurements by the hook method

The oscillator strength or f-value and population density were measured by the hook method,[7] which requires the interferometric measurement of anomalous dispersion near spectral lines. The optical setup was described in detail in our previous papers.[8,9] The discharge tube was placed in the test beam section of a Mach-Zehnder interferometer. A short Xe arc lamp (Ushio UXL-500D) was used as a continuum light source for the interferometer, and an Ebert-mount spectrograph of 170 cm focal length was employed to record the hook spectra with a grating of 1200 grooves/mm blazed at 3000 Å.

The simplified term diagram of CdI is shown in Fig.2 together with the transitions concerned. First, the population density N of the $5s5p\ ^3P_{0,1,2}$ levels was measured from the hooks formed near the visible transitions at 4678, 4800 and 5086 Å, where the known f-values for these lines[10] were used. Then, the f-values of the four transitions $5s5p\ ^3P_{0,1,2} - 5p^2\ ^3P_{0,1}$ were determined from the hooks near the ultraviolet lines at 2240, 2267, 2307 and 2329 Å. The N and f-value measurements were performed under several discharge conditions of different furnace temperature. The concentration of the ground state Cd atoms was also estimated from the hooks near the resonance line at 2288 Å.

The hook spectra were photographed with the slit width of 50 μm on Fuji Neopan-F film in the third order for the

visible lines and on Kodak SWR film in the first order for the ultraviolet lines. The reciprocal linear dispersion was 0.657 Å/mm at 5086 Å and 4.86 Å/mm at 2329 Å. The hook separation, for example, was in the range of 1.3 - 2.0 Å and 1.2 - 1.9 Å about the 5086 and 2329 Å lines, respectively. Figures 3 and 4 show examples of the hook spectrogram in the visible and ultraviolet regions, respectively. No hooks appeared near the autoionizing transitions at 2212 and 2270 Å on account of the broad line widths. Figure 5 represents N of the $5s5p\ ^3P_{0,1,2}$ levels as a function of furnace temperature.

2.2 Absorption measurement for the autoionizing transitions

Figure 6 shows the observed absorption spectrum and the densitometer trace which have a clear view of the autoionizing transitions $5s5p\ ^3P_{1,2} - 5p^2\ ^3P_2$ with the broad line width at 2212 and 2270 Å.

The fractional absorption measurement was carried out for these autoionizing transitions in the following procedure. No change was given to the experimantal arrangement in §2.1. In the interferometer with the continuum light source, the reference beam section was masked. An EMI 6256B photomultiplier was equipped as a detecter on the spectrograph with 100 μm slit-width. Then the transmission signal of the light source was detected by turning on and off the HF discharge, and the output signal was recorded on a strip chart. The period of the discharge-off was only a few seconds so that the same steady state of discharge was easily recovered. An example of the absorption spectrum so obtained is represented

in Fig.7. The population density of the lower 5s5p $^3P_{0,1,2}$ levels in the same discharge was determined by the hook method after the absorption measurement.

It was impossible to detect small absorption signal below about 1.5 % because of small and rapid fluctuation of the Xe arc. Non-resonant absorption of the excited Cd atoms, i.e., direct photoionization, was not also detectable even at the threshold wavelength.

§ 3. Experimental Results

The absorption cross section σ_ν of the autoionizing transitions is given by

$$\frac{I}{I_0} = \exp(-N\sigma_\nu l) \tag{3.1}$$

at a frequency ν, where I_0 is the intensity of the incident radiation, I is the intensity after passing through the Cd plasma and l is the absorption length or 57 cm in this case. The absolute value of σ_ν is plotted in Fig.8 (a) and (b) for the transitions 5s5p $^3P_1$ - 5p^2 $^3P_2$ and 5s5p $^3P_2$ - 5p^2 $^3P_2$, respectively. The profiles of these transitions are in good agreement with the Lorentzian profile with the same half-width of 232 cm^{-1}, which is represented by the solid line in Fig.8. The half width for the transitions determines the autoionization probability of the 5p^2 $^3P_2$ state to be 4.37 x 10^{13} sec^{-1}. The f-value of the transition is given by

$$\int \sigma_\nu d\nu = \frac{\pi e^2}{mc} f, \tag{3.2}$$

where m, e and c have the usual meanings.

The data on the $5p^2\ ^3P_2$ level are shown in Table I together with the previous date.

The f-values determined by the hook and absorption measurements are summerized in Table II, where f/f_λ is the relative value of f to the oscillator strength f_λ of the transitions $5s5p\ ^3P_{0,1,2} - 5s6s\ ^3S_1$, A is the radiative transition probability calculated from f and f_{ratio} is the theoretical f-ratio predicted from pure LS coupling. The comparison of f with f_{ratio} shows that the LS coupling scheme is almost valid for the $5p^2\ ^3P_{0,1,2}$ levels within the present experimental accuracy and the uncertainty of f_λ.

The f-value for the 2267 or 2329 Å line, for example in the LS limit, gives the transition integral $R^1(5s5p)$ in the dipole transition matrix as

$$R^1(5s5p) = \pm\ 2.2\ \text{au}. \qquad (3.3)$$

It is clear that $R^1(5s5p)$ of ± 5.5 au* given by Parkinson and Reeves[2] is too large to satisfy the f-sum rule.

§ 4. Discussion

The observed lines for the autoionizing transitions have the Lorentzian profile contrary to the ordinary asymmetric

---

* The capture cross section for the transitions from the $p^2\ ^3P_2$ state has been derived from the absolute line intensity measurement, on the assumption of thermal equilibrium in the arc plasma.

profile for an autoionization resonance. This fact will be explained as follows according to Fano.[6] The final state Ψ for an autoionizing transition is represented as

$$\Psi = \alpha\Phi + \int\beta\psi_E dE, \tag{4.1}$$

and

$$|\alpha|^2 = \frac{|V_E|^2}{(E - E_0)^2 + \pi^2|V_E|^4}, \tag{4.2}$$

where α and β are the interaction coefficients between a discrete atomic state Φ and a continuum state ψ_E, E_0 is the resonance energy of autoionization and V_E is an element of the energy matrix, i.e., $\langle\psi_E|H|\Phi\rangle$.

The $5p^2\ ^3P_2$ state is mixed with the $5p^2\ ^1D_2$ state by the spin-orbit interaction, as shown by Parkinson and Reeves.[2] The perturbed eigenfunction Φ of the $p^2\ ^3P_2$ state in the present case may be written in terms of the unperturbed eigenfunction ϕ:

$$\begin{aligned}\Phi(p^2\ ^3P_2) &= a\phi(p^2\ ^3P_2) - b\phi(p^2\ ^1D_2)\\ a^2 + b^2 &= 1,\end{aligned} \tag{4.3}$$

where b will be small. Then the only continuum state sE(d) $^1D_2$ is available for autoionization of $\Phi(p^2\ ^3P_2)$, so that we write

$$\psi_E = \psi_E(sd\ ^1D_2). \tag{4.4}$$

Using the eigenfunction $\phi(sp\ ^3P)$ of the initial $5s5p\ ^3P$ states, the absorption cross section σ of the transitions $5s5p\ ^3P_{1,2} - 5p^2\ ^3P_2$ is

$$\sigma \propto |\langle \Psi | D | \phi(sp\ ^3P) \rangle|^2$$

$$= |\alpha|^2 a^2 |\langle \phi(p^2\ ^3P_2) | D | \phi(sp\ ^3P) \rangle|^2 \qquad (4.5)$$

since

$$\langle \phi(p^2\ ^1D_2) | D | \phi(sp\ ^3P) \rangle$$

$$= \langle \psi_E(sd\ ^1D_2) | D | \phi(sp\ ^3P) \rangle = 0,$$

where D is the dipole transition operator. Equations (4.2) and (4.5) show that the observed spectra of σ are given by the Lorentzian profile and have the same half-width $2\pi|V_E|^2$. From the measured half-width,

$$\langle \psi_E(sd\ ^1D_2) | H | \Phi(p^2\ ^3P_2) \rangle = b\langle \psi_E(sd\ ^1D_2) | H | \phi(p^2\ ^1D_2) \rangle$$

$$= \pm\ 1.30 \times 10^{-2}\ \text{au}, \qquad (4.6)$$

where $\langle \psi_E(sd\ ^1D_2) | H | \phi(p^2\ ^3P_2) \rangle = 0$.

If configuration interaction is negligible, all levels in the $5p^2$ configuration are expressed as eq.(4.3)[11,12]

$$\Phi(p^2\ ^1D_2) = a\phi(p^2\ ^1D_2) + b\phi(p^2\ ^3P_2)$$

$$\Phi(p^2\ ^3P_1) = \phi(p^2\ ^3P_1)$$

$$\Phi(p^2\ ^3P_0) = c\phi(p^2\ ^3P_0) + d\phi(p^2\ ^1S_0) \qquad (4.7)$$

$$\Phi(p^2\ ^1S_0) = c\phi(p^2\ ^1S_0) - d\phi(p^2\ ^3P_0)$$

$$c^2 + d^2 = 1.$$

The experimental positions of the three ^3P levels determine the two parameters, i.e., the Slater integral $F_2(5s5p)$ and the spin-orbit integral ζ_p in the energy matrix components. The values of a, b, c, d and the unknown positions of the

$p^2\ ^1D_2$ and $^1S_0$ levels are estimated by these parameters:

$$a = 0.993,\ b = 0.117,\ c = 0.997,\ d = 0.082$$

and

$$E(5p^2\ ^1D_2) = 83268\ cm^{-1}$$
$$E(5p^2\ ^1S_0) = 95029\ cm^{-1}.*$$

The estimate shows the small mixing of $\phi(p^2\ ^1D_2)$ into $\phi(p^2\ ^3P_2)$ and also $\phi(p^2\ ^1S_0)$ into $\phi(p^2\ ^3P_0)$. As pointed out by the previous authors,[1,12] therefore, the $5p^2\ ^3P_0$ state would be expected to autoionize to the $sE(s)\ ^1S_0$-continuum. There are no acceptable interpretations on the reason why the spectral line from the $5p^2\ ^3P_0$ level at 2307 Å appears sharp yet (see Fig.6). The matrix element $\langle\psi_E(ss\ ^1S_0)|H|\phi(p^2\ ^1S_0)\rangle$ may be very small.

* These positions, of course, include some uncertainties because no configuration interactions are considered.

References

1) W.R.S.Garton and A.Rajaratnam: Proc. Phys. Soc. A 68 (1955) 1107.

2) W.H.Parkinson and E.M.Reeves: Proc. Roy. Soc. A 331 (1972) 237.

3) E.Majorana: Nuovo Cimento 8 (1931) 107.

4) K.Miyazaki and K.Fukuda: J. Phys. Soc. Japan 38 (1975) 906.

5) K.Miyazaki, T.Watanabe and K.Fukuda: J. Phys. Soc. Japan 38 (1975) 1551.

6) U.Fano: Phys. Rev. 124 (1961) 1866.

7) M.C.E.Huber: Modern Optical Methods in Gas Dynamic Research, ed. D.S.Dosanjh (Plenum Press, New York, 1971) p.85.

8) T.Fujimoto, K.Miyazaki and K.Fukuda: J. quant. Spectrosc. radiative Transfer 14 (1974) 377.

9) K.Miyazaki, Y.Ogata, T.Fujimoto and K.Fukuda: Japan. J. appl. Phys. 13 (1974) 1866.

10) T.Andersen and G.Sørensen: J. quant. Spectrosc. radiative Transfer 13 (1973) 369.

11) R.H.Garstang: Monthly Not. Roy. Astron. Soc. 111 (1951) 115.

12) E.U.Condon and G.H.Shortley: The Theory of Atomic Spectra (Cambridge University Press, London, 1935) Chap.11 and 15.

Figure captions

Fig.1. Schematic diagram of the discharge tube.

Fig.2. Simplified term diagram of CdI.

Fig.3. Examples of the hook spectrogram for the transitions $5s5p\ ^3P_{0,1,2} - 5s6s\ ^3S_1$.

Fig.4. Example of the hook spectrogram for the transitions $5s5p\ ^3P_{0,1,2} - 5p^2\ ^3P_{0,1}$.

Fig.5. Population density of the $5s5p\ ^3P_{0,1,2}$ levels as a function of furnace temperature. Ar (buffer gas): 1.0 Torr. Output power of the HF device: 475 W.

Fig.6. Example of absorption spectrum of the transitions $5s5p\ ^3P_{0,1,2} - 5p^2\ ^3P_{0,1,2}$ and the densitometer trace.

Fig.7. Absorption spectrum of the transitions $5s5p\ ^3P_{0,1,2} - 5p^2\ ^3P_{0,1,2}$. Furnace temperature: 340 °C.

Fig.8. Absorption cross section for the autoionizing transitions (a) $5s5p\ ^3P_1 - 5p^2\ ^3P_2$ and (b) $5s5p\ ^3P_2 - 5p^2\ ^3P_2$. The solid line represents the Lorentzian profile with the half width of 232 cm^{-1}. The maximum values of the cross section (a): 5.7×10^{-16} cm^2 at 2211.5 ± 0.2 Å and (b): 8.2×10^{-16} cm^2 at 2270.0 ± 0.3 Å.

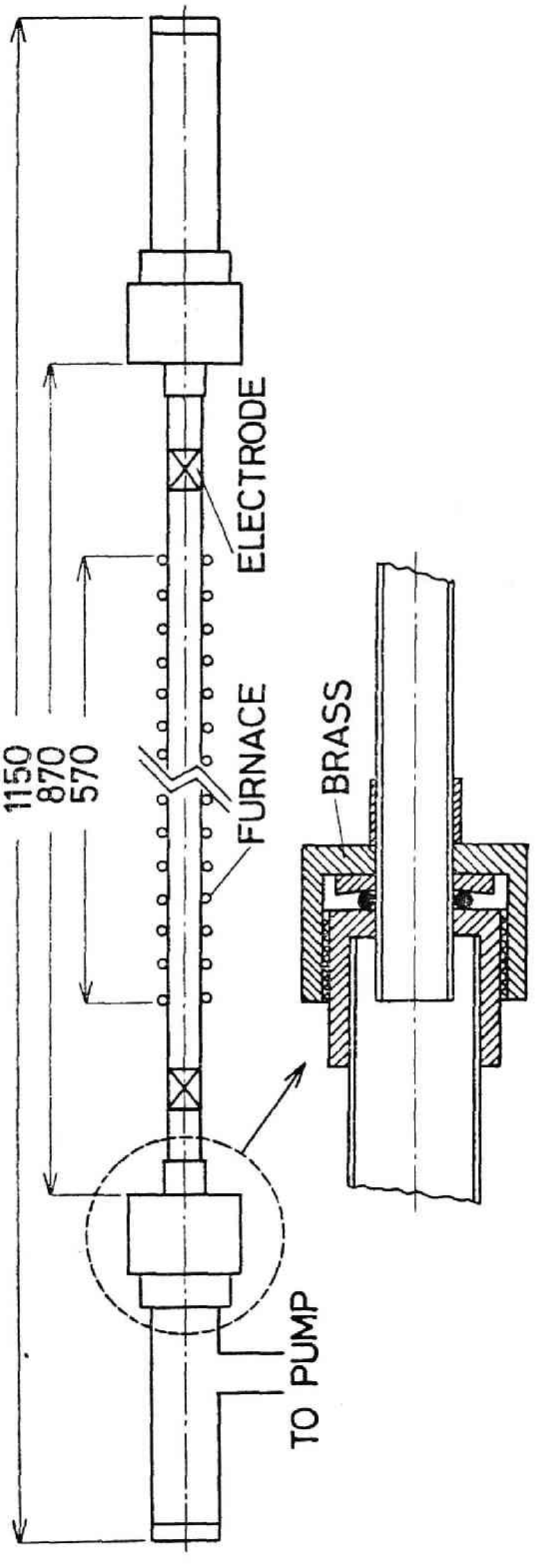

Fig.1

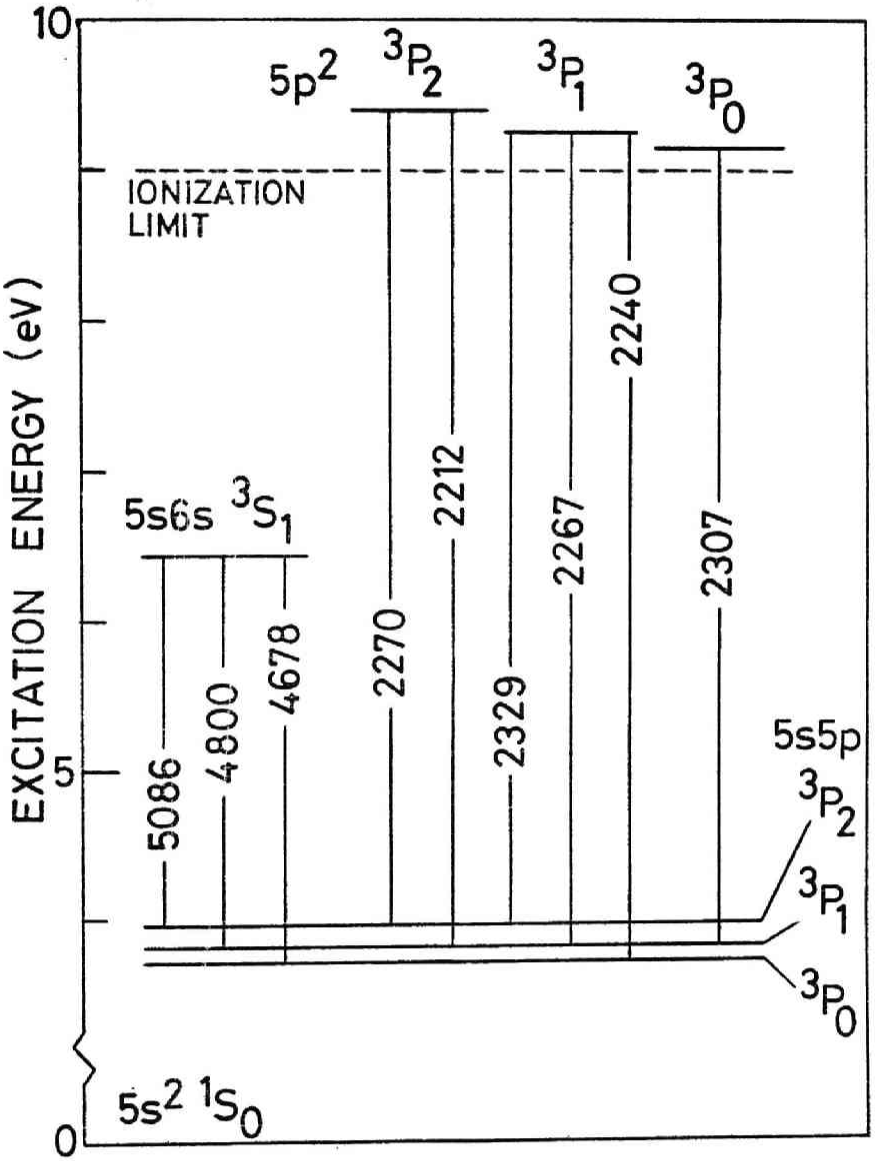
10
5
0
EXCITATION ENERGY (eV)
$5p^2$ $^3P_2$
$^3P_1$
$^3P_0$
IONIZATION LIMIT
2240
2212
2267
2307
2270
2329
5s6s $^3S_1$
5086
4800
4678
5s5p
$^3P_2$
$^3P_1$
$^3P_0$
$5s^2$ $^1S_0$

Fig.2

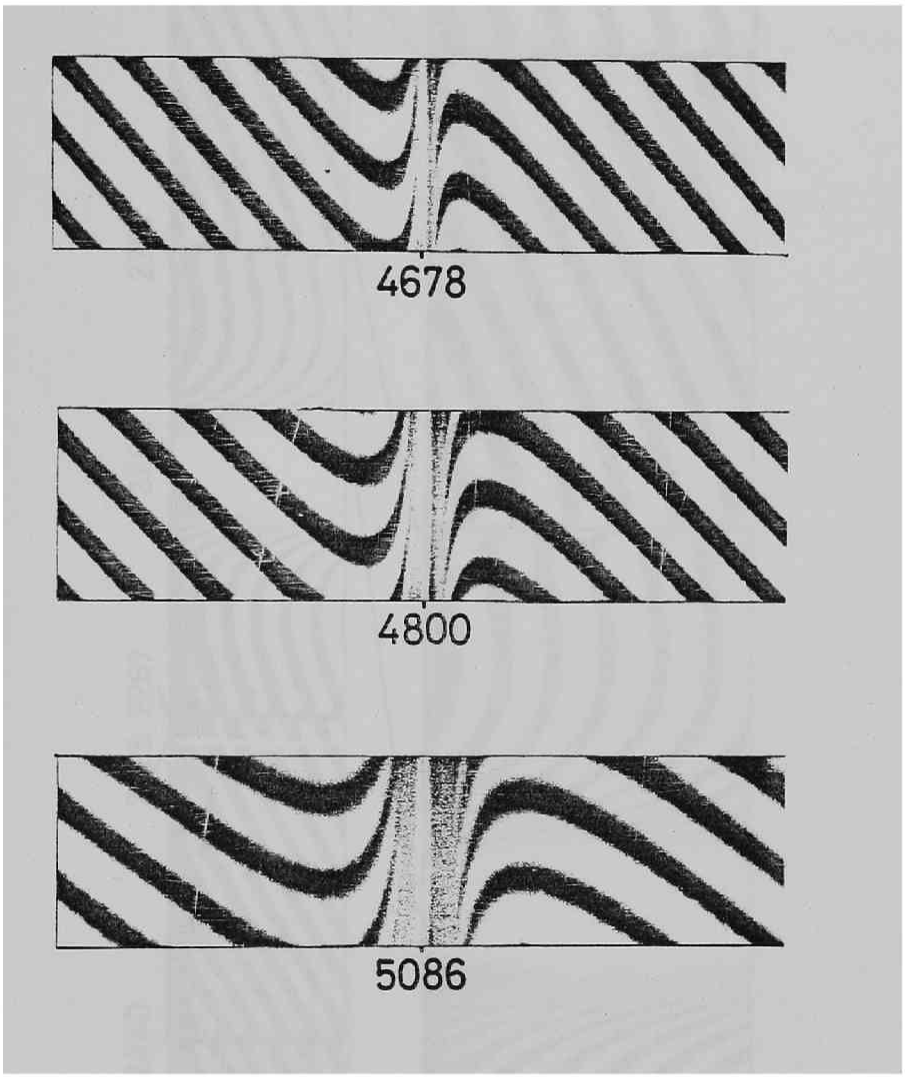

Fig.3

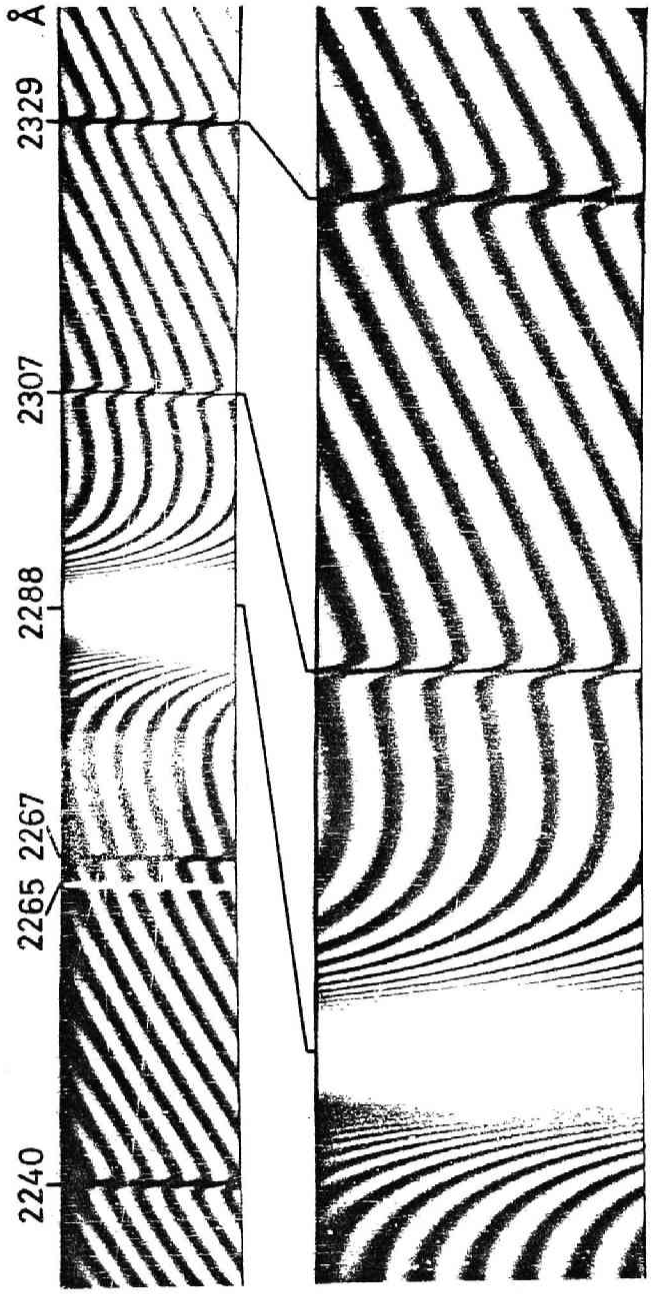

Fig.4

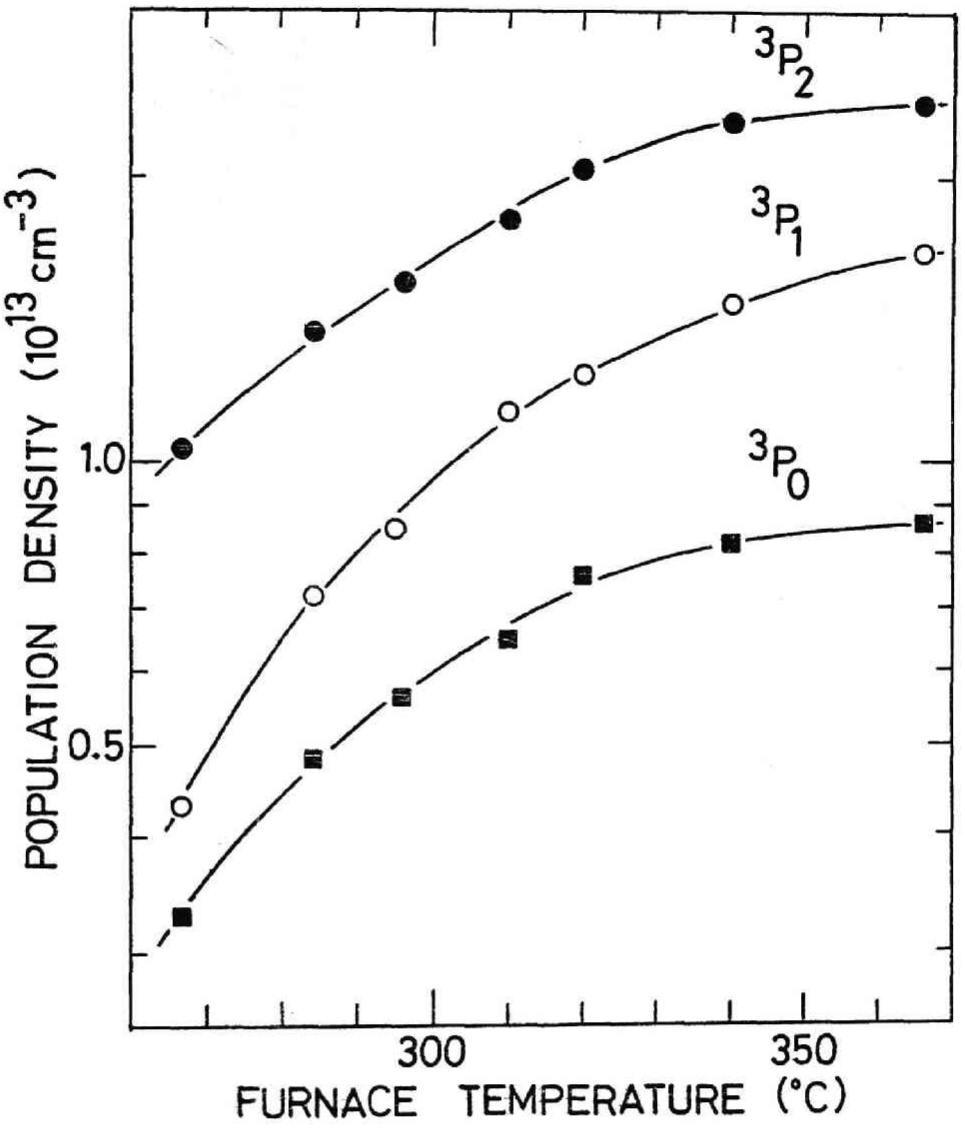
$^3P_2$
$^3P_1$
$^3P_0$
POPULATION DENSITY (10^{13} cm^{-3})
1.0
0.5
300
350
FURNACE TEMPERATURE (°C)

Fig.5

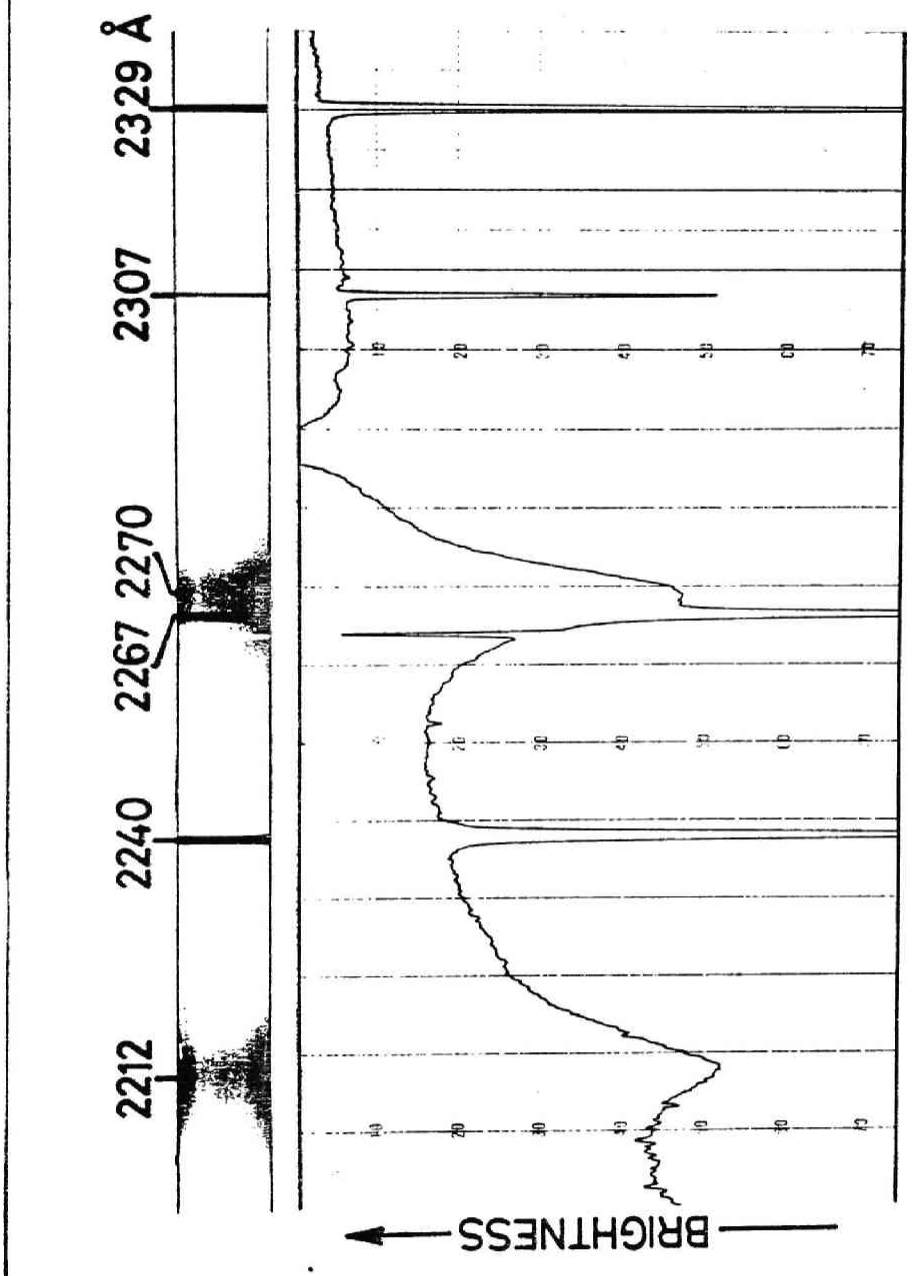

Fig.6

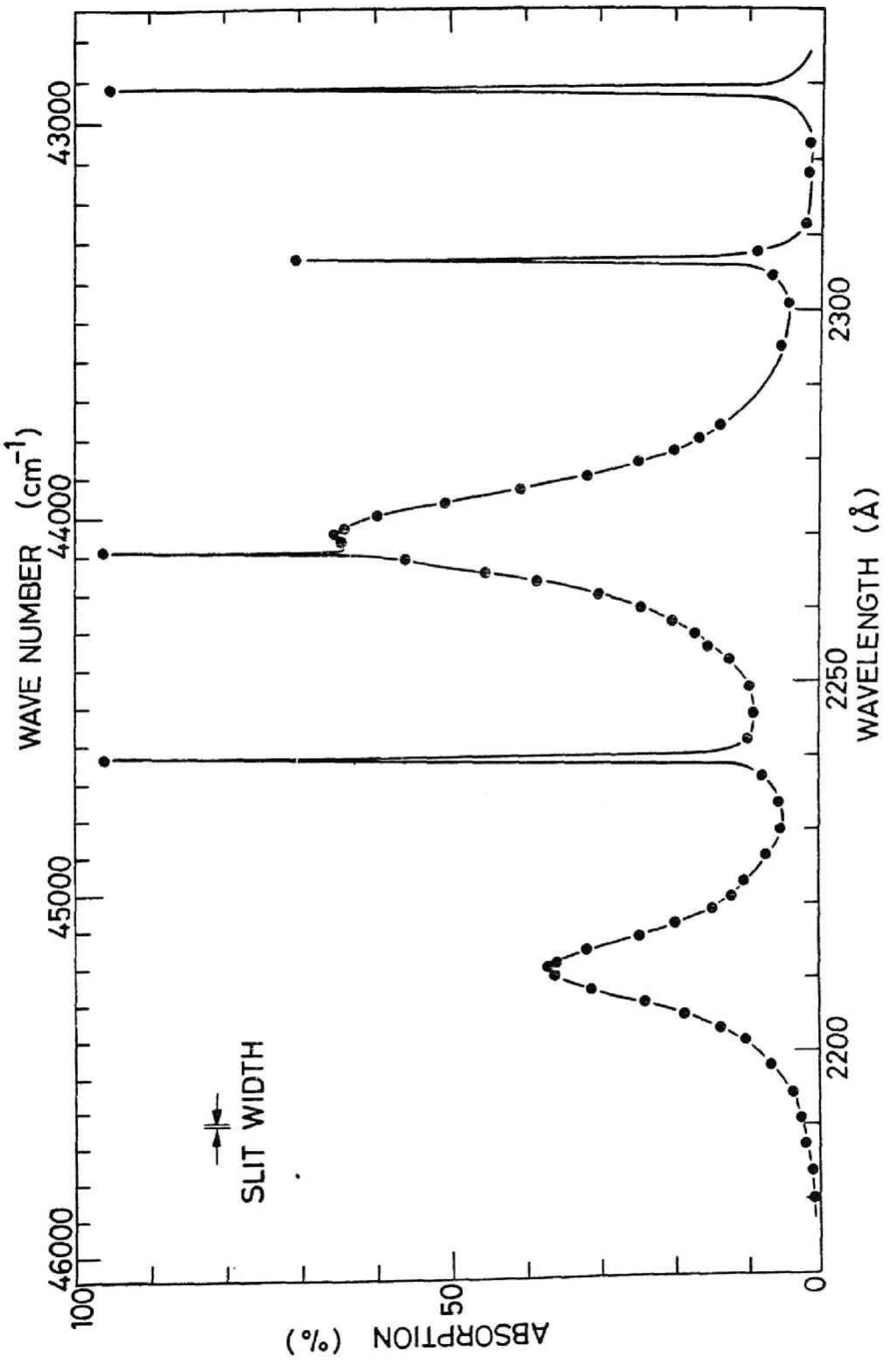
WAVE NUMBER (cm⁻¹)
46000
45000
44000
43000
WAVELENGTH (Å)
2200
2250
2300
ABSORPTION (%)
100
50
0
SLIT WIDTH

Fig.7

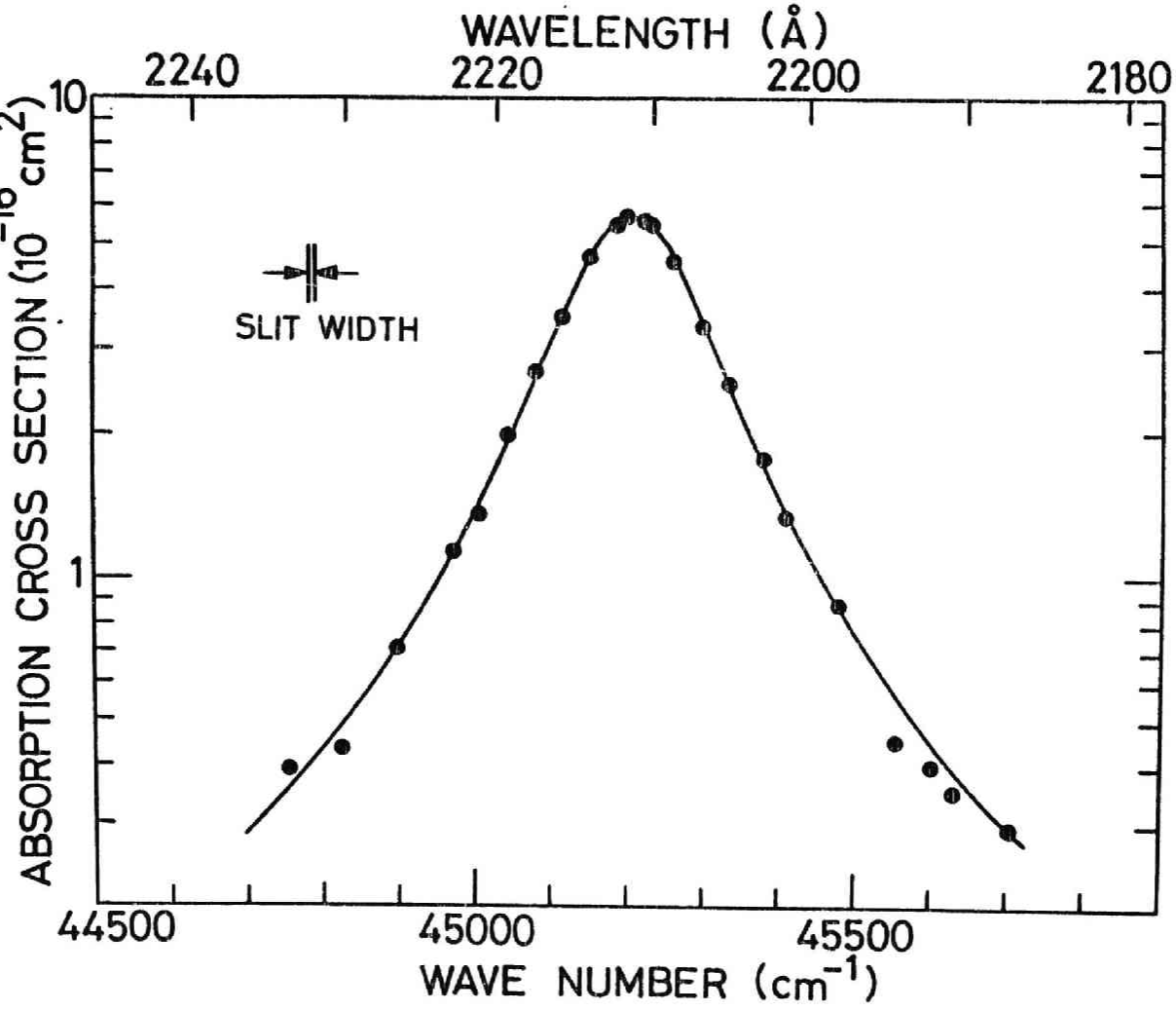
WAVELENGTH (Å)
2240
2220
2200
2180
10
1
ABSORPTION CROSS SECTION (10^{-16} cm^2)
SLIT WIDTH
44500
45000
45500
WAVE NUMBER (cm^{-1})

Fig.8(a)

ABSORPTION CROSS SECTION (10^{-16} cm^2)
1
10
SLIT WIDTH
43500
44000
44500
WAVE NUMBER (cm^{-1})
2300
2280
2260
2240
WAVELENGTH (Å)

Fig. 8 (b)

Table I. Half width $\Delta\nu$ and autoionization probability A_{aut} of the $5p^2\ ^3P_2$ state.

	Present experiment	Parkinson and Reeves[2]	Garton and Rajaratnam[1]
$\Delta\nu$ (cm^{-1})	232 ± 5	220	176
A_{aut} (10^{13} sec^{-1})	4.37 ± 0.09	4.15	3.32

Table II. Oscillator strengths of the transitions $5s5p\ ^3P_{0,1,2} - 5p^2\ ^3P_{0,1,2}$. A: radiative transition probability calculated from f. f_{ratio}: the ratio among f-values predicted from pure LS coupling.

Transition $5s5p - 5p^2$	Wavelength (Å)	f/f_λ	f [a)]	A (10^8 sec^{-1})	f_{ratio} (LS)
$^3P_2 - {}^3P_1$	2329	$/f_{5086}$: 0.89 ± 0.08	0.10	2.1	1.0
$^3P_1 - {}^3P_0$	2307	$/f_{4800}$: 0.97 ± 0.10	0.13	4.8	1.3
$^3P_1 - {}^3P_1$	2267	$/f_{4800}$: 0.80 ± 0.08	0.11	1.4	1.0
$^3P_0 - {}^3P_1$	2240	$/f_{4678}$: 3.2 ± 0.3	0.34	1.5	4.2
$^3P_2 - {}^3P_2$	2270	$/f_{5086}$: 2.8_8 ± 0.20	0.34	4.4	3.1
$^3P_1 - {}^3P_2$	2212	$/f_{4800}$: 1.7_8 ± 0.13	0.23	1.9	1.8

a) $f_{5086} = 0.117$, $f_{4800} = 0.132$ and $f_{4678} = 0.105$ are used.[10)]

Acknowledgement

The author would like to express his gratitude to Prof. K.Fukuda for his guidance and felicitous suggestions throughout this work and also wishes to express his thanks to the members of the laboratory, especially to Dr. T.Fujimoto for his collaboration and helpful discussion. The author is indebted to Dr. Y.Ogata for his help and discussion in the experiment on He-Cd laser discharge and to Mr. T.Watanabe, Mr. Y.Tomita and Mr. S.Watanabe for their assistance in performing the experiments.